A multilevel approach to assess the ecological impacts of hydroelectric infrastructures on local avifauna

Cheikh Tidiane Seck
Master in Ecology and Environment
Department of Biology
Faculty of Sciences of the University of Porto
2025

A multilevel approach to assess the ecological impacts of hydroelectric infrastructures on local avifauna

Cheikh Tidiane Seck

Dissertation carried out as part of the Master in Ecology and Environment

Department of Biology

2025

Supervisor
Dr. Rita Bastos, BIOPOLIS/CIBIO-InBIO, University of Porto

Co-supervisor
Dr. Joana Vicente, BIOPOLIS/CIBIO-InBIO, University of Porto

Co-supervisor
Prof. João Alexandre Cabral, CITAB, University of Trás-os-Montes e Alto Douro

Acknowledgements:

Embarking on a Master's degree in a new country presented a significant challenge for me. The landscape, language, and society all required adaptation, and I had to give my best to succeed in this endeavour. Numerous efforts were made, and many individuals contributed to this journey.

At the term of this Master's programme, I wish to express my profound gratitude to God and my family for their unwavering support. Their benevolent assistance accompanied me throughout my studies, particularly upon my arrival in Portugal. I would like to offer a heartfelt tribute to the memory of my late father, Souleymane Seck, may the Lord welcome his soul into paradise. He supported me throughout my childhood and never ceased to encourage me. His passing in 2022, shortly after my departure from Senegal, was a difficult time, but I cherish all his efforts to support me in my academic journey. May he rest in peace!

I also thank my mother, Ndeye Samb, who has always fought for her children and supported us with what little she had. Her prayers and constant support have been essential. Thank you, Mum!

To my brothers and sisters, for their love and their desire to see me succeed, I extend all my gratitude and respect. Special mention goes to my sister, Fatou Mbaye Seck, whose invaluable assistance during my settling in Portugal was decisive. Her generosity and support, as well as that of her husband, Mouhamed Wade, enabled me to overcome many difficulties. I am deeply grateful to them.

I would like to extend a very big thank you to Dr. Rita Bastos for her help and infinite support that she brought to me during this project. Her kindness and advice greatly helped me to refine this project and to have a broader vision on modelling and extensively on ecology. Without her, it would not be possible to successfully conclude this project. Rita, I extend my sincere gratitude. Thank you very much, Rita!

My thanks also go to Dr. Joana Vicente and Professor João Cabral for their availability, support and valuable explanations. Professor Cabral's analyses and advice were a great help in advancing this project. A big thank to you both!

I thank the University of Trás-os-Montes for making available the data that served as the basis for this work, as well as Professor Mário Santos, whose seminar in Vila Real introduced me to dynamic modelling and the use of NetLogo.

I thank the University of Porto for allowing me to integrate this Master's programme, and to all the professors of the Ecology and Environment Master's programme in the Biology Department of the University of Porto, I extend my gratitude for their contribution to enriching my knowledge. Special mention to Professor Nuno Formigo, Professor João Honrado and Professor Sara Antunes.

I thank the Camões Institute I.P. for the scholarship that was granted to me, a strong gesture that reflects the good cooperation between Senegal and Portugal.

Finally, I extend my greetings to my colleagues from the Ecology and Environment Master's programme, as well as to the members of the InvasionS group from CIBIO.

Abstract

The increasing demand for renewable energy sources has led to the development of numerous hydroelectric infrastructure projects worldwide. While these projects offer the potential for clean energy generation, they also introduce significant changes in the surrounding environment. This is particularly critical as projects expand into ecologically sensitive areas. Thus, assessing the effects of dams on wildlife is crucial for balancing renewable energy development with environmental management and biodiversity conservation.

The Hydroelectric Infrastructure of the Baixo Sabor (HIBS), located in northeast Portugal, was built within a Natura 2000 site, triggering changes in natural habitats and biological communities protected under EU directives. Based on field surveys conducted under the HIBS' environmental impact assessment, this thesis aims to evaluate the ecological impacts of this dam on bird communities, focusing on passerine and cliff-nesting birds. Particularly, the goals of this study are: (1) to understand passerine community responses to the combined effects of river flooding, land use (LU) changes and modifications in microclimatic conditions associated with the HIBS implementation, and (2) to assess whether river flooding have been causing changes in the population dynamics of cliff nesting raptors using the valley to breed.

A Stochastic Dynamic Model/Agent Based Model interface was developed to evaluate passerine community responses to the HIBS implementation. The metrics used to analyse passerine community responses were total species richness and total abundance of individuals, and the obtained spatio-temporal projections (passerine occurrence patterns and their seasonal and interannual variations) were analysed using landscape metrics (i.e. Shannon's Diversity Index, SHDI; Cohesion Index, CI; Division, DI). For cliff nesting birds, a Before-After-Control-Impact (BACI)-like approach was used to analyse changes in raptors territory occupancy, breeding population size, and breeding productivity before and after river flooding. This study leverages an extensive dataset (2010–2022) collected during the long-term monitoring of the HIBS project and focus on the three most abundant cliff-nesting birds using the study area for reproduction (Golden Eagle, Egyptian Vulture, and Gryffon Vulture).

Results suggest that elevation, slope ruggedness, proximity to water, and temperature are important drivers of passerine community dynamics. Overall, higher passerine diversity and abundance were associated with shrublands and olive orchards at lower elevations, located at greater distances from the reservoir. Furthermore, areas subjected to flooding and increased urbanization did not seem to promote changes in passerine occurrence patterns within the study period considered (2013-2016), suggesting passerine community stability associated with the reservoir filling phase. Landscape metrics analysis revealed distinct spatial configuration in passerine occurrence patterns: SHDI indicated reduced diversity in passerines diversity/abundance classes during summer months, CI suggested strong spatial connectivity of similar diversity/abundance classes during peak breeding season and DI indicated more cohesive distribution patterns of passerine diversity/abundance classes during mid-spring. These results suggest that while passerine community maintained stable spatial organization across years despite reservoir development, they exhibited pronounced seasonal dynamics driven by breeding phenology and microclimatic conditions. Regarding cliff-nesting birds, results showed that Egyptian vultures exhibited steeper declines in breeding productivity in territories most affected by flooding, likely due to habitat loss and potential competition. Golden eagles showed fluctuating population trends and a decline in breeding productivity

over time, though not directly linked to flooding extent. Conversely, Griffon vultures experienced increases in breeding colony occupancy and population size after flooding, regardless of flooding levels, possibly benefiting from supplementary feeding as a mitigation measure.

Overall, this study underscores the complex ecological impacts of hydroelectric infrastructures on avifauna, revealing community and population-based responses of passerine and cliff-nesting birds to environmental changes. The findings emphasize the importance of preserving diverse, connected habitats and implementing targeted conservation strategies to mitigate impacts, particularly for vulnerable species like Egyptian vultures and Golden eagles. By integrating long-term monitoring and dynamic modelling, this research provides a framework for balancing renewable energy development with biodiversity conservation in Mediterranean ecosystems, offering actionable insights for adaptive management within protected areas.

Keywords: *BACI approach, Biodiversity conservation, Cliff-nesting birds, community patterns, Impact assessment, Passerine birds, population dynamics, Spatially-explicit dynamic modelling, spatial-temporal trends*.

Table of Contents

List of Figures

List of Tables

List of Appendixes

List of Abbreviation

ABM	Agent Based Model
AIC	Akaike Information Criterion
BACI	Before-After-Control-Impact
HIBS	Hydroelectric Infrastructure of the Baixo Sabor
CI	Patch Cohesion Index
COS	Carta de Ocupação do Solo
DEM	Digital Elevation Model
DI	Landscape Division Index
GLMMs	Generalized Linear Mixed Models
GLMs	Generalized Linear Models
K.W	Kruskal Wallis
LTER	Long-Term Ecological Research
LU	Land Use
LULC	Land Use/ Land Cover
MMI	Multi-model inference
PIMA	Integrated Environmental Monitoring Program
SHDI	Shannon Diversity Index
SPA	Special Protection Area
StDM	Stochastic Dynamic Methodology
TRI	Terrain Ruggedness Index
VIF	Variance Inflation Factor

General introduction

The global transition to renewable energy has positioned hydropower as a cornerstone of sustainable development, providing a renewable source that contributes for reductions in greenhouse gas emissions (International Energy Agency, 2021). However, the ecological trade-offs between hydropower development and nature conservation remain poorly understood, particularly in ecologically sensitive areas.

The Iberian Peninsula, recognized as a biodiversity hotspot, exemplifies the tension between renewable energy development and biodiversity conservation. Its Mediterranean ecosystems harbour unique avian communities but increasing hydropower development threatens to destabilize these systems (Margalida & Colomer, 2012; Cortés-Avizanda et al., 2015). In northeastern Portugal, the Baixo Sabor region epitomizes these challenges. The Hydroelectric Infrastructure of the Baixo Sabor (HIBS), constructed within a Natura 2000 site, has transformed a protected Mediterranean landscape by flooding 60 km of the Sabor River valley and fragmenting critical habitats for avian communities (Santos et al., 2021). This creates a conservation paradox: a renewable energy initiative embedded in a biodiversity hotspot where endemic avifauna face compounded pressures from habitat fragmentation, climatic stressors, and direct infrastructure impacts.

Environmental impact assessment (EIA) enables the identification of critical habitats, vulnerable species, and ecosystem processes at risk by systematically evaluating potential ecological consequences associated with project implementation (Geneletti, 2003). It plays a pivotal role in the management of sensitive areas and the conservation of biodiversity, particularly in regions affected by large-scale infrastructure such as hydropower (Bidoglio et al., 2019). In the context of avian conservation, EIA facilitates the development of targeted mitigation measures—such as habitat restoration, buffer zones, and adaptive management protocols—that can reduce negative impacts on bird populations and maintain ecological integrity (Bidoglio et al., 2019). Moreover, the integration of EIA findings into decision-making processes supports compliance with international conservation frameworks and enhances the effectiveness of protected areas (Lemieux et al., 2018). In this regard, the Integrated Environmental Monitoring Program (PIMA) was implemented as part of the HIBS project to monitor and mitigate the environmental impacts of the dam (EDP, 2015). PIMA's primary goals include assessing the conservation status of ecosystems and species affected by the dam, ensuring the ecological efficiency of compensatory and mitigation measures, and maintaining the long-term ecological balance of the Sabor Valley (EDP, 2015). Specific objectives within the Sabor dam context involve monitoring of aquatic and adjacent terrestrial ecosystems, main

faunistic groups (i.e. mammals, avifauna, herpetofauna, freshwater mussels), and key species such as the Iberian wolf (*Canis lupus signatus*) and the Iberian desman (*Galemys pyrenaicus*), while also evaluating the effectiveness of habitat restoration and compensation measures (EDP, 2015).

Assessing the ecological impacts of hydropower infrastructures also requires robust methodologies that integrate long-term monitoring. In this regard, the Baixo Sabor region hosts a Long-Term Ecological Research (LTER) site, which serves as a platform for monitoring the long-term impacts of dam construction, habitat fragmentation, and climate change (eLTER, 2019). The Baixo Sabor LTER site is part of the broader European Long-Term Ecosystem Research (eLTER) network, a distributed infrastructure of research sites designed to understand ecosystem structure and functions across Europe. This network facilitates systematic, long-term observation of representative sites to enhance understanding in the fields of ecosystem, biodiversity, and socio-ecological research (eLTER, 2019). Integrated within the Natura 2000 network, the Baixo Sabor LTER site provides valuable insights into biodiversity dynamics and ecosystem services in response to human activities and environmental pressures (Beja & Cabral, 2012). This LTER site is particularly valuable for studying the ecological consequences of river damming on freshwater and adjacent terrestrial ecosystems, and how these effects interact with other socio-economic and environmental drivers operating at scales from local (e.g. land use changes) to global (e.g. climate change, biological invasions) (eLTER, 2019).

Hydropower projects disrupt ecosystems through cascading effects, ranging from microhabitat alterations that reduce invertebrate prey availability for insectivorous passerines to large-scale habitat loss that threatens key predators like cliff-nesting raptors (Zarfl et al., 2015; He et al., 2024). These disturbances highlight the vulnerability of avian communities, which are highly sensitive to both environmental and anthropogenic changes, making them effective bioindicators of ecosystem health (Gregory et al., 2004; Şekercioğlu et al., 2016). Within these communities, passerine birds, positioned at intermediate trophic levels, capture fine-scale habitat heterogeneity by responding rapidly to changes in Land use/Land cover (LU/LC) and microclimatic variability (Santos & Cabral, 2004; Bastos et al., 2016). In contrast, cliff-nesting raptors serve as sentinels for broader landscape disturbances, given their extensive territorial needs and susceptibility to habitat loss (Margalida et al., 2014b). By examining both groups, this study employs a hierarchical framework to unravel the ecological impacts of hydropower at two distinct scales: (1) community-level responses of passerines to habitat fragmentation and microclimatic changing conditions, and (2) population-level dynamics of raptors in response to habitat loss due to flooding.

This study aims to advance understanding on how renewable energy infrastructures interacts with biodiversity in Mediterranean ecosystems, offering insights for balancing decarbonization goals with conservation imperatives. Specifically, it investigates:

1. passerine community responses to the combined effects of river flooding, land use (LU) changes and modifications in microclimatic conditions
2. The long-term effects of reservoir flooding on the breeding occurrence and productivity of cliff-nesting raptors. *Paper under review in Global Ecology and Conservation*

By analysing long-term monitoring data and employing a multidisciplinary approach that integrates field surveys, statistical and dynamic modelling, this research examines trends in ecological indicators responses to human-induced changes associated with hydropower infrastructures. The findings aim to provide critical insights into the resilience of bird communities in changing Mediterranean ecosystems and inform adaptive management strategies to balance renewable energy development with biodiversity conservation.

Study area

This research was conducted in the Baixo Sabor region, located in northeast Portugal, a landscape profoundly influenced by the HIBS. Situated in the Trás-os-Montes region within the District of Bragança (Figure 1), the study area spans the lower Sabor river valley and its surrounding habitats, encompassing both human-altered environments and a protected ecological corridor critical for bird conservation. At the core of the HIBS is a concrete double-curvature arch dam, 123 meters high, which creates a reservoir extending approximately 60 km north along the Sabor River (Figure 1), with a storage capacity of 630 million cubic meters. Its construction, initiated in 2006 and completed in 2014, has significantly altered the local landscape through reservoir flooding and habitat modification (Santos et al., 2021).

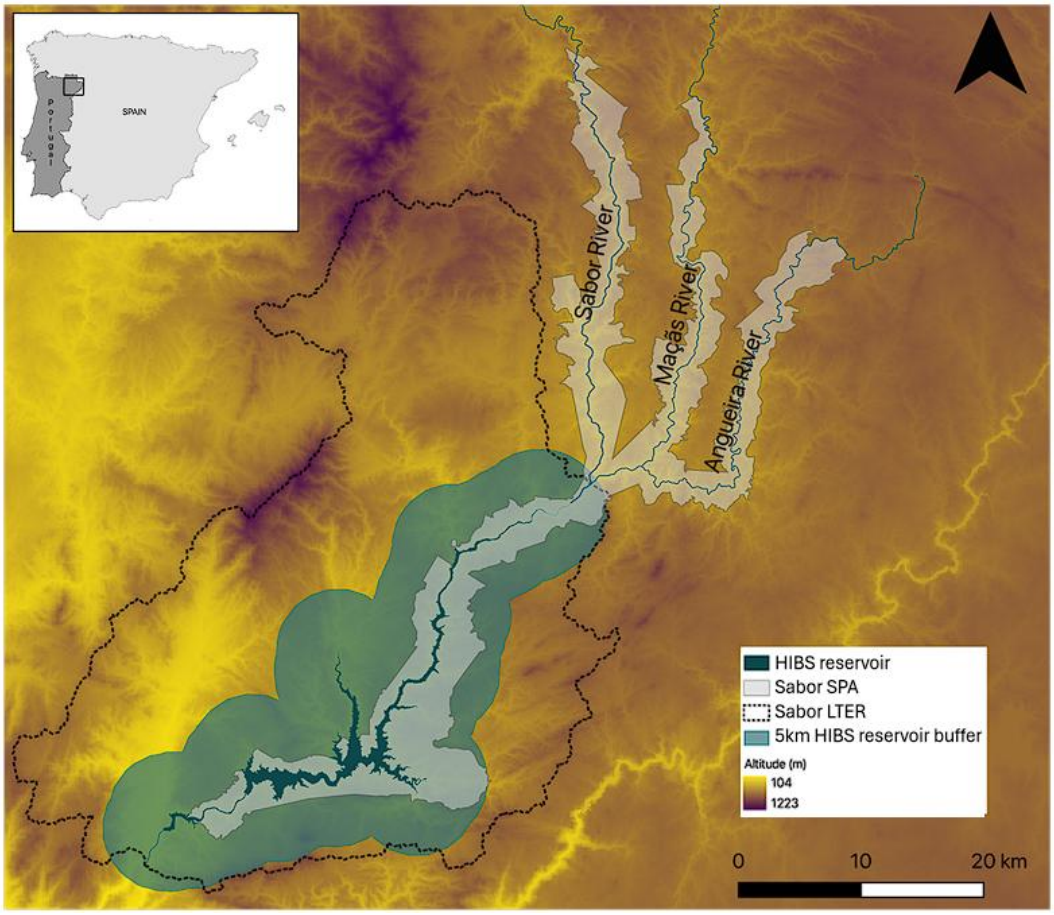

Figure 1 - Location of the Baixo Sabor study area in northeastern Portugal, showing the HIBS reservoir and its 5 km buffer, the boundaries of the Sabor Special Protection Area (SPA), and the Sabor LTER site. The map also displays the main tributary rivers (Sabor, Maçãs and Angueira Rivers) and altitude gradients.

The region is characterized by a transitional climate between the meso- and the supra-Mediterranean bioclimatic zones, with cold winters (average temperature of the coldest month

<6ºC) and dry summers (total annual precipitation <600 mm, with <5% occurring in July–August; Monteiro-Henriques, 2010). The landscape is a mosaic historically shaped by traditional agriculture, rural depopulation, and afforestation dynamics (Azevedo et al., 2011; Bastos et al., 2015). Over the past decades, the region has experienced significant LU changes, primarily due to agricultural abandonment and afforestation efforts. Agricultural land, which once covered 22% of the landscape in 1958, declined to less than 5% by 2005, replaced by shrublands and forests (Azevedo et al., 2011). This shift was driven by rural exodus and low-intensity traditional farming activities, such as extensive livestock grazing and forestry logging, which continue to shape the humanized areas of the region (Azevedo et al., 2011; Bastos et al., 2015). These changes have also increased wildfire frequency and intensity, further transforming the landscape (Azevedo et al., 2011). Presently, the area includes a mosaic of land uses, with agriculture and pasturelands dominating the lowlands, while forest plantations and natural vegetation covering the higher elevations (*Comunidade Intermunicipal das Terras de Trás-os-Montes*, 2019). The association of these habitats creates a dynamic landscape that reflects the ecological heterogeneity of the region. The northern part of the region is characterized by chestnut production, extensive forest areas with Pyrenean oak, and pastures, while the southern part supports olive and almond cultivation, interspersed with shrublands and pastures (*Comunidade Intermunicipal das Terras de Trás-os-Montes*, 2019).

The Baixo Sabor Special Protection Area (SPA), designated under the Natura 2000 network (Figure 1), lies within this region. Covering approximately 33,476 hectares (ICN-B, 1999), the SPA is recognized as a Site of Community Importance (SCI) and a Special Protected Zone (SPZ, code PTZPE0037) under the European Commission's Habitats and Birds Directives. The SPA encompasses a diversity of habitats, including Mediterranean scrublands, oak woodlands, pine forests, steep cliffs, rocky outcrops, and riparian zones. These features provide critical nesting and foraging habitats for cliff-nesting raptors, such as Egyptian vulture (*Neophron percnopterus*), Griffon Vulture (*Gyps fulvus*), Golden eagle (*Aquila chrysaetos*), Bonelli's eagle (*Aquila fasciata*), and Peregrine falcon (*Falco peregrinus*) (Margalida & Colomer, 2012; Santos et al., 2019a). In addition, the Baixo Sabor SPA supports other endemic fauna, such as the Iberian wolf (*Canis lupus signatus*), the Iberian frog (*Rana iberica*), the Gold-striped salamander (*Chioglossa lusitanica*), the Iberian wall lizard (*Podarcis hispanicus*) and the Schreiber's green lizard (*Lacerta schreiberi*) (Cabral et al., 2017; Mota et al., 2020a). The SPA is also renowned for its diverse passerine community, which includes rare and/or conservation-priority species. Some examples are the Rufous-tailed Rock-thrush (*Monticola saxatilis*; Linnaeus, 1766), Eurasian Bullfinch (*Pyrrhula pyrrhula*; Linnaeus, 1758), Dartford Warbler (*Curruca undata*; Boddaert, 1783), and Rock Bunting (*Emberiza cia*; Linnaeus, 1766).

Chapter 1: Combined effects of river flooding, land use and microclimatic changes at the community level: Modelling the spatially-explicit trends of passerine abundance and richness

1.1 Introduction

Passerine species constitute the largest and most diverse order of birds and play critical ecological functions as pollinators, seed dispersers and insect predators (Chen et al., 2019; Eriksson, 2014), thus being important elements for ecosystem regulation. Besides their visual and acoustic conspicuous presence, their sensitivity to environmental changes makes them reliable indicators of ecosystem health (Santos et al., 2018). For example, their presence and abundance often reflect habitat suitability conditions, as they respond to changes in vegetation structure, food availability, and habitat fragmentation (Díaz et al., 2011). Moreover, their conspicuousness and cost-effective monitoring makes them relatively easy to study (Bibby et al., 2000). Therefore, Passerine birds are good ecological indicators providing useful whole-system information, such as by capturing species diversity trends in face of disturbances (Carignan and Villard, 2002) or, when expressed as guilds or traits, by reflecting the trophic responses to land use gradients of change, both in composition and functioning terms (Santos and Cabral, 2004; Vandewalle et al., 2010).

The construction of dams introduces profound changes in natural systems. Dams alter hydrological regimes, fragment habitats, and create reservoirs that transform terrestrial and aquatic environments (Zarfl et al., 2015; Abreu et al., 2020). These changes have cascading effects on avian communities by modifying habitat availability, disrupting food webs, and altering microclimatic conditions (Kingsford, 2000; Pearce-Higgins et al., 2015). For example, reservoir-induced flooding often results in the submergence and loss of riparian habitats, which are critical for many passerine species as breeding and foraging sites. The destruction of these structurally complex and resource-rich zones can also lead to declines in passerine species richness and abundance, particularly habitat specialists (Hanowski et al, 1995; Nilsson & Berggren, 2000; Poff & Zimmerman, 2010), while promoting the dominance of generalist species; thus leading to shifts in community composition and reduced overall biodiversity (Newbold et al., 2015). Microclimatic conditions, such as temperature and humidity, are also critical determinants of species distribution and ecosystem functioning (Heikkinen et al., 2004). Dams influence these conditions by altering local hydrology and creating new thermal and moisture gradients around reservoirs (Gardner et al., 2016). These changes can have significant implications for bird communities, particularly during the breeding season when birds are highly dependent on stable microclimatic conditions for nesting and foraging (Pearce-Higgins et al., 2015).

Despite all these consequences, the combined effect of multiple drivers shaping avifauna responses to dam construction remains poorly understood. In this context, spatially explicit dynamic modelling tools such as the Stochastic Dynamic Methodology (StDM) and agent-

based modelling (ABM) can be useful to address these knowledge gaps. The StDM is a sequential hybrid modelling protocol developed in order to predict the ecological status of changed ecosystems, from which management strategies can be designed (Cabral et al., 2008; Santos et al., 2013). Particularly, the StDM is based on the premise that the general statistical patterns of ecological phenomena are emergent indicia of complex ecological processes that do indeed reflect the operation of universal law-like mechanisms (Cabral et al., 2008). StDMs are well-suited for predicting ecological responses to environmental changes, as they combine statistical and dynamic modelling techniques to simulate relevant holistic ecological metrics, such as species richness and abundance under contrasting scenarios (Santos & Cabral, 2004; Bastos et al., 2015). ABMs complement this approach by simulating process-based changes in spatially explicit landscapes, thus providing a mechanistic understanding of the species responses to modified environmental conditions (e.g. Carter et al. 1999; Faust et al. 2003; Zurell et al. 2015; Santos et al., 2016a; Johnston et al. 2018; Boyd et al. 2018). The integration of these methods therefore allows for the visualization of outputs in dynamic, interactive interfaces, enhancing the interpretation of results and supporting decision-making processes.

By using de principles of the Stochastic Dynamic Methodology (StDM), implemented into an agent-based modelling (ABM) environment, this study intends to evaluate passerine community responses (in terms of species richness and abundance of individuals) to the combined effects of river flooding, land use (LU) changes and modifications in microclimatic conditions associated with the HIBS implementation. For this, the developed StDM/ABM framework allowed to project passerine spatio-temporal trends (i.e. occurrence patterns and their seasonal and interannual variations) before (2013-2014) and after (2015-2016) reservoir filing phase, which were further analysed using landscape metrics. In fact, while traditionally applied to assess landscape physical patterns (e.g. habitat fragmentation) and its influence on biological communities, this study innovatively uses landscape metrics (i.e. Shannon's Diversity Index, SHDI; Cohesion Index, CI; Division, DI) to evaluate passerine community spatial responses, offering a novel perspective on the spatial configuration of ecological indicators responses to infrastructural impacts. By addressing these objectives, this study contributes to a better understanding of how hydropower infrastructure interacts with biodiversity in Mediterranean ecosystems, offering insights for balancing renewable energy development with conservation imperatives.

1.2. Methodology

1.2.1. StDM/ABM interface framework

The proposed StDM/ABM framework (Figure 2) is a sequential modelling procedure developed to predict ecological indicators responses to environmental and/or anthropogenic changes. Initiated with the characterization of environmental data layers obtained throughout representative gradients of prevailing conditions (i.e. passerine occurrence in sampling points, river flooding characteristics, topographic features, LU maps and microclimatic conditions) (Figure 2a), the analysis of landscape and habitat composition defines the convenient statistical parameters, derived from multi-model inference (Figure 2b), that contextualize the physical and biotic descriptors at the study unit level (1x1km) (Figure 2c). Based on the algorithms created in the statistical analysis (Figure 2b), the ABM is prepared to perform iterative updates of spatial data layers to predict passerine community responses (e.g. total species richness and abundance) at each time step (Figure 2c). In this way, the ABM dynamically update ecological indicators responses based on surrounding conditions, providing an integrative picture, in space and time, of passerine community responses to environmental changes (Figure 2d).

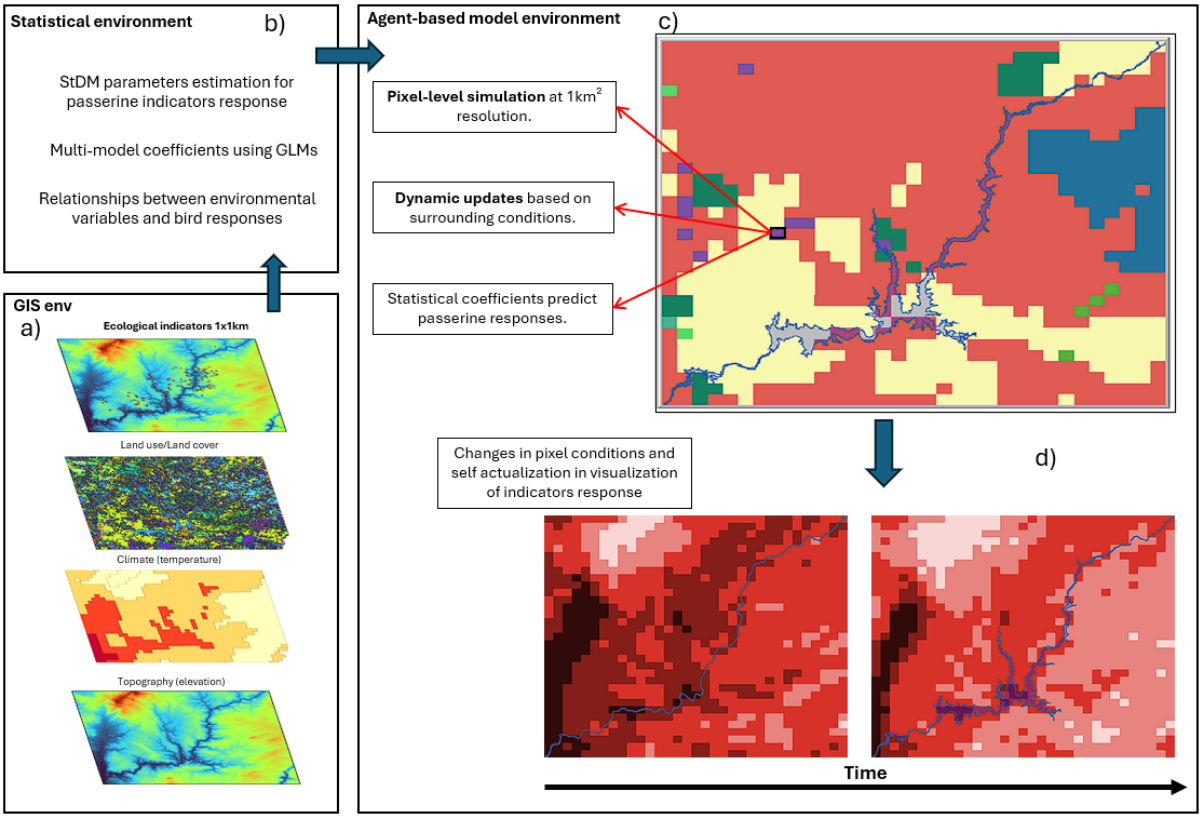

Figure 2 - The proposed StDM/ABM framework to predict ecological indicators responses to environmental changes: (a) characterization of spatial data layers (passerine sampling points, river flooding characteristics, topographic features, LU maps and microclimatic conditions) at the study unit level - GIS environment; (b) estimation of statistical relationships between passerine

occurrence and environmental variables at the study unit level - Statistical environment; (c) dynamic integration of spatial data layers and statistical algorithms into the ABM environment and (d) iterative updates of environmental data layers to predict passerine community responses (e.g. total species richness and abundance) through time and space.

1.2.2. Passerine data

The database used in this study was based on point count surveys of passerine bird species (Figure 3) conducted from March to July over a four-year period (2013–2016) and selected throughout a representative gradient of environmental conditions. This period corresponds to the passerine breeding season, during which birds rely on specific habitats and resources for nesting and foraging (Santos & Cabral, 2004). The surveys were part of two monitoring programs: the Long-Term Ecological Research (LTER) program (2013–2014) and the Integrated Environmental Monitoring Program (PIMA, 2015–2016), both associated with the HIBS. These programs provided a robust framework for monitoring passerine assemblages across different phases of the HIBS: the reference phase (2013), the construction phase (2013–2014), and the flooding phase (2015–2016).

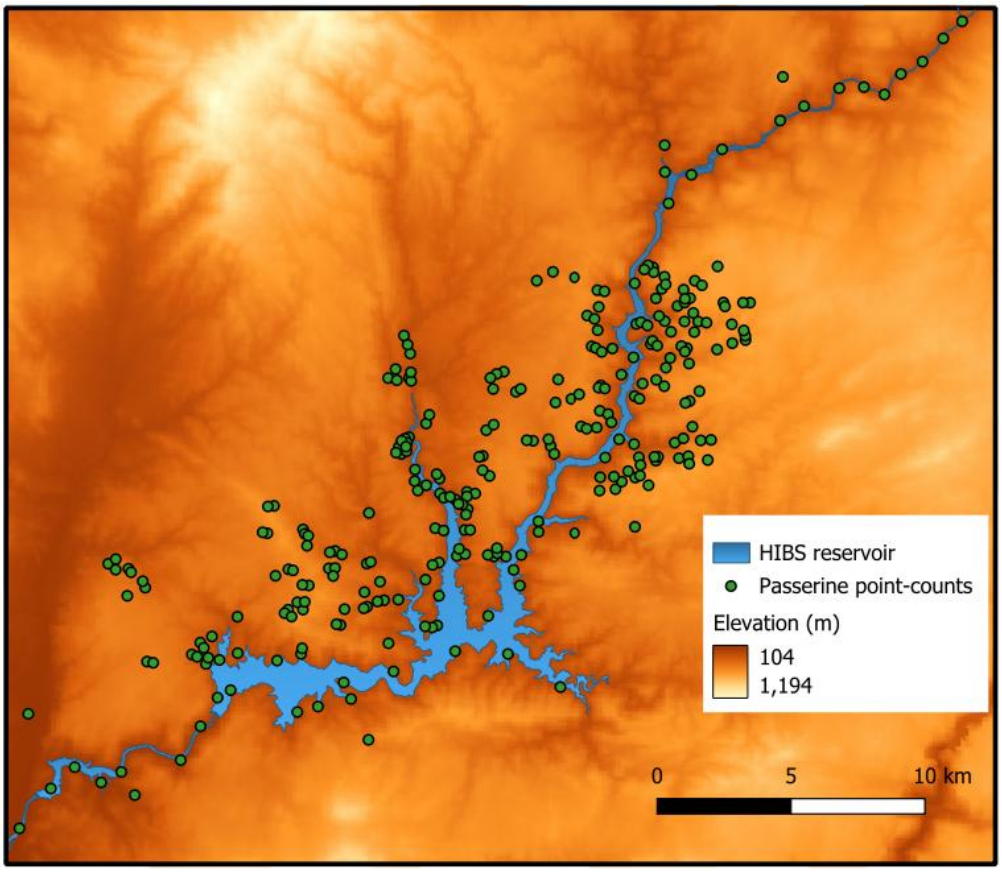

Figure 3 - Distribution of passerine point-counts during the study period (2013-2016), selected throughout a representative gradient of environmental conditions.

Passerine species richness and relative abundances were recorded using unlimited 10-minute point-counts conducted up to five hours after sunrise, a timeframe widely recognized as

optimal for capturing a representative snapshot of avian populations due to peak bird activity during early morning hours (Ralph et al., 1993). Experienced ornithologists recorded all individuals seen or heard within two distance bands (0–50 m and 50–100 m) and categorized them by species and distance band. Both visual and auditory detections were included in the records, with species richness representing the total number of different species detected per point-count and abundance representing the total number of individuals recorded. This dual approach ensured comprehensive data collection, capturing both conspicuous and cryptic species.

According to expert knowledge, previously reported in the scientific literature (e.g. Gil-Tena et al., 2009; Moreira et al., 2001; Regos et al., 2015), species were grouped into three foraging groups, namely grassland species, shrubland species and woodland species, considering their degree of functional specialization on open habitats (including heterogeneous open habitats with hedgerows) and habitats dominated by shrubs or forests, respectively (Bastos et al., 2016).

1.2.3. Environmental data

A set of environmental variables was selected to characterize the habitats surrounding each passerine point count, such as LU, topography, distance to water, and microclimatic conditions (Table 1). For this, a standardized 500 m buffer zone around each sampling point was used, assumed as suitable to capture local passerine responses to habitat features and environmental gradients (Heikkinen et al., 2004).

Table 1 - The environmental classes of the variables used in the procedure for the passerine foraging groups and the respective main data sources, according to the respective reference scales (i.e. 1 km UTM cells), and supporting literature references.

Environmental classes	Variables	Source
Topographic data	Elevation at the point count (m) Slope Rugosity in the buffer (°)	https://csidotinfo.wordpress.com/data/srtm-90m-digital-elevation-database-v4-1/
Landscape composition	Coniferous forest (m²) Deciduous forest (m²) Temporary crops (m²) Traditional agricultural mosaic (m²) Olives & Orchards (m²) Vineyards (m²)	COS2010 COS2015 http://www.dados.gov.pt

	Pastures (m²) Shrublands (m²) Water source (m²) Reservoir (m²) Urban areas (m²)	
Microclimatic	Mean temperature per month (from March to July) (°) Mean precipitation per month (from March to July) (mm)	Fonseca et al., 2019

LU characterization was based on *Carta de Ocupação do Solo* (COS) for the years 2010 and 2015 (dados.gov.pt, 2010, 2015). Data were aggregated into ecologically relevant categories following the criteria established by Bastos et al. (2016). These categories included agricultural and forested areas, urban lands, and water bodies, grouped into broader classes based on their ecological relevance and similarity in terms of passerine habitat use (Appendix I). The area (in m²) of each LU category was calculated for each buffer using the QGIS field calculator tool. This approach allowed for a detailed assessment of habitat composition and its potential influence on passerine community patterns.

Topographic features, including elevation and slope rugosity, were derived from a high-resolution Digital Elevation Models (DEMs) within a 10 km grid. Elevation data were extracted for each point-count (measured in meters above sea level), while slope rugosity (hereinafter named TRI) was calculated within each buffer zone according to the formula (Sappington et al., 2007):

$$\mathrm{TRI}_{\mathrm{slope}} = \sqrt{\left(\frac{\sum_{i=1}^{n}(s_i - \bar{s})^2}{n}\right)}$$

Where:

- s_i is the slope value of each pixel within the buffer.
- $\bar{s}$ is the mean slope value of all pixels within the buffer.
- n is the number of pixels within the buffer.

TRI is a reliable measure of topographic complexity (Sappington et al., 2007), and is expressed in degrees (°), quantifying the mean angular difference in elevation between a

central pixel and its surrounding cells. It captures the intricate details of terrain features, which can affect habitat suitability and species distribution (Santos et al., 2016b).

The proximity to water bodies was measured to assess the influence of the Sabor River and the reservoir on passerine community patterns. For point counts performed before the dam's filling phase (2013–2014), the distance to the Sabor River was calculated, while for those recorded after the filling phase (2015–2016), the distance to the newly formed reservoir was measured. These distances were calculated using the Euclidean distance in meters.

Microclimatic variables, including monthly precipitation and temperature, were extracted from raster datasets produced for the study area at 1km resolution (Fonseca et al., 2019). These datasets were derived using a methodology that incorporates daily precipitation totals at 20 km resolution (Fonseca et al., 2019) and daily average temperatures at 25 km resolution (Fonseca et al., 2019) for Portugal. Daily precipitation and temperature values were linearly interpolated (in latitude and longitude coordinates) to a 1 km resolution for mainland Portugal (Fonseca et al., 2019).

To obtain average values within the 500 m buffer zones around passerine point-counts, a spatial intersection was performed in QGIS. Specifically, the 'intersect' tool was used separately for temperature and precipitation. For each variable, the tool identified all raster cells (representing either temperature or precipitation values) that fell within each buffer. The resulting intersected data were then exported to Excel, where the 'AVERAGE' function was applied to calculate the mean temperature and precipitation values for each buffer zone separately. Precipitation was measured in millimetres (mm), while temperature was recorded in degrees Celsius (°C).

All data analysis were performed in QGIS (QGIS Development Team (2024).

1.2.4. Statistical analysis

The StDM/ABM interface was preceded by a statistical procedure, for parameter estimation, to test for relationships between dependent and independent variables (Santos and Cabral, 2004). The dependent variables correspond to total passerine species richness and abundance of individuals per study unit, also discriminated by functional groups (i.e. species richness and abundance of grassland, shrubland, woodland passerine birds) (Figure 2). The independent variables were derived from geospatial, environmental, and climatic data, including LU categories, topographic features, and proximity to water bodies (Table 1).

In order to avoid multicollinearity, the selected 16 predictors (habitat classes; Table 1) were tested for pairwise correlation using Spearman’s rho correlation coefficient and only predictors with correlation lower than 0.7 (Elith et al., 2006; Wisz and Guisan, 2009) and Generalized

Variance Inflation Factor lower than 5 were considered (Neter et al., 1996). Rather than a single best model, we fitted a set of competing models and applied Multi-Model Inference (Burnham and Anderson, 2002) to assess how well each model was supported by the data. We used a particular implementation of the Akaike information criterion for small sample sizes (AIC_C; Shono, 2000), as recommended when the ratio between n (the number of observations used to fit the model) and K (the number of parameters in the largest model) is less than 40 (Shono, 2000; Burnham and Anderson, 2002). To overcome dependence on sample size and allow comparability among models, we calculated the AIC_C difference ($Di = AIC_{C\ initial} - AICc_{minimum}$) for each candidate model to rank the candidate models (Burnham and Anderson, 2002). We applied data dredge statistics (dredge – MuMIn R package) to run Generalized Linear Models with all (valid) combinations of environmental predictors, and different variance distributions based on the nature of the response variables. For count data such as species richness and abundance of grassland and shrubland species, a Poisson variance distribution with a log link function was applied. In cases of over-dispersed count data, specifically total species richness, total abundance, woodland species richness and woodland abundance, negative binomial GLMs were used (O'Hara et al., 2010). We selected all the models with $Di < 2$ as recommended by Burnham and Anderson (2002), and finally we calculated the averaging model to incorporate in the StDM. All statistical analyses were conducted in R software using several specialized packages: "*glmtoolbox*" for generalized linear model diagnostics and validation, "*MASS*" for fitting negative binomial models to handle over-dispersed count data, "*MuMIn*" for multi-model inference and model averaging procedures, and "*regclass*" for assessing multicollinearity through variance inflation factors (R Core Team, 2024).

1.2.5. Conceptualization and implementation of the Agent-Based Model (ABM):

In a holistic perspective, the partial regression coefficients obtained in the previous statistical analysis represent the global influence of the selected environmental variables that are proxies of complex ecological processes in each study unit (Santos and Cabral, 2004). Their potential influence was considered in the ABM simulations by explicitly incorporating the respective algorithms into the model. The spatial resolution of the model was standardized to a grid of 1 km² UTM cells, compatible with the study unit dimension, resulting in a total of 1089 patches covering the study area (Figure 4). The temporal resolution was the month in coherence with passerine surveys periodicity.

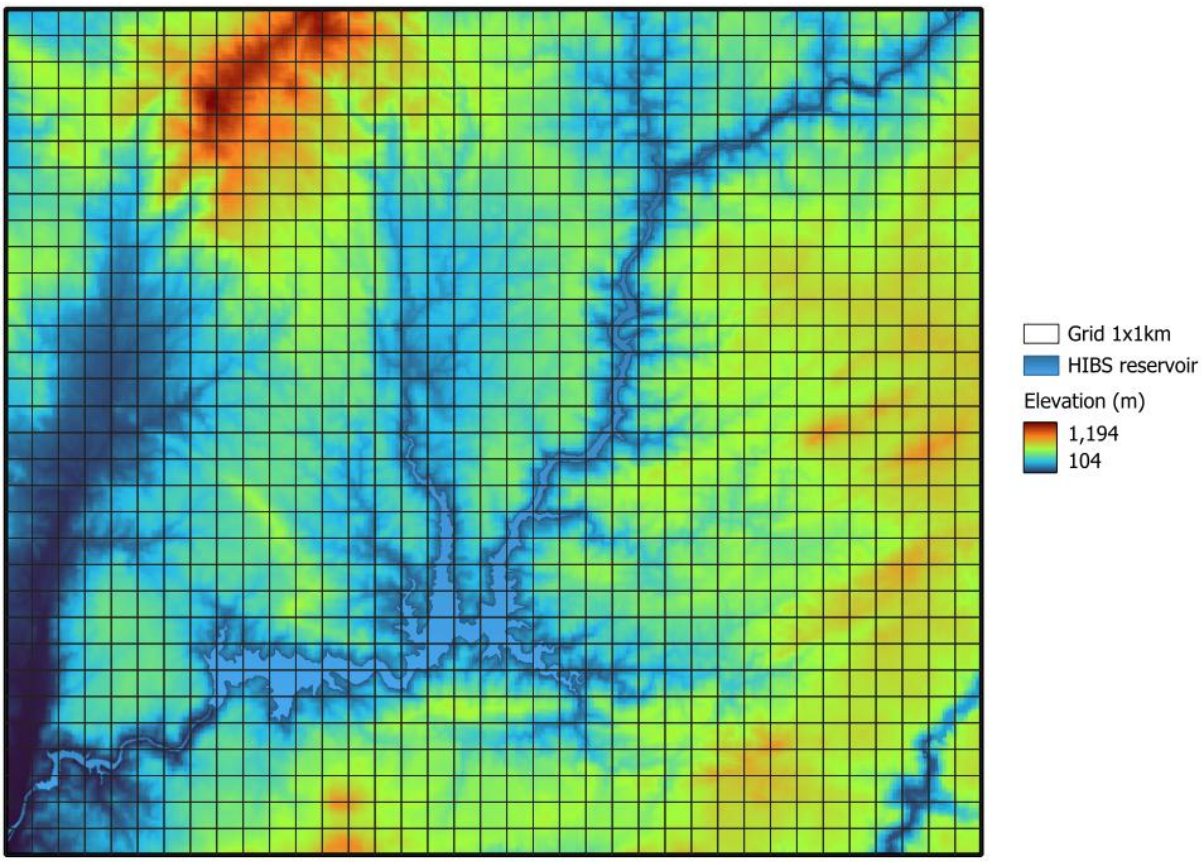

Figure 4 - Grid of 1x1km UTM cells superimposed to the study area.

The model was prepared to import spatial environmental data layers (i.e. LU, topographic features and microclimatic data) in order to predict passerine community responses to the HIBS implementation. For this, LU data before the dam filling phase (2013, 2014) was based on COS2010 and after the dam filling phase from COS 2015 (2015, 2016), assuming that those were the most representative LU patterns before and after the dam implementation. Microclimatic variables, such as temperature and precipitation, assumed monthly variability. Topographic maps were used to incorporate elevation and slope rugosity characteristics. For each simulation, the corresponding LU maps, topographic characteristics and monthly climatic data were imported and processed, ensuring temporal and spatial variability throughout simulations (Appendix III-a). This approach allowed the model to capture the dynamic interactions between environmental conditions and passerine community responses over space and time.

Each patch in the model was characterized by its dominant LU, topographic characteristics, and distance to water. The model was designed to import and process spatial data from shapefiles (using the *GIS extension*), representing LU and microclimatic variables. Monthly temperature and precipitation data were dynamically loaded using procedures that construct

file paths based on the selected month and year (Appendix III-a). Additionally, the Sabor river and reservoir layers were incorporated into the model for visualization of water distance. The Sabor river shapefile was used for simulations before the filling phase, while the reservoir shapefile was used for simulations after the filling phase.

The spatial extent of the model was defined using `*gis:set-world-envelope*`, ensuring all layers aligned within the same coordinate system (Appendix III-c). Each patch in the model was assigned with values from the imported shapefiles using `*gis:apply-coverage*` (Appendix III-c).

The calculation of passerine responses was based on the coefficients derived from prior statistical analysis to predict response variables based on environmental variables (Appendix III-d). The formula for the prediction was expressed as:

$$\text{log\_prediction} = \text{intercept} + \sum(\text{coefficient} \times \text{variable})$$

where the prediction was transformed back to the original scale using the exponential function (`*exp*`) and rounded to ensure non-negative values (Appendix III-d). The model included checks to handle missing or invalid data, ensuring all patches have valid values (Appendix III-d).

Visualization is a key component of the model, with several procedures designed to display the spatial configuration of environmental and response variables. The `*dominant_variable*` procedure assigned colours to patches based on the dominant land use type, while the `update-visuals` procedure discriminated species richness using a colour gradient based on natural breaks imported from a CSV file (Appendix III-e & f). For the prediction maps, patches were coloured from light to dark red, representing increasing richness. Additional features, such as water sources, the Sabor River, and the reservoir, were overlaid on the map using transparent or solid colours for better interpretation (Appendix II; Appendix III-g).

The model also included functionality to export data and visualizations. The `*export-data-for-metrics-year*` procedure allowed to save response variables values from each patch to a CSV file (further used for landscape metrics calculation), while the `*export-maps*` procedure enabled visualization as a PNG image. Dynamic updates of microclimate data and recalculations of response variables were handled through the `*refresh-climate-data*` procedure (Appendix III-h).

The model was initialized using the `setup` procedure, which loaded all datasets, estimated response variables and allowed to visualize the results. Iterative updates were performed

through the `*go*` procedure, which recalculated the response and updated visualizations at each step (Appendix II).

The model was developed using the software NetLogo 6.4.0. (Wilensky, 1999). Full details on model conceptualization and assumptions are displayed in Appendix II, according to the overview, design concepts, and details (ODD) protocol (Grimm et al. 2010).

1.2.6 Visual inspection and quantitative assessment of passerine community responses to the HIBS implementation

The results of the StDM/ABM framework were used to evaluate the spatial and temporal trends of passerine community responses to the HIBS implementation. For visual inspection of the results, spatially explicit maps of total species richness and total abundance, including discriminated by functional group, were produced for each month (March to July) throughout the study period (2013–2016). To enhance the interpretability of spatial patterns, the Jenks natural breaks optimization method (Jenks, 1967) was applied to the predicted range of values (i.e. total species richness and abundance). This method objectively partitions the data into classes that reflect natural groupings within the distribution, minimizing within-class variance and maximizing between-class differences. Based on this approach, five categories were defined for both response variables (i.e. passerine total species richness and abundance): “very low”, “low”, “medium”, “high”, and “very high”.

For the quantitative assessment of passerine community responses to the HIBS implementation, landscape metrics were applied. Although landscape metrics are commonly used to quantify changes in spatial heterogeneity, connectivity, and fragmentation of the physical landscape, in this work landscape metrics were applied to quantify changes in spatial-temporal distribution patterns of passerine response to the HIBS implementation. Three metrics were tested in this scope: Shannon’s Diversity Index (SHDI), Patch Cohesion Index (CI), and Division Index (DI).

SHDI is a measure of landscape diversity that quantifies the relative abundance and evenness of different patch types (in this case expressed by classes of total species richness and abundance of individuals) within the landscape (McGarigal et al., 2002). It is adapted from the Shannon entropy concept in information theory and ecology.

$$SHDI = -\sum_{i=1}^{m} p_i \ln(p_i)$$

where:

- *m* = number of patch types (classes)
- *Pi* = proportion of the landscape occupied by patch type *i*
- ln(pi): The natural logarithm of *Pi*

Since higher SHDI indicates a more diverse and heterogeneous landscape, in this study higher SHDI reflects greater variety and more even distribution of species richness/abundance classes (McGarigal et al., 2002).

The Patch Cohesion Index (CI) quantifies the physical connectedness of patches of the same class across the landscape (McGarigal et al., 2002). It measures the degree to which habitat patches are physically connected, thus reflecting landscape connectivity.

$$CI = \left[1 - \sum_{i=1}^{m} \left(\frac{P_{ij}}{\sum_{i=1}^{m} P_{ij}}\right)\right] \times \left[1 - \frac{1}{\sqrt{A}}\right]^{-1} \times 100$$

where:

- *Pij* = perimeter of patch *j* of class *i*
- *m* = number of patch types
- A = total landscape area (in cells or hectares)

Higher CI value indicates greater connectivity among patches of the same class (McGarigal et al., 2002). In this study, it reveals greater spatial connectivity within passerine community classes.

The Division Index (DI) measures the probability that two randomly chosen points in the landscape are not situated in the same patch (Jaeger, 2000). It is a robust indicator of landscape fragmentation.

$$DI = 1 - \sum_{j=1}^{n} \left(\frac{a_{ij}}{A}\right)^2$$

where:

- *aij* = area of patch *j* of class *i*
- *n* = total number of patches
- *A* = total landscape area

Higher DI value indicates more fragmented landscapes, with many small, isolated patches. In this study, it reveals greater fragmentation and isolation among passerine community classes.

Landscape metrics were therefore used to address two main questions: (1) Do passerine total species richness and abundance vary significantly among months within the same breeding season? (2) Do passerine species richness and abundance vary significantly among years across the study period? For this, intra-annual (monthly) and inter-annual (annual) variations in passerine total species richness and abundance (in terms of Shannon's Diversity Index - SHDI, Patch Cohesion Index - CI), and Division Index - DI) were analysed using box-and-whisker plots generated with the *ggplot2* package in R (R Core Team, 2024). To assess whether significant differences existed among months and years, a non-parametric Kruskal-Wallis (K-W) test was performed. When significant differences were detected, Dunn's post-hoc tests were used for pairwise comparisons ($\alpha = 0.05$; Corder & Foreman, 2014). All landscape metrics and statistical analyses were conducted in R 4.3.1, using the *landscapemetrics, FSA*, and *PMCMRplus* packages (Hesselbarth et al., 2019; R Core Team, 2024).

1.3. Results

Due to the large amount of information produced (i.e. spatial projections of total species richness and abundance of individuals, also discriminated per functional group – grassland, shrubland and woodland species), for demonstrative purposes the results presented in the main body of this thesis were directed to total passerine species richness and abundance. This section therefore includes: 1) the outcomes of statistical analysis (MMI), identifying key environmental predictors of passerine responses to the HIBS implementation; 2) description of passerine spatial-temporal patterns facing the potential influence of the HIBS implementation; 3) comparative analysis of the seasonal and inter-annual patterns of passerine spatial occurrence using landscape metrics as an innovative proposal for ecological response assessments at the community level.

1.3.1. Key environmental predictors of passerine responses to the HIBS implementation

The MMI analysis revealed distinct environmental drivers of species richness. Total species richness was negatively associated with elevation (coefficient = -9.07e-04, $p < 0.001$), slope ruggedness (coefficient = -1.95e-02, $p < 0.001$), and the presence of the reservoir (estimate = -6.24e-07, $p = 0.045$), indicating that topographical complexity and reservoir-related habitat alteration limit overall passerine diversity (Table 2). In contrast, distance to water had a significant positive effect (coefficient = 3.53e-05, $p = 0.001$), suggesting that proximity to water bodies supports higher species richness. Average temperature also showed a negative

association (coefficient = -1.08e-02, p = 0.037), reflecting the sensitivity of passerine communities to changes in microclimatic conditions (Table 2).

Table 2 - The model coefficients for passerine total species richness. The table includes the coefficient estimate (direction and strength of the relationship), standard error (precision of the estimate), adjusted standard error (Adj. SE), z value (test statistic), and p-value (statistical significance: *p<0.05; **p<0.01; ***p<0.001).

Variables	Coefficient	Std. Error	Adj. SE	z value	p-value
(Intercept)	2.646e+00	1.925e-01	1.929e-01	13.715	< 2e-16 ***
reservoir	-6.248e-07	3.113e-07	3.120e-07	2.003	0.045227 *
coniferous_forest	-2.057e-07	1.603e-07	1.605e-07	1.282	0.199967
olives_orchards	2.613e-07	1.753e-07	1.756e-07	1.488	0.136625
average_temperature_buffer	-1.078e-02	5.174e-03	5.185e-03	2.080	0.037547 *
distance_water	3.525e-05	1.070e-05	1.073e-05	3.286	0.001016 **
elevation_pc	-9.077e-04	1.623e-04	1.627e-04	5.579	< 2e-16 ***
rugosity_slope_buffer	-1.945e-02	5.319e-03	5.332e-03	3.648	0.000264 ***
pasture	2.449e-07	6.084e-07	6.092e-07	0.402	0.687733
average_precipitation_buffer	-2.314e-04	5.127e-04	5.133e-04	0.451	0.652152
urban_areas	-2.025e-07	5.867e-07	5.874e-07	0.345	0.730261
temporary_crops	3.909e-08	1.649e-07	1.652e-07	0.237	0.812893
shrublands	2.982e-09	3.508e-08	3.515e-08	0.085	0.932396

For total passerine abundance, abundance was negatively associated with the presence of the reservoir (coefficient = -6.77e-07, p = 0.030), elevation (coefficient = -1.11e-03, p < 0.001), and slope ruggedness (coefficient = -2.46e-02, p < 0.001), indicating that both topographical complexity and reservoir-related habitat alteration reduce overall passerine abundance (Table 3). In contrast, olive orchards (coefficient = 5.53e-07, p = 0.001), average temperature (coefficient = -1.31e-02, p = 0.008), and distance to water (coefficient = 3.72e-05, p = 0.001) emerged as significant predictors, with olive orchards and proximity to water supporting higher abundance, while higher temperatures promoting lower abundances (Table 3).

Statistical outputs of passerine species richness and abundance discriminated by functional groups are provided in supplementary material (Appendix IV in supplementary material).

Table 3 - The model coefficients for passerine total abundance. The table includes the coefficient estimate (direction and strength of the relationship), standard error (precision of the estimate), adjusted standard error (Adj. SE), z value (test statistic), and p-value (statistical significance: *p<0.05; **p<0.01; ***p<0.001).

Variables	Coefficient	Std. Error	Adj. SE	z value	p-value
(Intercept)	3.248e+00	1.834e-01	1.838e-01	17.670	< 2e-16 ***
reservoir	-6.765e-07	3.113e-07	3.120e-07	2.168	0.030146 *
olives_orchards	5.526e-07	1.468e-07	1.471e-07	3.757	0.000172 ***
average_temperature_buffer	-1.307e-02	4.914e-03	4.926e-03	2.652	0.007991 **
distance_water	3.720e-05	1.125e-05	1.128e-05	3.300	0.000969 ***
elevation_pc	-1.114e-03	1.742e-04	1.746e-04	6.378	< 2e-16 ***
rugosity_slope_buffer	-2.463e-02	6.071e-03	6.084e-03	4.048	5.17e-05 ***
temporary_crops	1.636e-07	3.169e-07	3.172e-07	0.516	0.606078
vineyards	-1.806e-07	5.182e-07	5.188e-07	0.348	0.727800
shrublands	2.058e-08	7.537e-08	7.548e-08	0.273	0.785127
pasture	1.048e-07	4.342e-07	4.349e-07	0.241	0.809555
coniferous_forest	-7.701e-09	4.610e-08	4.618e-08	0.167	0.867552
average_precip_buffer	-2.717e-05	2.026e-04	2.030e-04	0.134	0.893528
watersource	-4.376e-08	3.966e-07	3.974e-07	0.110	0.912319
traditional_agricultural_mosaic	2.238e-08	2.545e-07	2.550e-07	0.088	0.930081

1.3.2. Spatial-temporal patterns of passerine responses to the HIBS implementation

The obtained results indicate subtle interannual differences in spatial patterns of both passerine total species richness (Figure 5a) and total abundance (Figure 5b) between 2013 and 2016. Particularly, both species richness and abundance remained relatively elevated in areas that were later transformed by the reservoir, suggesting passerine community stability associated with the reservoir filling phase (Figure 5a, 5b). Furthermore, both species richness and abundance were higher in areas where shrublands, olive orchards, and patches of deciduous forest predominated (see Figure 6a, 6b). In contrast, areas of higher elevations (see Appendix V in supplementary material) and temporary crops (Figure 6a, 6b) consistently exhibited lower values of passerine richness and abundance (Figure 4a, 4b). Additionally, areas where shrublands were associated with coniferous forest (see Figure 6a, 6b) tended to support lower passerine species richness and abundance (Figure 5a, 5b), suggesting that this particular habitat combination may be less suitable for diverse and abundant passerine assemblages.

Seasonally, both richness and abundance peaked in the earlier months (March to May), with a gradual decline towards July (Figure 5a, 5b). This trend was consistent across the study period and was especially pronounced in areas subject to higher temperatures and lower precipitation during the summer (see Figure VI in supplementary material). The spatial overlap between areas of high passerine richness/abundance and regions with more stable or favourable microclimatic conditions (moderate temperatures and higher spring precipitation) was also apparent (Figure 5a, 5b; Appendix VI in supplementary material).

Maps of passerine species richness and abundance discriminated by functional groups are provided in supplementary material (Appendix VII, VIII in supplementary material).

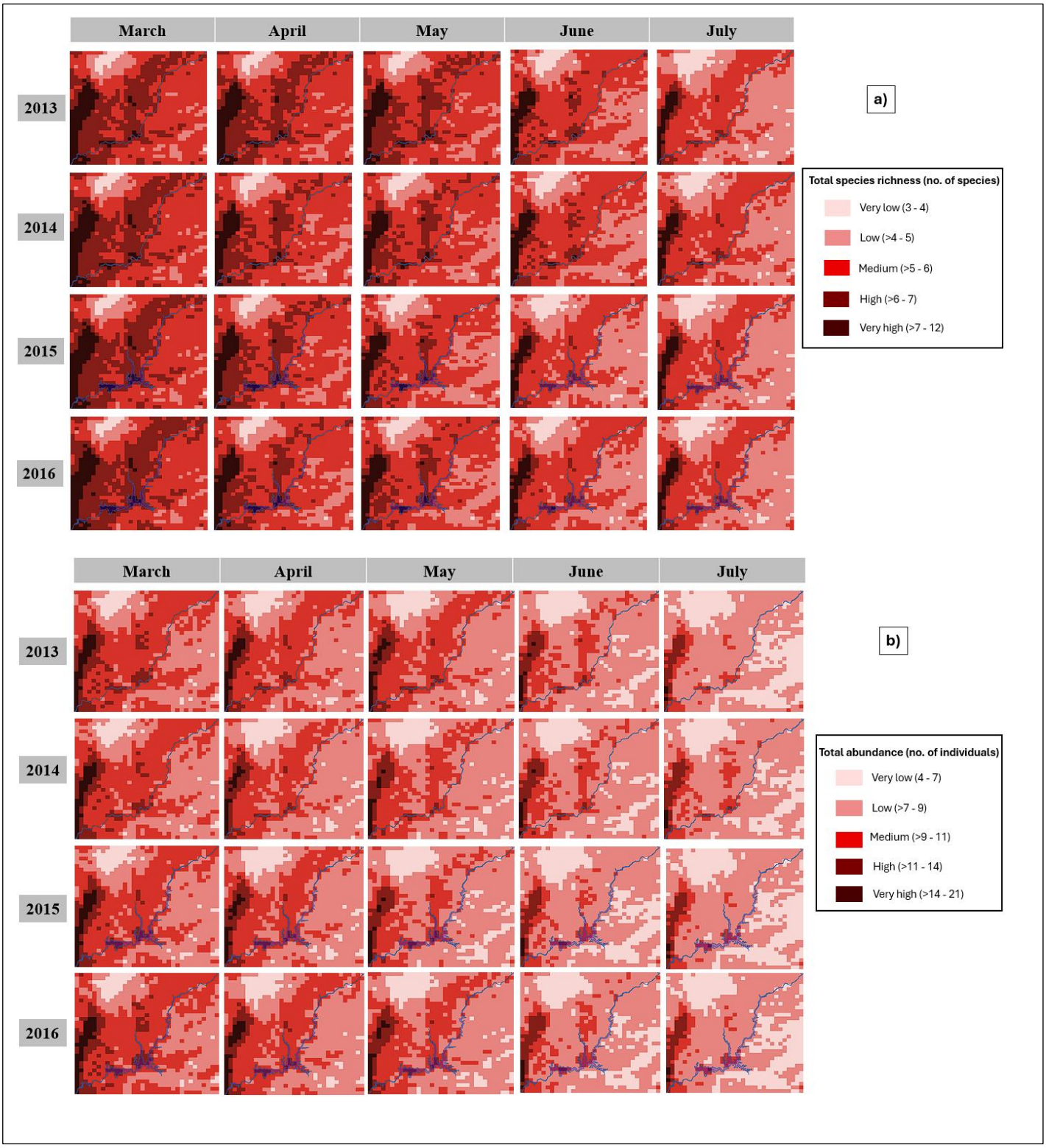

Figure 5 - Spatio-temporal variation in total passerine species richness (a) and total abundance (b), from March to July, between 2013 and 2016.

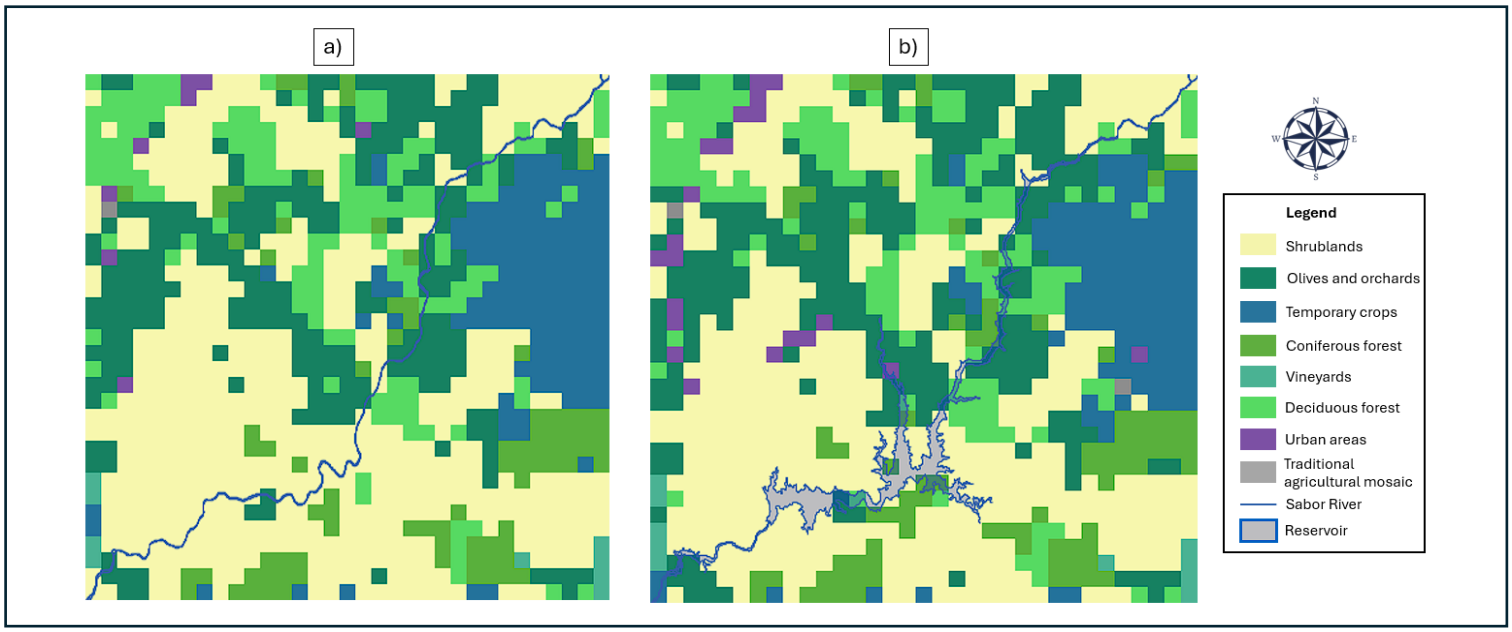

Figure 6 - Spatial configuration of LU and river flooding in the study area (ABM interface visualization): a) before reservoir filing phase; b) after reservoir filing phase.

1.3.3. Interannual landscape metrics applied to passerine community occurrence patterns (2013-2016)

The SHDI values for total species richness (Figure 7a) remained relatively stable throughout the four years, with median values ranging from 1.20 to 1.22 (see Appendix IX-1.1; supplementary material). The interquartile range (IQR) and whiskers indicate moderate variability within each year, with a few outliers presented, reflecting occasional months with slightly higher or lower diversity (Figure 7a). The Kruskal-Wallis (K-W) test ($\chi^2 = 1.71$, df = 3, $p = 0.635$) indicates no statistically significant differences in SHDI among years (Appendix IX-1.1).

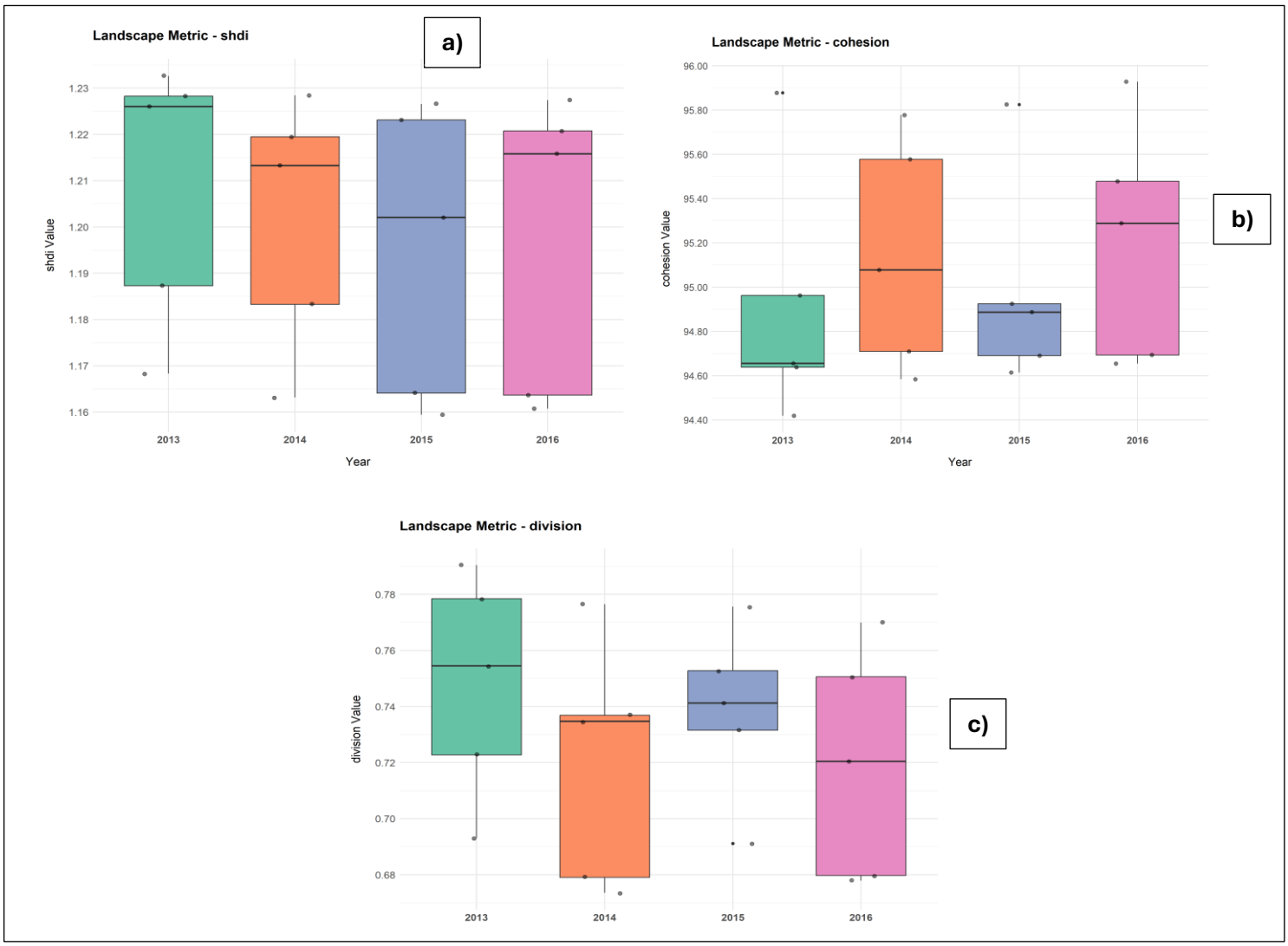

Figure 7 - Box and whisker plots expressing landscape metrics for the interannual variation of passerine species richness between 2013 and 2016: (a) Shannon's Diversity Index (SHDI), (b) Patch Cohesion Index, and (c) Division Index. Box plots represent the median (horizontal line), upper and lower quartiles (box limits), and whiskers indicate the range of values within 1.5 times the interquartile range from the quartiles. Outliers are plotted as individual points.

Cohesion values for species richness (Figure 7b) were consistently high throughout the years (medians ranging from 94.66–95.29), indicating strong connectivity among patches of the same class. The IQRs were moderate, with a few outliers presented. The K-W test ($\chi^2 = 1.33$, df = 3, p = 0.722) indicated no significant differences among years (Appendix IX-1.2).

Division index values (Figure 7c) for species richness were moderate throughout the years (medians ranging from 0.72–0.75) (Appendix IX-1.3). The K-W test ($\chi^2 = 2.63$, df = 3, p = 0.452) confirmed no significant differences among years (Appendix IX-1.3).

For total abundance (Figure 8a), SHDI values ranged approximately from 1.01 to 1.21, with median values between 1.11 and 1.18 among years (Appendix X-1.1). The interquartile ranges (IQRs) were moderate, and several outliers were present each year, indicating occasional months with notably higher or lower diversity in abundance classes (Figure 8a). The K-W test ($\chi^2 = 0.57$, df = 3, p = 0.904) indicated no statistically significant differences in SHDI among years (Appendix X-1.1).

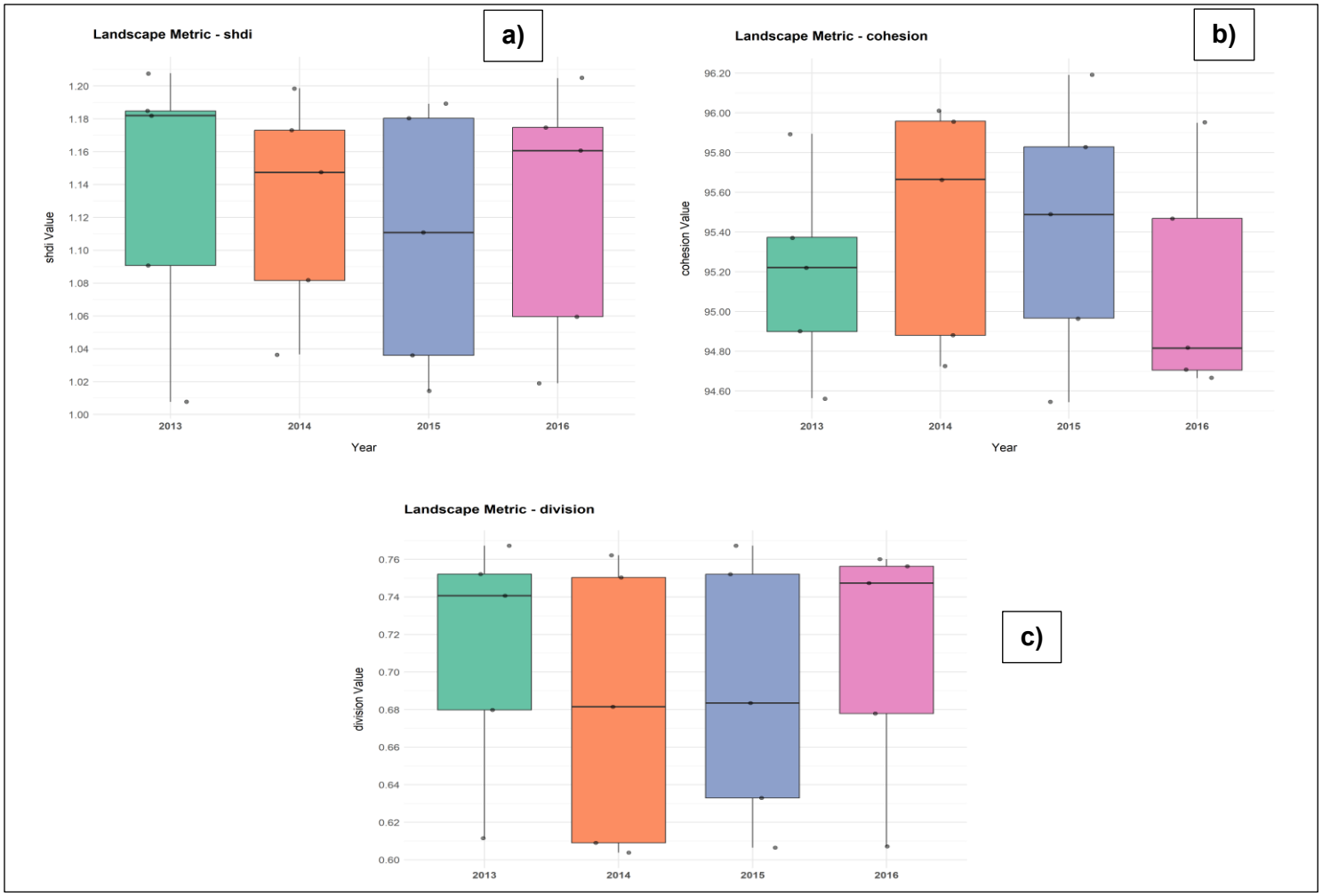

Figure 8 - Box and whisker plots expressing landscape metrics for the interannual variation of passerine total abundance landscape metrics between 2013 and 2016: (a) Shannon's Diversity Index (SHDI), (b) Patch Cohesion Index, and (c) Division Index. Box plots represent the median (horizontal line), upper and lower quartiles (box limits), and whiskers indicate the range of values within 1.5 times the interquartile range from the quartiles. Outliers are plotted as individual points.

Cohesion values for total abundance (Figure 8b) were consistently high throughout the years, with medians ranging from 95.0 to 95.7. The IQRs presented some variations relatively small, and a few outliers were observed (Figure 8b), particularly in 2014 and 2015, reflecting occasional months with slightly lower or higher patch connectivity. The K-W test ($\chi^2 = 1.61$, df = 3, $p = 0.658$) showed no significant interannual differences (Appendix X-1.2).

Division index values for total abundance (Figure 8c) exhibited median values between 0.68 and 0.74 throughout the years, with moderate IQRs and several outliers each year. The K-W test ($\chi^2 = 0.61$, df = 3, $p = 0.894$) indicated no significant differences among years (Appendix X-1.3).

1.3.4. Seasonal passerine occurrence patterns (march-july) expressed by landscape metrics

Seasonal analysis of SHDI for passerine species richness (Figure 9a) revealed a significant decline in passerine occurrence diversity from early spring (March-April) to midsummer (June-July). SHDI values were higher in March (mean = 1.23), remaining relatively stable in April and May (means = 1.22), and dropping markedly in June (mean = 1.17); reaching their lowest in July (mean = 1.16) (Appendix XI-1.1; supplementary material). Variability among years was generally low, except for June, which showed greater interannual variation (Figure 9a). The K-W test confirmed a significant seasonal effect ($\chi^2 = 15.87$, df = 4, p = 0.0032) (Appendix XI-1.1). Post-hoc Dunn's tests indicated that heterogeneity among passerine classes were significantly lower for both June and July compared to March (p.adj = 0.0125 for both comparisons) (Appendix XI-1.1).

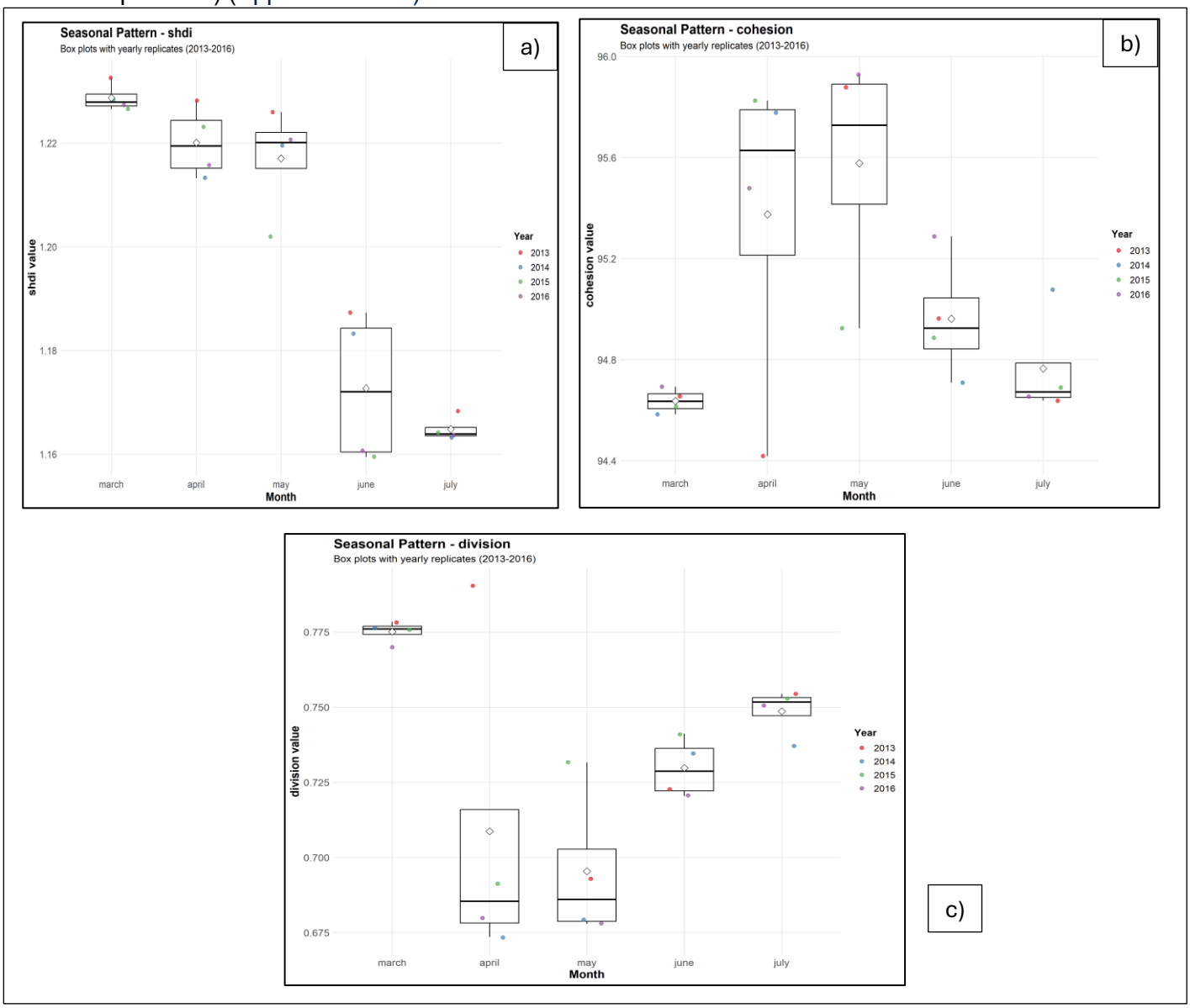

Figure 9 - Seasonal variation in landscape metrics for passerine species richness between March and July: (a) SHDI, (b) CI, and (c) DI. Box plots represent the interquartile range (IQR), with the horizontal line indicating the median and the diamond symbol representing the mean. Whiskers extend to the minimum and maximum values within 1.5×IQR. Individual coloured dots correspond to yearly replicates (red: 2013, blue: 2014, green: 2015, purple: 2016).

CI analysis revealed significant variations in passerine species richness connectivity among months (Figure 9b). CI values were relatively stable and high from March to May (means = 94.6–95.6), indicating strong connectivity among patches of similar species richness. However, a slight decline was observed in June (mean = 95.0) and July (mean = 94.8) (Appendix XI-1.2). The K-W test indicated a significant seasonal effect ($\chi^2 = 9.74$, df = 4, p = 0.045). Post-hoc Dunn's tests showed that cohesion among passerine classes was significantly higher in May compared to March (p.adj = 0.0497) (Appendix XI-1.2).

DI analysis revealed significant variations in passerine species richness fragmentation among months (Figure 9c). DI values were higher in March (mean = 0.775), indicating greater passerine species richness fragmentation in the beginning of the breeding season (March). A marked decrease was observed in April (mean = 0.709) and May (mean = 0.695), followed by a gradual increase in June (mean = 0.730) and July (mean = 0.749) (Appendix XI-1.3). The K-W test confirmed a significant seasonal effect ($\chi^2 = 11.13$, df = 4, p = 0.025). Post-hoc Dunn's tests indicated that fragmentation among passerine classes was significantly lower in May compared to March (p.adj = 0.028) (Appendix XI-1.3).

Seasonal analysis of SHDI for total abundance classes (Figure 10a) revealed the highest values in March (mean = 1.20), followed by a progressive decline through April (mean = 1.18), May (mean = 1.15), and June (mean = 1.07), reaching the lowest values in July (mean = 1.02) (Appendix XII-1.1). The K-W test indicated a significant seasonal effect ($\chi^2 = 17.51$, df = 4, p = 0.0015), and Dunn's post-hoc tests showed that heterogeneity among passerine classes was significantly lower in both June and July compared to March (p.adj = 0.034 and 0.0017, respectively) (Appendix XII-1.1).

For total abundance classes (Figure 10b), the seasonal pattern of CI was more pronounced. CI values increased from March (mean = 95.0) and April (mean = 94.7) up to June (mean = 96.0), further declining in July (mean = 95.5). The K-W test confirmed a significant seasonal effect ($\chi^2 = 11.83$, df = 4, p = 0.019) (Appendix XII-1.2). Dunn's post-hoc tests revealed that cohesion among passerine classes was significantly higher in April compared to June (p.adj = 0.0125), while no other pairwise comparisons were significant after adjustment (Appendix XII-1.2).

A more pronounced seasonal pattern was observed for DI based on total abundance classes (Figure 10c). DI values were highest in April (mean = 0.760), then declined sharply through May (mean = 0.710) and reached their lowest in June (mean = 0.607), before increasing again in July (mean = 0.663) (Appendix XII-1.3). The K-W test indicated a significant seasonal effect ($\chi^2 = 14.07$, df = 4, p = 0.007). Dunn's post-hoc tests showed that fragmentation among

passerine classes was significantly lower in June compared to April (p.adj = 0.0066) (Appendix XII-1.3)

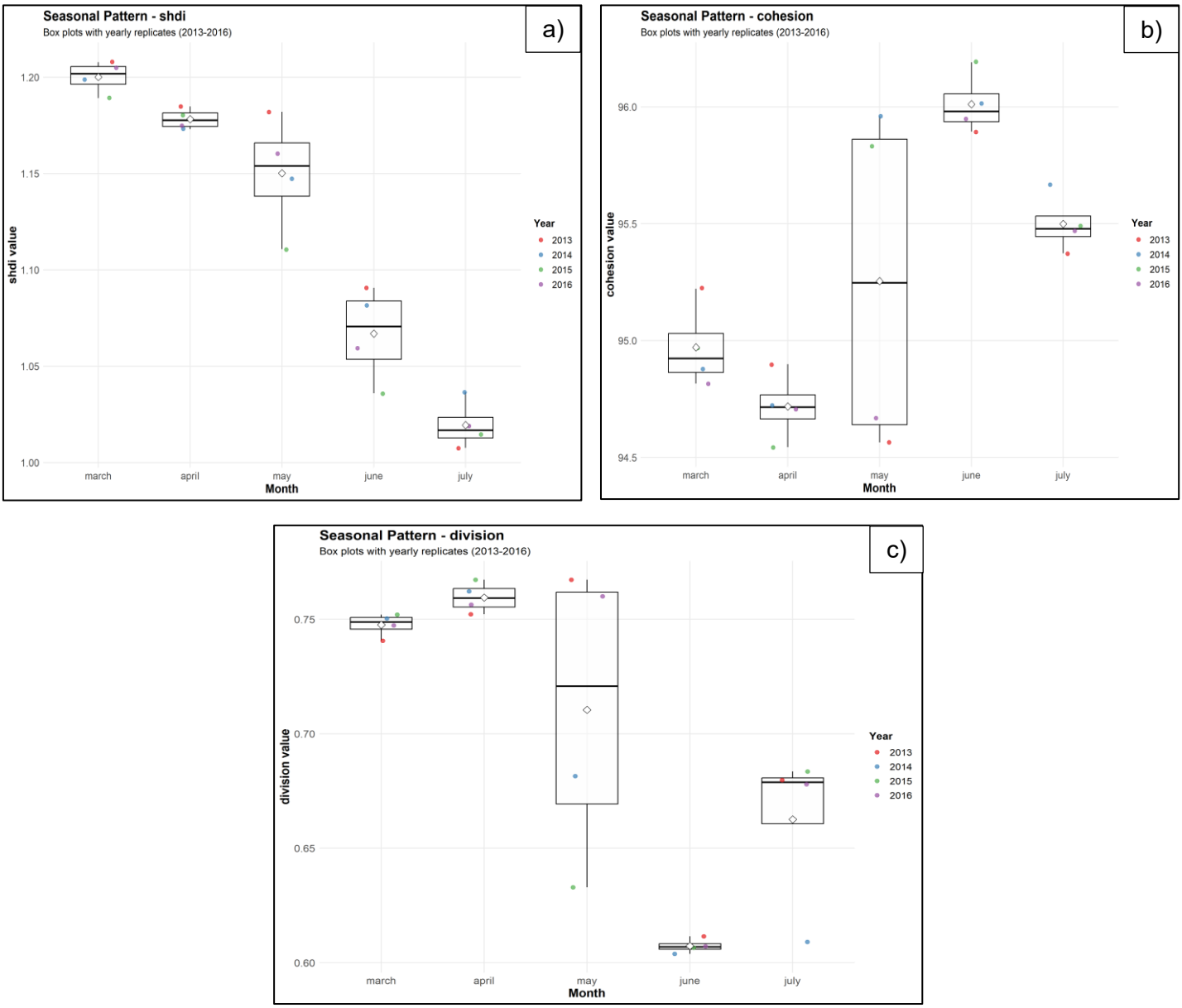

Figure 10 - Seasonal variation in landscape metrics for total abundance between March and July: (a) SHDI, (b) CI, and (c) DI. Box plots represent the interquartile range (IQR), with the horizontal line indicating the median and the diamond symbol representing the mean. Whiskers extend to the minimum and maximum values within 1.5×IQR. Individual coloured dots correspond to yearly replicates (red: 2013, blue: 2014, green: 2015, purple: 2016).

1.4. Discussion

This study aimed to evaluate passerine community responses to the HIBS implementation, focusing on spatial and temporal patterns of species richness and abundance from 2013 to 2016. Key patterns emerged from the analysis, revealing relatively stable spatial patterns of passerine diversity and abundance among the study years (Figures 7 and 8). In particular, higher passerine species richness and abundance were consistently observed in areas less affected by the reservoir (i.e. flooded areas), dominated by shrublands, olive orchards, and deciduous forests (Figure 5). In contrast, pronounced seasonal dynamics were evident, with diversity peaking in early spring and declining towards midsummer, accompanied by distinct changes in landscape metrics applied to passerine community patterns. Notably, the SHDI decreased significantly from March to July for species richness classes (Figure 9a), reflecting reduced variety and evenness in species richness distribution, while a similar declining trend was observed for abundance classes from March to July (Figure 10a). Concurrently, the CI showed a slight peak in May before declining in June and July (Figures 9b and 10b), indicating varying connectivity among patches of similar richness or abundance over the breeding season. Overall, these findings suggest that while short-term landscape alterations associated with the HIBS may not immediately disrupt overall community diversity, intra-annual ecological processes (i.e. phenology) and habitat associations (i.e., preference for shrublands and olive orchards) play a critical role in shaping passerine diversity in this Mediterranean ecosystem.

1.4.1. Spatial-temporal patterns of passerine responses to the HIBS implementation

According to the obtained results, areas dominated by olive orchards and shrublands consistently supported higher passerine richness and abundance in the Baixo Sabor region. This pattern mirrors findings from other Mediterranean landscapes, where habitat heterogeneity enhances avian diversity by offering a mosaic of resources, including nesting sites, foraging opportunities, and shelter (Mulatu et al., 2016; Santos et al., 2016b; Bouvier et al., 2020; Morgado et al., 2020; Santos et al., 2022). Structurally diverse agricultural landscapes, particularly those with traditional agroecosystems, not only promote higher biodiversity compared to monocultures or fragmented habitats but also foster ecological interactions vital for maintaining bird communities (Railsback & Johnson, 2014; Olimpi et al., 2022).

The consistently high passerine richness and abundance in structurally heterogeneous habitats, as evidenced by stable spatial patterns in shrublands and olive orchards after the HIBS implementation (Figure 5), suggest that preserving a variety of LU categories is critical for supporting bird communities subjected to landscape changes. This aligns with evidence that edge effects and fragmentation, triggered by human development, reduce avian species

richness (Reino et al., 2009), whereas heterogeneous agricultural landscapes provide essential resources that sustain passerine diversity under infrastructural pressures (Moreira et al., 2012). This diversity of habitats likely helps birds adapting to alterations by providing different feeding sources and safe areas to live (Reino et al., 2009; Moreira et al., 2012), which is particularly important in the context of the Baixo Sabor region where traditional farming practices exist alongside with modern infrastructural developments (Beja & Cabral, 2012; Santos et al., 2019a,b; Fonseca & Santos, 2023).

In contrast, topographic complexity, particularly in higher elevation zones with rugged slopes, was significantly associated with lower passerine diversity and abundance in the Baixo Sabor region. This is evidenced by strong negative relationships with elevation and slope ruggedness in our models (Tables 2 and 3). This pattern aligns with findings from Mediterranean and mountainous landscapes, where topographic complexity often constrains bird diversity by limiting habitat accessibility and resource distribution, such as nesting sites or insect prey availability (Carrascal et al., 2012; Katuwal et al., 2016). In the context of HIBS implementation, our spatial analyses (Figure 5; Appendix V) indicate that areas at higher elevation and rugged terrain, often distant from the reservoir, consistently supported lower passerine diversity and abundance, suggesting that topographic constraints naturally shape passerine distribution patterns across the Sabor region.

For microclimate gradients, warmer areas and those with lower precipitation were often associated with reduced passerine diversity and abundance during the breeding season (see Tables 2 and 3; Appendix VI in supplementary material). This pattern resonates with research highlighting the sensitivity of passerines to thermal stress and water availability constraints in Mediterranean climates (Carrascal et al., 2012), where temperature extremes and reduced moisture can influence foraging efficiency and reproductive success (Zuckerberg et al., 2018; Herrando et al., 2019; Tirozzi et al., 2024). This observation suggests that microclimatic variability plays a pivotal role in shaping habitat suitability for passerines, especially during critical life stages such as breeding when energy demands are likely elevated due to reproductive activities (Salaberría et al., 2013; Zuckerberg et al., 2018; Tirozzi et al., 2024).

Additionally, the presence of the HIBS may contribute to changes in microclimatic conditions, and while temperature gradients, precipitation patterns, and landscape fragmentation affect bird communities, their combined influence on stress levels remains to be fully explored (Bastos et al., 2015; Zuckerberg et al., 2018; Herrando et al., 2019). Warmer and drier conditions in open or fragmented areas could potentially limit access to shaded refugia or abundant insect prey, though this requires further investigation (Zuckerberg et al., 2018; Herrando et al., 2019). Moreover, the pronounced seasonal decline in passerine occurrence

patterns from early spring to midsummer, as observed in the study (Figures 10a and 11a), points to the temporal dimension of microclimatic influence, where harsher summer conditions—characterized by higher temperatures and lower precipitation—likely exacerbate resource scarcity (Salaberría et al., 2013; Zuckerberg et al., 2018; Herrando et al., 2019). Given the projected increases in temperature extremes and potential shifts in precipitation patterns under climate change in Mediterranean regions, these findings highlight the need to consider microclimatic regulation—through the preservation of shaded habitats or vegetation cover that retains moisture—as a key strategy for supporting passerine persistence in dam-impacted areas (Salaberría et al., 2013; Herrando et al., 2019).

Regarding the influence of river flooding, our findings indicate a significant negative association between proximity to the HIBS reservoir and passerine diversity and total abundance, with areas farther from the reservoir exhibiting higher species richness and abundance (Tables 2 & 3). Visual inspection of the patterns obtained further reveal that higher passerine diversity and abundance often correspond to shrubland and agricultural landscapes, such as olive orchards and mixed forests, located at greater distances from the reservoir (Figure 5). This pattern aligns with research suggesting that terrestrial passerines favour habitats distant from aquatic or edge environments created by dam reservoirs (Reino et al., 2009; Nasruddin-Roshidi et al., 2021). Near the reservoir, the observed reduction in species richness and abundance (see Table 2 & 3) is likely associated with habitat loss due to flooding and urbanization, which alter vegetation cover (e.g. loss of riparian gallery), potentially impacting nesting opportunities for shrub-dependent and/or ground-nesting species (Moreira et al., 2012; Nasruddin-Roshidi et al., 2021). However, interannual stability in the broader spatial organization of passerine community patterns from 2013 to 2016 (Figures 9 and 10), suggests that the localized effects near the reservoir did not immediately translate into detectable declines across the entire study area within such short timeframe. In fact, the combined effects of habitat fragmentation, microclimatic shifts, and flooding create cumulative stressors that challenge passerine resilience over long timeframes (Pearce-Higgins et al., 2015; Abreu et al., 2020; Fonseca & Santos, 2021). These stressors disproportionately affect passerines due to their sensitivity to environmental changes (Abreu et al., 2020; Nasruddin-Roshidi et al., 2021), small body size, and dependence on specific habitat mosaics (Moreira et al., 2012), potentially leading to declines in species richness and abundance over time (Beja et al., 2013; Nasruddin-Roshidi et al., 2021). In the Mediterranean context, where climatic variability and anthropogenic pressures are already pronounced (Santos et al., 2019b; Srinivasan et al., 2019), these impacts are amplified (Fonseca & Santos, 2021), exacerbating the vulnerability of passerine communities to further ecological disruptions (Srinivasan et al.,

2019; Abreu et al., 2020). Nonetheless, future studies should explore long-term ecological adjustments to confirm these trends.

In summary, the combined influence of landscape composition, topography, microclimatic gradients, and reservoir presence highlights the multifaceted environmental dynamics shaping passerine community patterns in the Baixo Sabor region. These factors collectively illustrate the complexity of maintaining avian assemblages in dam-impacted Mediterranean ecosystems, where habitat diversity and microclimatic moderation emerge as pivotal elements for ecological resilience (Abreu et al., 2020; Nasruddin-Roshidi et al., 2021). Addressing these influences through integrated conservation approaches could help balance the ecological trade-offs of large-scale infrastructure with the imperatives of biodiversity conservation, both at local and global levels (Moreira et al., 2012; Santos et al., 2016b; Nasruddin-Roshidi et al., 2021).

1.4.2. Seasonal Versus Inter-Annual passerine occurrence patterns: landscape metrics analysis

This study introduces a novel approach by applying landscape metrics—SHDI, CI, DI—to quantify the spatial organization of passerine community responses (species richness and abundance) to the HIBS implementation. This methodological innovation, supported by the StDM/ABM framework, enables the examination of passerine community patterns, revealing distinct inter-annual and seasonal trends (Figures 7-10). Specifically, inter-annual analysis reveals a general stability in passerine community patterns across the study period (2013–2016). SHDI, which measures the diversity and evenness of species richness and abundance classes across the landscape, remained consistent over the years. Similarly, the CI, indicating how well areas with similar passerine presence are linked spatially, showed consistently high values across years, while the DI, reflecting fragmentation among these classes, exhibited moderate levels (Figures 7 and 8). Taken all together, these findings suggest stable spatial distribution patterns of passerine diversity and abundance over time, potentially indicating resilience or limited impact from HIBS-related changes during the study period. In fact, other studies suggest that bird assemblages can remain stable under changing conditions, especially when habitat connectivity is maintained (Benton et al., 2003; Abreu et al., 2020).

In contrast, seasonal dynamics were pronounced, with SHDI for both species richness and abundance declining from early spring (March) to midsummer (July), alongside shifts in CI and DI, suggesting increasing homogeneity and varying connectivity in the spatial distribution of passerine species richness and abundance classes across the landscape as the breeding season progressed (see Figures 9 and 10). Notably, CI often peaked in mid-season, reflecting potential aggregation during breeding, while DI indicated reduced fragmentation between

classes of passerine occurrence in late spring. These seasonal patterns correspond with phenological cycles of passerines in Mediterranean ecosystems, where breeding activity and resource availability peak in spring and decline under harsher summer conditions, as reflected by increasing temperatures and decreasing precipitation (Appendix VI; Moreira et al., 2005; Carrascal et al., 2012). The spatial overlap of high species richness and abundance with moderate microclimatic conditions in spring (Figure 5, Appendix VI) further supports this interpretation, emphasizing the role of temperature and precipitation in shaping passerine community distribution.

The stronger effect of seasonal over inter-annual patterns, as captured by landscape metrics applied to passerine community responses, underscores that, short-term ecological fluctuations—particularly triggered by microclimatic and phenological conditions—, had greater influence in passerine community structure than immediate HIBS-related landscape changes within the 2013-2016 timeframe (Pearce-Higgins et al., 2015). This finding has critical implications for understanding dam impacts in the Baixo Sabor SPA. The inter-annual stability suggests that the initial phases of HIBS implementation did not disrupt overall spatial organization of passerine community responses across the landscape, potentially due to the buffering capacity of heterogeneous habitats distant from the reservoir (Figure 6). While the four-year timeframe (2013-2016) of this study captures initial passerine responses to the HIBS implementation, it also highlights the necessity of long-term monitoring beyond this period to detect possible lagged responses to habitat loss or fragmentation, as ecological adjustments may unfold over decades (Nasruddin-Roshidi et al., 2021). In seasonal terms, the marked declines in diversity and shifts in connectivity of passerine species richness and abundance classes, as categorized by spatial distribution patterns, indicate that management interventions, such as habitat restoration and/or mitigation measures, should be prioritized during early spring (March-May) to support breeding success and maintain community aggregation in key habitats. Integrating these temporal insights into frameworks like the Long-Term Ecological Research (LTER) can enhance adaptive conservation strategies, ensuring that renewable energy development aligns with avian biodiversity protection in Mediterranean regions impacted by these infrastructures.

1.4.3. Strengths, Limitations, and Methodological Advances

This study introduces a novel approach by applying landscape metrics to assess passerine community patterns, offering a perspective on the spatial organization of biological communities' response to environmental/anthropogenic change. This methodological innovation provides a community-level lens to impact assessments, distinguishing it from conventional landscape ecology applications, which typically use these metrics to quantify spatial patterns of physical landscape features (McGarigal et al., 2002). By shifting the focus

to the spatial configuration of biological responses, this approach provides a novel perspective on the patterns of ecological impacts, describing how passerine diversity and abundance are distributed and connected across the Baixo Sabor region in response to dam-induced changes, providing a complementary tool for evaluating biodiversity responses in altered ecosystems. Additionally, the integration of StDM with ABM enables spatially explicit predictions of passerine community patterns (Bastos et al., 2012; Santos et al., 2013), allowing for the visualization of ecological trends across space and time. This combined framework captures multi-scale interactions, from local habitat features to broader landscape patterns, strengthening the robustness of the analysis (Bastos et al., 2015). A key strength of this approach lies in its potential to predict future ecological outcomes under realistic socio-ecological scenarios, such as projected land use changes or microclimatic shifts, thereby supporting long-term conservation planning (Topping et al., 2013). The StDM/ABM framework is also adaptable to other ecosystems and species affected by environmental gradients, demonstrating its versatility for broader impact assessments (Cabral et al., 2008). Moreover, it can serve as a multi-scale modelling tool to guide strategic monitoring and mitigate cumulative impacts on biodiversity, while offering credible projections for decision-makers and environmental managers (Brotons et al., 2007; Roscioni et al., 2013). In fact, when compared to alternative modelling methodologies, this hybrid approach is adjustable in relation to the local management requirements (objectives and parameters) and capable of responding with flexibility to more specific contexts. Although widely applied in predicting species distributions under global change scenarios, the deterministic assumptions of Species Distribution Models (SDMs) limit the accuracy in capturing ecological responses under scenarios of more local changes. Therefore, this proposal also provides a useful synergistic contribution in this scope, allowing the precise improvement of subsequent hybrid multi-scale approaches where both model paradigms, correlative and dynamic models, will result in promising future outcomes, combining holistic landscape composition trends with the species occurrence dynamics at a local level, namely by the integration of techniques such as remote-sensing based predictors, statistical inference, stochastic-dynamic simulations and spatial projections in a common and interactive approach (Bastos et al. 2018).

Despite these strengths, limitations exist, notably the short study timeframe of four years (2013-2016), which may constrain the detection of long-term ecological shifts following the HIBS implementation. Passerine responses to large-scale infrastructure may manifest over extended periods (Bastos et al., 2015). Therefore, predictive modelling tools, such as those integrated within spatio-temporal distribution models, can be employed to simulate potential future changes in the Sabor region over a long-term perspective. Furthermore, this study did not include a formal validation process, where model predictions are compared against

independent observed data to assess accuracy, as is often recommended to ensure the reliability of predictive ecological models (Santos & Cabral, 2004). Future work should address this by incorporating independent datasets or extended monitoring to test the model's predictive performance. Future research should also build on this foundation by extending temporal coverage, training the algorithm with more data to achieve more accurate future predictions, and incorporating additional ecological variables, such as prey availability or interspecific interactions, to refine the predictive capacity of the StDM/ABM framework.

1.4.4. Management applications within network frameworks

The insights from this study offer practical applications for managing avian biodiversity within monitoring and conservation frameworks such as the LTER and PIMA associated with the HIBS (e.g., EDP, 2015; eLTER, 2019). The persistence of passerine diversity in heterogeneous landscapes suggests that conservation efforts should prioritize the preservation of diverse habitats to buffer against infrastructure-related impacts (Bastos et al., 2015; Santos et al., 2016b). Management strategies could integrate these findings by enhancing habitat connectivity and protecting key refugia within the Baixo Sabor SPA.

Furthermore, the pronounced seasonal dynamics indicate that management activities, such as habitat restoration or infrastructure maintenance, should be timed to minimize disturbance during the critical breeding period in early spring (Zuckerberg et al., 2018). Aligning such actions with the LTER and PIMA frameworks can ensure sustained monitoring of avian responses to the HIBS, supporting adaptive management that balances renewable energy development with biodiversity conservation in Mediterranean ecosystems (Nasruddin-Roshidi et al., 2021). These applications underscore the value of long-term ecological data in informing evidence-based strategies for avifauna conservation in dam-impacted regions (Bastos et al., 2015; Santos et al., 2016b).

Chapter 2: Long-term effects of river flooding at upper-trophic levels: A BACI approach applied to metrics of cliff-nesting raptors population dynamics[1]

[1] The content of this chapter is based on a manuscript currently under review in Global Ecology and Conservation, entitled "Long-Term Effects of Hydropower Development on Cliff-Nesting Raptors in a Mediterranean Landscape" (*Bastos, R., Seck, C., Travassos, P., Carvalho, D., Gomes, C., Palma, L., Vicente, J.R., Honrado, J.P., Santos, M., Cabral, J.A., & Beja, P.*).

2.1. Introduction

As global energy demand continues to rise, hydropower has become a cornerstone of sustainable energy strategies, providing a renewable source that contributes for reductions in greenhouse gas emissions (International Energy Agency, 2021). However, despite its potential for clean energy generation, the ecological impacts of hydropower on terrestrial wildlife are often underestimated or overlooked (Fearnside, 2016; Nasruddin-Roshidi et al., 2021; Amorim et al., 2022). While environmental impact assessments and monitoring are typically required for new hydropower developments, these studies are often short-term, making it difficult to capture long-term effects on ecosystems and wildlife populations. Understanding these long-term impacts is particularly crucial when hydropower projects intersect with protected areas and species of high conservation concern, including rare, endangered, and/or priority species (Sánchez-Zapata et al., 2016).

Cliff-nesting raptors are among the species potentially vulnerable to hydropower developments, as their habitats can be greatly modified by dam construction and the subsequent flooding of river valleys (Sánchez-Zapata et al., 2016). These changes can lead to the loss and degradation of raptors' breeding and foraging grounds, causing a decrease in local population sizes as well a decline in breeding success and productivity. Previous studies support these concerns, showing that: (1) the inundation of breeding sites often results in nest abandonment and displacement of individuals, leading to breeding failure (Kajtoch & Figarski, 2013; Mateo-Tomás et al.,, 2010b); (2) increased human presence near nesting areas alters parental investment strategies, reducing breeding performance (Zuberogoitia et al., 2008, 2014; Morant et al., 2018); (3) the disruption of riverine food webs due to damming has cascading effects on prey availability, ultimately impacting raptors' foraging efficiency and breeding productivity (Mor et al., 2018; Nasruddin-Roshidi et al., 2021); and (4) habitat loss caused by flooding may intensify competition among raptor species (Kajtoch & Figarski, 2013; Nasruddin-Roshidi et al., 2021; Elas et al., 2023). Consequently, the effects of dam construction extend beyond immediate habitat loss, potentially influencing population and community dynamics (Elas et al., 2023). Understanding these long-term ecological impacts is crucial for identifying priority conservation actions and developing effective mitigation strategies.

The construction and environmental impact monitoring of the HIBS in Portugal provided an opportunity to assess the effects of dam construction and river valley flooding on both terrestrial and aquatic species (Amorim et al., 2022; Mota-Ferreira et al., 2021). The dam was built within a Natura 2000 site, designated under the EU Birds (79/409/EEC) and Habitats (92/43/EEC) Directives, leading to significant opposition from environmental NGOs and a legal

dispute between the Portuguese government and the European Commission (Jackson, 2011). The project was ultimately approved under the condition that extensive mitigation and compensation measures, alongside a long-term monitoring program, would be implemented (Santos et al., 2019a,b). Given the relevance of the river valley for cliff-nesting raptors, particular attention was given to the most emblematic species of conservation concern, including the Egyptian vulture (*Neophron percnopterus*), Griffon Vulture (*Gyps fulvus*), Golden eagle (*Aquila chrysaetos*), Bonelli's eagle (*Aquila fasciata*), and Peregrine falcon (*Falco peregrinus*). To mitigate potential impacts, efforts were made to minimize disturbances near nesting sites during the construction phase, while habitats were managed to improve prey availability for eagles and supplementary feeding was provided at vulture feeding stations during the operational phase. Additionally, systematic monitoring was conducted to track breeding pairs in both impact and control areas, with annual assessments of breeding productivity for species of conservation concern.

This study leverages an extensive dataset (2010–2022) collected during the long-term monitoring of the HIBS project to assess the impacts of hydropower infrastructure on cliff-nesting raptors. Using an analytical framework akin to a Before-After-Control-Impact (BACI) approach (Smith, 2006), we specifically aimed to determine whether dam construction resulted in reductions in territory occupancy, breeding population size, and breeding productivity, and whether the severity of impacts was greater in areas with increasing extent of river valley flooding. We focused on the three most abundant cliff-nesting birds (Golden eagle, Egyptian vulture, and Griffon Vulture), due to small sample sizes for the other species. This study will contribute to a deeper understanding of the long-term ecological consequences of hydropower development on terrestrial wildlife. Furthermore, it will inform the design of more effective mitigation and compensation strategies, ensuring better conservation outcomes for affected raptor populations.

2.2. Methods

2.2.1. Cliff-nesting bird data

Data on cliff-nesting raptors was collected through monthly surveys conducted yearly during the breeding season (primarily January to August) from 2010 to 2022 (Mota et al., 2020b,c; Cabral et al., 2024). Surveys focused on a 5-km buffer surrounding the future reservoir area to ensure comprehensive coverage of nesting sites potentially impacted by river valley flooding due to dam construction (Figure 1). Experienced field ornithologists conducted the surveys, systematically scanning rocky cliffs and outcrops along river valleys using binoculars (10×42 or 12×50) and telescopes (20–60× magnification) to locate and identify occupied raptor nests. To enhance detection probability while minimizing disturbance, observations were made from

multiple strategic vantage points. Researchers recorded key reproductive behaviours, including territorial displays, courtship, nest occupancy, nest defence, incubation, and chick provisioning (Zuberogoitia et al., 2008; Dias et al., 2017). In addition to systematic monitoring, opportunistic observations from travel across the study area and in the scope of other bird monitoring programs were also considered. These supplementary data helped refine survey efforts and identify previously overlooked breeding territories. Nest detection efforts were further informed by baseline data from the previous EIA phase of the hydropower project (2006–2008).

Each year, all known nests were visited at least once during each key reproductive stage, including mating, incubation, post-hatching, and pre-emancipation of juveniles. From a safe observation distance, researchers used telescopes to confirm breeding activity, such as the presence of incubating adults, eggs, nestlings, or fledglings. The number of fledged juveniles per nest was recorded to estimate breeding productivity (Zuberogoitia et al., 2008, 2014; Margalida et al., 2014b).

For Golden eagles, a territory was identified as a cluster of nests used by the same breeding pair over multiple years. This definition accounts for the tendency of these eagles and other large raptors to alternate between different nests within a territory across breeding seasons (Kochert & Steenhof, 2012). The same criterion was applied to Egyptian vultures, though this species can sometimes form loose aggregations, when suitable cliffs are limited. In such cases, we treated a cluster of nearby nests as a single territory, even if used by more than one breeding pair. For the gregarious Griffon vulture, which nests colonially, we defined a colony as a spatially discrete cluster of nests used by one or more breeding pairs over multiple years. This information was used to estimate the annual occupancy of each territory or colony, defined as the presence of at least one confirmed breeding attempt in a given year during the study period. To ensure the reliability of occupancy estimates, only nests with at least one confirmed reproduction event over the study period were included in the analysis. Occupancy was determined either directly, by the presence of eggs, chicks, or fledglings, or indirectly through the observation of adult breeding behaviour. All spatial analyses were conducted using QGIS software (QGIS Development Team, 2024).

2.2.2. Data analysis

We estimated temporal trends of demographic parameters for Golden eagles, Griffon vultures, and Egyptian vultures over the study period. Specifically, we analysed interannual variation in the number of occupied breeding territories and the number of breeding pairs. Additionally, we assessed breeding productivity, measured as the average number of fledged juveniles per breeding nest. We used the number of flying juveniles as a proxy for breeding productivity,

given the difficulty and higher uncertainty associated with estimating clutch size or hatchling count. The year 2020 was excluded from all trends analyses due to significantly reduced monitoring efforts related to the COVID-19 pandemic (Appendix XIII).

To evaluate the impact of dam construction on cliff-nesting raptor species, we employed a Before-After-Control-Impact (BACI) design with multiple sites and years (Smith, 2006). For each species, we modelled territory/colony occupancy as a binary variable (occupied vs. unoccupied) in relation to: (i) a binary variable coding the period before (2010–2014) and after (2015–2022) the flooding of the river valley; (ii) a continuous variable coding the maximum extent of flooded area within 2-km and 5-km buffers around the breeding nest; and (iii) an interaction term between the two variables. Similarly, we modelled the number of breeding pairs and the number of fledged juveniles per breeding territory using the same explanatory variables. We hypothesized that if the dam had a negative impact, territory/colony occupancy, population size and breeding productivity would decline after flooding, but primarily in territories with a larger area affected.

We conducted the modelling using Generalized Linear Mixed Models (GLMMs) to account for the lack of independence among samples, treating breeding territories/colonies and sampling year as random effects (Pinheiro & Bates, 2000). Occupancy for each target species was modelled using a binomial distribution with a logit link function, while the number of pairs was modelled using a Poisson distribution and a log link. For breeding productivity, a Poisson distribution (with a log link) was used for Golden eagles to model the number of fledged juveniles per breeding pair, while for Egyptian and Griffon vultures we used a Gamma distribution with a log link to model the average number of fledged juveniles per breeding pair per territory/colony. In each case, we fitted the full model with the two main effects and their interaction term. Analyses were conducted using the ‘lme4’, ‘siPlot’ and ‘ggplot2’ packages in R software (R Core Team, 2024).

2.3. Results

2.3.1. Population trends

During the study, we identified six and five breeding territories for Golden eagles and Egyptian vultures, respectively, and six Griffon Vulture colonies (Appendix XIV). The number of Golden eagle territories (equal to the number of pairs) fluctuated considerably over time, without a clear trend (Mean ± SD, Min–Max: 3.3 ± 1.6, 1–6; Figure 11).

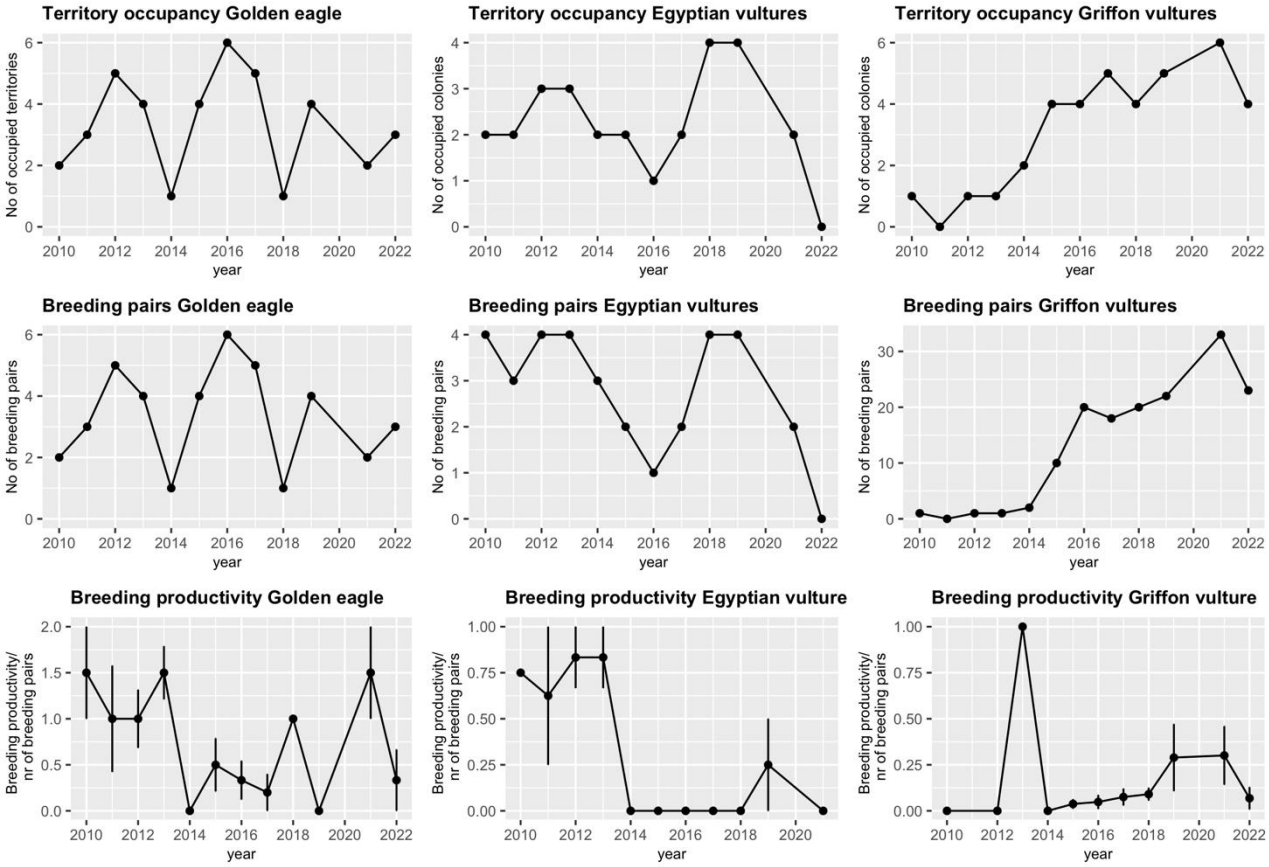

Figure 11 - Demographic trends of three cliff-nesting birds breeding along the lower reaches of the River Sabor (NE Portugal) before (2010-2014) and after (2015-2022) the flooding of the valley by the reservoirs of the Baixo Sabor Hydroelectric System. The panels represent trends in the number of territories/colonies, number of breeding pairs and breeding productivity (average number of fledglings per breeding pair) for Golden eagles, Egyptian vultures and Griffon vultures.

Annual breeding productivity for this species (0.74 ± 0.58, 0–1.5 fledglings/pair) increased between 2010 and 2013, declined sharply in 2014, and remained low thereafter, except for the highly productive year of 2021. For Egyptian vultures, the annual number of both territories (2.2 ± 1.1, 0–4) and total breeding pairs (2.8 ± 1.4, 0–4) largely declined between 2010 and 2016, rebounded to a peak in 2018–2019, and then declined again until the end of the study (Figure 11). Annual productivity (0.30 ± 0.38, 0–0.8 fledglings/pair) remained relatively stable at high levels from 2010 to 2013 but dropped sharply in 2014, staying extremely low or null in

subsequent years (Figure 11). Griffon vultures showed a markedly different pattern, with the annual numbers of colonies (3.1 ± 2.0, 0–6) and total breeding pairs (12.6 ± 11.4, 0–33) increasing steadily throughout the study period (Figure 11). The rise in breeding pairs was particularly striking, with at most one pair between 2010 and 2013, followed by a rapid increase from 2 to 33 pairs between 2014 and 2021. Productivity had a peak in 2013, which was an artefact resulting from a single pair breeding successfully for the first time in the study area. From 2014 onwards, productivity increased gradually alongside population growth but later plateaued and then decreased in the final year.

2.3.2. Modelling of dam impacts

For Golden eagles, GLMMS showed no significant effects of the explanatory variables on the numbers of territories and breeding pairs (Table 4). There was, however, a marginal tendency (P<0.10) for lower productivity in the post-flooding period, though this trend does not seem to be directly linked to the extent of flooding (i.e. non-significant interaction term) (Table 4). For Egyptian vultures, there was a marginal tendency (P<0.10) for higher occupancy probability along with the extent of river flooding within 2 km of the colony, with no other effects observed on either occupancy or the number of breeding pairs. For productivity, however, there were significant (P<0.05) and marginally significant (P<0.10) effects of the interaction term between time period and the extent of flooding within 2 km and 5 km from the colonies, respectively (Table 4). This effect underlined a tendency for productivity increasing with the amount of potentially flooded area in the pre-flooding period, while remaining at much lower levels irrespective of the extent of flooding in the post-flooding period (Figure 12). For Griffon vultures, the colony occupancy and number of breeding pairs increased significantly in the post-flooding period (Table 4). Breeding productivity could not be modelled for Griffon Vulture in relation to the time of flooding, as only a single pair bred during pre-flooding. Griffon Vulture productivity was not affected by the extent of flooding (Table 4).

Table 4 – Summary of Generalized Linear Mixed Model (GLMM) results examining the relationships between territory/colony occupancy, population size, and breeding productivity of Golden eagle, Egyptian vulture, and Griffon Vulture in relation to key explanatory variables. The full model includes the sampling period relative to the timing of river flooding (BA; 2010–2014 vs. 2015–2022), the proportion of flooded area within 2-km and 5-km buffers around territories/colonies (FLOODED_AREA), and their interaction (BA:FLOODED_AREA). For each model, summary statistics include regression coefficients (± standard error) and their significance levels (***P < 0.001; **P < 0.01; *P < 0.05; • P<0.1), as well as test statistics and significance levels for the full model. Due to convergence issues, GLMMs for Griffon Vulture productivity were fitted only to FLOODED_AREA (see the main text for further details).

	Golden eagle 2km	Golden eagle 5km	Egyptian vulture 2km	Egyptian vulture 5km	Griffon vulture 2km	Griffon vulture 5km
TERRITORY/COLONY OCCUPANCY						
Intercept	0.46±0.66	0.72±0.70	-2.04±1.31	-1.14±0.93	-2.60±2.81	-3.65±1.86 (*)
BA	-0.17±0.85	-0.47±0.89	1.31±1.29	0.45±0.93	5.59±2.85 (*)	4.62±1.92 (*)
FLOODED_AREA	-5.17±4.58	-13.31±8.50	29.05±16.71 (•)	25.62±17.60	1.48±32.75	30.42±33.60
BA:FLOODED_AREA	6.98±5.80	16.76±10.43	-23.30±16.29	-17.70±17.19	-16.05±29.92	-8.06±30.83
Observations	72	72	60	60	72	72
Chisq (Full Model)	2.11	3.85	3.87	2.56	19.79 (***)	20.38 (***)
POPULATION SIZE						
Intercept	-0.49±0.35	-0.36±0.36	-1.00±0.71	-0.74±0.54	-1.92±1.61	-2.93±1.06 (**)
BA	-0.08±0.44	-0.23±0.46	-0.35±0.68	-0.49±0.52	4.63±1.39 (***)	4.07±0.83 (***)
FLOODED_AREA	-2.55±3.27	-7.06±6.40	6.74±8.33	5.27±8.28	-1.23±19.36	19.50±20.44
BA:FLOODED_AREA	3.15±3.85	8.17±7.21	-2.30±8.04	-0.61±7.54	-22.81±16.83	-28.58±15.33 (•)
Observations	72	72	60	60	72	72
Chisq (Full Model)	1.07	33.88 (***)	2.88	2.64	33.80 (***)	31.65 (***)
PRODUCTIVITY						
Intercept	0.15±0.35	0.17±0.35	0.19±0.24	0.37±0.20 (•)	0.43±0.23 (•)	0.32±0.17 (•)
BA	-1.00±0.55 (•)	-1.06±0.56 (•)	-0.30±0.30	-0.34±0.21		
FLOODED_AREA	-0.40±3.61	-1.15±6.41	3.00±2.04	0.63±1.67	-2.42±2.49	-2.32±2.90
BA:FLOODED_AREA	-0.36±4.84	0.66±8.24	-2.78±1.32 (*)	-2.25±1.18 (•)		
Observations	40	40	27	27	37	37
Chisq (Full Model)	6.36 (•)	6.34 (•)	8.04 (*)	7.41 (•)	0.78	0.65

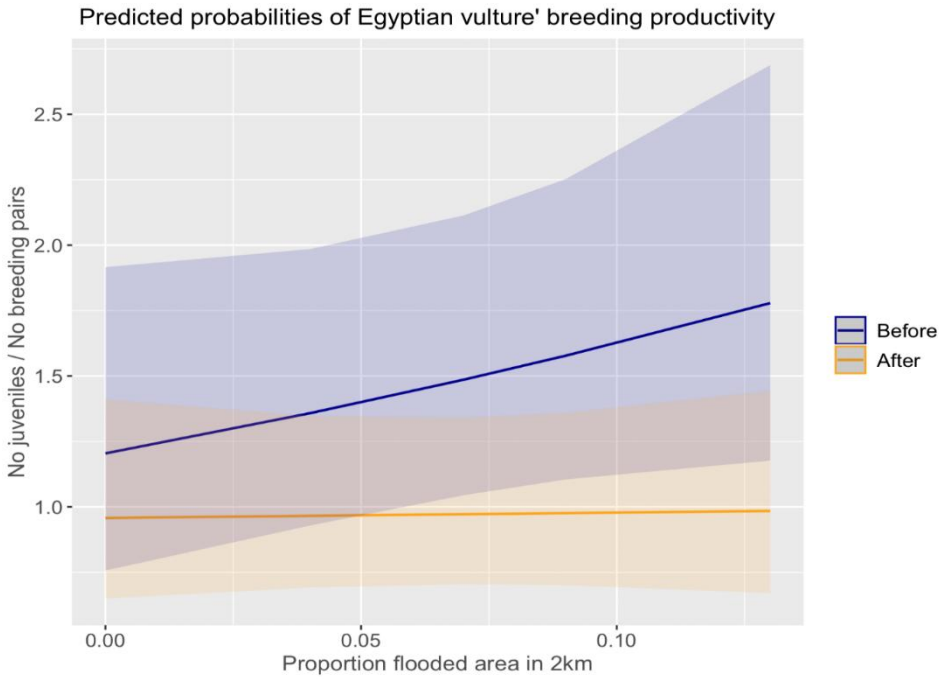

Figure 12 - Generalized Linear Mixed Model (GLMM) predictions of Egyptian vulture breeding productivity in relation to the extent of flooded area within a 2-km buffer around breeding colonies, before (2010–2014) and after (2015–2022) river flooding. The blue and orange lines represent model-predicted trends for the pre-flooding and post-flooding periods, respectively, with shaded areas indicating 95% confidence intervals.

2.4. Discussion

This study offers valuable insights into the long-term effects of hydropower development on cliff-nesting raptors within a designated conservation area. By analysing demographic trends before (2010-2014) and after (2015-2022) the flooding of a river valley caused by dam construction, we identified species-specific responses, with Egyptian vultures experiencing a marked decline in breeding productivity, Griffon vultures showing rapid population expansion, and Golden eagles displaying fluctuating but stable occupancy patterns. While these findings partially align with initial expectations that hydropower-driven habitat alteration would negatively impact cliff-nesting raptors, they also reveal high significant intraspecific variation, including potential benefits for more generalist and competitively dominant species. Such variation was likely influenced by additional, unmeasured factors, such as regional population dynamics of each species, construction- and operation-related disturbances, and the effectiveness of mitigation measures implemented to offset impacts. Overall, our results highlight the complex ecological effects of hydropower development on terrestrial wildlife, with consequences for the design of effective impact mitigation and compensation programs.

2.4.1. Raptor Responses to the Baixo Sabor Hydropower Development

The decline in Egyptian vulture breeding productivity following the flooding event suggests that hydropower development introduced environmental pressures that disproportionately affected this species. Several mechanisms can underlie this pattern, including the loss or degradation of optimal nesting sites, increased predation risk due to exposure in newly selected nesting locations, and reduced foraging efficiency due to landscape modification (Mateo-Tomás et al., 2010; Velevski et al., 2014). Egyptian vultures typically select nests on small, secluded cliffs along deep valleys to protect against predators and provide favourable microclimatic conditions. However, flooding may have forced individuals into more exposed nesting sites, increasing vulnerability to nest predation, heat stress, and dehydration (Velevski et al., 2014). Another potential negative impact might be related to increased human activity near the reservoir after flooding, including recreational use, which can contribute to nest abandonment and decreased parental investment (Zuberogoitia et al., 2008, 2014; Morant et al., 2018). However, disturbance already occurred prior to flooding, initially concentrated near the dam construction site, and later expanding progressively throughout the valley due to vegetation clearing operations, albeit outside the breeding period.

Another plausible factor for the decline in Egyptian vulture productivity is the concurrent expansion of the Griffon Vulture population. As a larger and more dominant scavenger, the Griffon Vulture may be exerting competitive pressures on Egyptian vultures, both for food and nesting sites. Griffon vultures can outcompete Egyptian vultures for carrion resources and

exhibit aggressive behaviours that may limit food access for smaller scavengers (Cortés-Avizanda et al., 2010; Margalida et al., 2014b). Competition at supplementary feeding stations is particularly relevant, with Griffon vultures monopolizing these supplementary food sources, reducing the benefits for Egyptian vultures and potentially altering their foraging efficiency and reproductive success (Moreno-Opo et al., 2015; Duriez et al., 2012). The increasing Griffon Vulture population may also contribute to nest-site interference, potentially exacerbating the challenges faced by Egyptian vultures (Beest et al., 2008).

The rapid expansion of Griffon vultures in the Baixo Sabor region is likely part of the broader recovery of the species across the Iberian Peninsula, where populations have been increasing due to legal protection, reduced persecution, and improved food availability (Zuberogoitia et al., 2013; Arrondo et al., 2020). However, local factors may have also played a role, particularly the establishment of vulture feeding stations, which are known to support higher densities of scavengers by providing a predictable and abundant food source (Cortés-Avizanda et al., 2016; Moreno-Opo et al., 2020). In fact, these artificial food supplies may have facilitated colony establishment and growth in the study area, potentially accelerating population increases beyond what would be expected from regional trends alone. Supplementary feeding has been documented to promote rapid aggregation of Griffon vultures, sometimes even influencing their movement patterns and breeding site selection (Arrondo et al., 2018).

Unlike the other two species, Golden eagles did not exhibit a clear decline in occupancy or population size. Although we observed demographic fluctuations for this species, they seemed unrelated to the hydropower development and may likely be a consequence of natural interannual variation in meteorological conditions, changes in prey availability, and other factors. As a territorial, long-lived species with low reproductive rates, Golden eagles may be less immediately affected by habitat modifications than opportunistic scavengers like Griffon vultures (Watson, 2010; Hunt et al., 2017). However, these results might be seen as surprising, because the flooding of the river valley may have caused the loss of foraging areas, which could have affected territory occupancy and reproductive output (Fernández-Gil et al., 2023, Tack et al., 2019). It should be noted, however, that Golden Eagles usually have large ranges, and so flooding likely affected only a minor proportion of the foraging areas. Moreover, It is possible that the loss of these habitats was at least partly offset by compensation measures targeted at increasing rabbit (*Oryctolagus cuniculus*) and red-legged partridges (*Alectoris rufa*), though evidence to support this idea is lacking.

2.4.2. Limitations and potential shortcomings

While our study benefits from a long-term dataset and a BACI-like approach, some methodological limitations should be acknowledged. The relatively small sample sizes may

have limited our ability to detect subtle demographic trends, a common challenge in studies involving rare and long-lived raptors (Hunt et al., 2017; Fernández-Gil et al., 2023). Limited sample sizes also constrained our capacity to explore in more detail the drivers of spatial heterogeneity across territories, including potential effects of prey availability and localised human disturbance. Moreover, although we analysed demographic changes before and after the flooding of the river valley, some ecological impacts may have occurred earlier, during the dam construction phase. While early disturbances were initially concentrated near the dam site, they expanded progressively from 2012 to 2014 due to vegetation clearing in the future reservoir area. These operations were conducted outside the main breeding season and were therefore assumed to have a limited direct impact on cliff-nesting raptors. Nevertheless, possible indirect or cumulative effects cannot be entirely excluded. The absence of true control areas unaffected by hydropower development further complicates causal attribution, as observed trends could partially reflect broader regional or environmental changes (Smith, 2006). Other unaccounted-for influences, such as interspecific interactions, climate variability, and anthropogenic pressures beyond the valley, may also have shaped the observed patterns. Despite these constraints, our findings remain ecologically meaningful and offer a basis for evaluating the long-term impacts of hydropower infrastructures on raptor populations.

2.4.3. Conservation and Management Recommendations

Our findings highlight the need for targeted conservation actions to mitigate the impacts of hydropower infrastructure on cliff-nesting raptors, with broader implications for similar developments. Given the decline in Egyptian vulture productivity and the expansion of Griffon vultures, adaptive management should focus on food resource management and long-term monitoring to minimize potential interspecific competition and ensure population stability. The rapid increase in Griffon vultures suggests that supplementary feeding programs, originally designed as a compensation measure, may have unintentionally favoured the disproportionate population growth of this dominant scavenger. Adjusting feeding station management could help mitigate these effects by spatially separating feeding sites to ensure that Egyptian vultures have exclusive access to food sources, providing smaller carrion pieces that are less accessible to larger scavengers, and regulating the availability and predictability of food to prevent monopolization by Griffon vultures (Cortés-Avizanda et al., 2010; Donázar et al., 2010; López-López et al., 2014; Moreno-Opo et al., 2015). Research has shown that optimizing food size, placement, and timing can reduce competition at feeding sites and improve access for subordinate scavengers, ensuring that multiple species benefit from conservation interventions (Donázar et al., 2010; García-Heras et al., 2013).

Golden eagles exhibited stable occupancy but fluctuating reproductive success, emphasizing the need for continued long-term monitoring to detect potential delayed ecological responses

(Fernández-Gil et al., 2023). Given the complex interplay between food availability, habitat modifications, and interspecific competition, regular assessments of population trends will be essential for guiding adaptive conservation strategies that maintain a balanced raptor community in the Baixo Sabor landscape. Understanding how species respond over time to changes in resource distribution and habitat structure will be critical to refining conservation actions and ensuring their effectiveness in mitigating hydropower-related impacts.

2.4.4. Broader implications and future perspectives

Our study provides insights into the complex ecological consequences of hydropower development, particularly in protected areas hosting species of conservation concern. While the impacts of hydropower on aquatic biodiversity are well documented (Geist, 2021; He et al., 2024), our findings support the view that terrestrial wildlife can also be affected (Sánchez-Zapata et al., 2016; Lees et al., 2016). Moreover, we found that these effects can occur in less predictable ways, driven by changes in resource availability and interspecific interactions that likely enhance the effects of direct habitat loss. The contrasting responses of cliff-nesting raptors observed in our study illustrate how hydropower-induced alterations can create ecological winners and losers, with some species adapting or even thriving under new conditions, including those derived from compensatory measures, while others experience negative demographic effects, including possible secondary effects from compensatory measures. These results underscore the importance of comprehensive environmental impact assessments that incorporate long-term monitoring to detect delayed and indirect effects on terrestrial biodiversity (Gracey & Verones, 2016; Zarfl et al., 2019).

To mitigate these effects, conservation planning must integrate species-specific management approaches that account for competitive dynamics, resource shifts, and habitat modifications (Botelho et al., 2017; Sánchez-Zapata et al., 2016). Understanding how different species respond to hydropower-induced environmental changes is essential for designing mitigation strategies that effectively balance biodiversity conservation with renewable energy expansion (Gracey & Verones, 2016). Future research should focus on cumulative hydropower impacts at the landscape scale, considering both direct and indirect effects of infrastructure projects and their prescribed mitigation measures. By strengthening the connection between energy policy and conservation science, decision-makers can develop more sustainable hydropower models that align with biodiversity goals, ensuring that renewable energy development does not come at the cost of wildlife conservation (Lees et al., 2016; Dorber et al., 2020).

3. Conclusions and Further perspectives

This study provides a comprehensive assessment of the HIBS ecological impacts on local avifauna of a Mediterranean landscape, focusing on passerine community patterns and cliff-nesting raptors population dynamics. Findings from the first chapter reveal that passerine species richness and abundance exhibit relative interannual stability from 2013 to 2016, with higher values consistently observed in areas less affected by flooding, dominated by shrublands and olive orchards. However, pronounced seasonal declines in passerine diversity likely reflect the sensitivity of passerine birds to phenological cycles and resource availability. Key environmental drivers, including elevation, slope ruggedness, proximity to water, and temperature, emerged as significant predictors of passerine community patterns, underscoring the complex interplay of topographic, climatic, and anthropogenic factors shaping avian assemblages.

In the second chapter, long-term monitoring (2010–2022) of cliff-nesting raptors revealed species-specific responses to river flooding, with Egyptian vultures and Golden eagles experiencing declines in breeding productivity linked to habitat loss, while Griffon vultures showed population expansion, potentially influenced by supplementary feeding and regional recovery trends. Specifically, Egyptian vultures exhibited a significant drop in productivity post-flooding (2015–2022), particularly in territories with greater flooded areas within 2-km and 5-km buffers, likely due to degraded nesting sites and increased competition. Golden eagles showed fluctuating but marginally lower productivity after flooding, though not directly tied to flooding extent, suggesting other environmental factors at play. Conversely, Griffon vultures experienced a steady increase in colony occupancy and breeding pairs, from just one pair pre-flooding to 33 by 2021, likely benefiting from feeding stations and broader Iberian recovery. These contrasting outcomes illustrate the varied ecological consequences of hydropower development across trophic levels (Margalida et al., 2014a; Pearce-Higgins et al., 2015; Nasruddin-Roshidi et al., 2021).

The results of this research have direct implications for EIA and decision-making in the management of sensitive areas and bird conservation within the Baixo Sabor SPA and broader Natura 2000 network. In the case of passerines, results suggest that maintaining habitat mosaics and mitigating microclimatic stressors through vegetation preservation are critical strategies to buffer against infrastructure-related impacts (Benton et al., 2003; Moreira et al., 2012). For cliff-nesting raptors, the decline in Egyptian vulture productivity underscores the need for targeted conservation actions, such as adjusting supplementary feeding programs to reduce interspecific competition with Griffon vultures, while continued monitoring of Golden eagles is essential to detect delayed responses to habitat alteration (Mateo-Tomás et al.,

2010a; Margalida et al., 2014a; Velevski et al., 2014; Watson & Davies, 2015; Cortés-Avizanda et al., 2016). Integrating these findings into frameworks, like the LTER network, can enhance adaptive management, ensuring that renewable energy development aligns with biodiversity conservation goals in Mediterranean ecosystems (e.g., Zuberogoitia et al., 2014; Bastos et al., 2015). Specifically, conservation strategies should prioritize protecting terrestrial habitats distant from reservoir edges as refugia for passerines and implement species-specific measures for raptors to address habitat loss and inter-specific interactions (e.g., Margalida et al., 2014a; Zuberogoitia et al., 2014).

From a methodological perspective, this study highlights the added value of integrating StDM with ABMs to predict ecological indicators responses to environmental changes (Santos et al., 2013). This approach not only enable the visualization of spatial-temporal patterns but also provides a robust framework for simulating complex ecological processes under realistic scenarios of change (e.g., Bastos et al., 2015; Hughes et al., 2016). Looking forward, there is significant potential to advance this methodology by incorporating process-based landscape changes (e.g. via socio-economic rules in the ABM), rather than relying solely on map importation. In fact, by simulating environmental/anthropogenic changes based on dynamic processes within ABMs, ecological indicator responses could emerge directly from a mechanistic understanding of the system (Bastos et al.,2016; Santos et al., 2016b). This would allow for more realistic predictions of long-term impacts and support the design of management strategies tailored to evolving landscape management. Additionally, the BACI-like approach applied to cliff-nesting raptors offers a valuable framework for long-term monitoring of infrastructure effects, and future refinements could incorporate multi-scale spatial analyses and additional ecological variables (e.g., prey dynamics) to enhance the precision of impact detection across species and habitats. Extending temporal coverage by collecting more data over longer periods is particularly valuable for these studies, as it captures delayed or cumulative impacts more effectively than modelling alone.

Overall, this thesis underscores the necessity of balancing renewable energy development with biodiversity conservation through evidence-based impact assessments and adaptive management. The differential responses of passerines and raptors to the HIBS emphasize the importance of long-term monitoring to capture delayed and/or cumulative ecological effects.

References

Abreu T.L.S., Berg S.B., de Faria I.P., *et al.* (2020). River dams and the stability of bird communities: A hierarchical Bayesian analysis in a tropical hydroelectric power plant. *Journal of Applied Ecol*ology, 57: 1124–1136. https://doi.org/10.1111/1365-2664.13607

Almeida J., Catry P., Encarnação V., Franco .C, Granadeiro J.P., Lopes R., Moreira F., Oliveira P., Onofre N., Pacheco C., Pinto M., Pitta Groz M.J., Ramos J., Silva L. (2005). Sterna albifrons Chilreta Pp - in Livro Vermelho dos Vertebrados de Portugal (Cabral M.J. et al.(eds.)). *Instituto da Conservação da Natureza*. Lisboa.

Amorim, F., Pita, R., Mata, V. A., Beja, P., & Rebelo, H. (2022). Crowding after sudden habitat loss affects demography and social structure in a bat population. *Journal of Animal Ecology*, 91(3), 668-680. https://doi.org/10.1111/1365-2656.13659

Arrondo, E., Sanz-Aguilar, A., Pérez-García, J. M., Cortés-Avizanda, A., Sánchez-Zapata, J. A., & Donázar, J. A. (2020). Landscape anthropization shapes the survival of a top avian scavenger. *Biodiversity and Conservation*, 29, 1411-1425. https://doi.org/10.1007/s10531-020-01942-6

Arrondo, E., Moleón, M., Cortés-Avizanda, A., Jiménez, J., Beja, P., & Sánchez-Zapata, J. A. (2018). Invisible barriers: Differential sanitary regulations constrain vulture movements across country borders. Biological Conservation, 220, 254-261. https://doi.org/10.1016/j.biocon.2018.01.029

Azevedo, J., Moreira, C. A., Castro, J. P., & Loureiro, C. (2011). Agriculture abandonment, land-use change and fire hazard in mountain landscapes in northeastern Portugal. *Landscape Ecology in Forest Management and Conservation*, 329-351. https://doi.org/10.1007/978-3-642-12754-0_14

Bastos, R., Santos, M., Ramos, J. A., Vicente, J., Guerra, C., Alonso, J., et al. (2012). Testing a novel spatially-explicit dynamic modelling approach in the scope of the laurel forest management for the endangered Azores bullfinch (*Pyrrhula murina*) conservation. *Biological Conservation*, 147, 243–254. https://doi.org/10.1016/j.biocon.2012.01.009

Bastos, R., Pinhanços, A., Santos, M., Fernandes, R., Vicente, J., Morinha, F., & Cabral, J. (2015). Evaluating the regional cumulative impact of wind farms on birds: how can spatially explicit dynamic modelling improve impact assessments and monitoring? *Journal of Applied Ecology*, 53(5), 1330-1340. https://doi.org/10.1111/1365-2664.12451

Bastos, R., D'Amen, M., Vicente, J., Santos, M., Yu, H., Eitelberg, D., & Cabral, J. (2016). A multi-scale looping approach to predict spatially dynamic patterns of functional species richness in changing landscapes. *Ecological Indicators*, 64, 92-104. https://doi.org/10.1016/j.ecolind.2015.12.025

Bastos, R., D'Amen, M., Marcos, B., Santos, M., Braz, L., Vicente, J., et al. (2018). Towards functional biodiversity predictions: a hierarchical modelling framework from primary productivity to biomass of upper trophic levels. *Landscape Ecology*, 33. https://doi.org/10.1007/s10980-018-0735-8

Beest, F. M. v., Bremer, L. v. d., Boer, W. F. d., Heitkönig, I., & Monteiro, A. (2008). Population dynamics and spatial distribution of Griffon vultures (Gyps fulvus) in Portugal. *Bird Conservation International*, 18(2), 102-117. https://doi.org/10.1017/s0959270908000129

Beja, P., & Cabral, J. (2012). LTSER-Sabor - Portugal. DEIMS-SDR Site and Dataset Registry. https://deims.org/45722713-80e3-4387-a47b-82c97a6ef62b

Beja, P. et al., (2013). Predators and livestock reduce bird nest survival in intensive mediterranean farmland. *European Journal of Wildlife Research*, 60(2), 249-258. https://doi.org/10.1007/s10344-013-0773-0

Benton, T. G., Vickery, J. A., & Wilson, J. D. (2003). Farmland biodiversity: Is habitat heterogeneity the key? *Trends in Ecology & Evolution, 18*(4), 182–188. https://doi.org/10.1016/S0169-5347(03)00011-9

Bibby, C. J., Burgess, N. D., Hill, D. A., & Mustoe, S. H. (2000). Bird Census Techniques (2nd ed.). *Academic Press*.

Bidoglio, G., Berger, M., & Finkbeiner, M. (2019). An environmental assessment of small hydropower in India: the real costs of dams' construction under a life cycle perspective. *The International Journal of Life Cycle Assessment*, *24*, 419-440. https://doi.org/10.1007/s11367-018-1458-4

Boddaert, P. 1783. Table des planches enluminéez d'histoire naturelle, de M. D'Aubenton. Avec les dénominations de M.M. de Buffon, Brisson, Edwards, Linnæus et Latham. Precedé d'une notice des principaux ouvrages zoologiques enluminés. - pp. I-XV, [1], 1-58, 1-9. *Utrecht*.

Botelho, A., Ferreira, P., Lima, F., & Pinto, L. M. C. (2017). Assessment of the environmental impacts associated with hydropower. *Renewable and Sustainable Energy Reviews*, 70, 896-904. https://doi.org/10.1016/j.rser.2016.11.271

Boyd, R., Roy, S., Sibly, R., Thorpe, R., & Hyder, K. (2018). A general approach to incorporating spatial and temporal variation in individual-based models of fish populations with application to Atlantic mackerel. *Ecological Modelling*, *382*, 9-17. https://doi.org/10.1016/j.ecolmodel.2018.04.015

Brotons, L., Herrando, S., & Pla, M. (2007). Updating bird species distribution at large spatial scales: applications of habitat modelling to data from long-term monitoring programs. *Diversity and distributions*, *13*(3), 276-288. https://doi.org/10.1111/j.1472-4642.2007.00339.x

Burnham, K.P., Anderson, D.R., 2002. Model Selection and Multi Model Inference: A Practical Information-Theoretic Approach, second ed. *Springer*.

Cabral, J. A., Marques, J. C., & Nielsen, S. N. (2001). Modelling mosquito fish (Gambusia holbrooki) responses to Genapol OXD-080, a non-ionic surfactant, in rice fields. *Ecological Engineering*, 16(4), 537–544. https://doi.org/10.1016/S0925-8574(00)00106-2

Cabral J. A., Cabecinha E., Santos M., Travassos P. & Silva-Santos P. (2008) Simulating the ecological status of changed ecosystems by holistic applications of a new Stochastic-Dynamic Methodology

(StDM). In: Alonso M. S. and Rubio I. M. (Eds), Ecological Management: New Research. Chapter 4: 123-141, *Nova Science Publishers, Inc., New York*. ISBN: 978-1-60456-786-1.

Cabral, J. A., Barros, P., Vale-Gonçalves, H. M., Travassos, P., Madeira, J., & Figueira, R. (2017). EDP Baixo Sabor: Herpetology – Baseline Studies [2009]. v1.1. *EDP* - Energias de Portugal. Dataset/Occurrence.

http://ipt.gbif.pt/ipt/resource?r=edp_sabor_herpetology_baseline&v=1.4

Cabral J. A., Jesus J., Travassos P., Carvalho D., Gomes C., Brás L., Barros P., Múrias T. (2024). Movhera Baixo Sabor: Exploration Phase - Cliff-nesting species: Breeding sites [2021-2023]. Movhera - Hidroelétricas do Norte, S.A. Sampling event dataset. https://doi.org/10.15468/sdh3c5 accessed via GBIF.org on 2025-01-21.

Carignan, V., Villard, MA. Selecting Indicator Species to Monitor Ecological Integrity: A Review. *Environ Monit Assess,* 78, 45–61 (2002). https://doi.org/10.1023/A:1016136723584

Carrascal, L. M., Seoane, J., & Villén-Pérez, S. (2012). Temperature and food constraints in wintering birds — an experimental approach in montane mediterranean oakwoods. *Community Ecology*, 13(2), 221-229. https://doi.org/10.1556/comec.13.2012.2.12

Carter, J., Ackleh, A. S., Leonard, B. P., & Wang, H. (1999). Giant panda (*Ailuropoda melanoleuca*) population dynamics and bamboo (subfamily *Bambusoideae*) life history: a structured population approach to examining carrying capacity when the prey are semelparous. *Ecological Modelling*, *123*(2-3), 207-223. https://doi.org/10.1016/S0304-3800(99)00145-3

Chen, K., Lu, J., & Wang, C. (2019). Effective pollination of aeschynanthus acuminatus (Gesneriaceae) by generalist passerines, in sunbird-absent east Asia. *Scientific Reports*, 9(1). https://doi.org/10.1038/s41598-019-53035-2

Comunidade Intermunicipal das Terras de Trás-os-Montes, (2019). In the Lands of Trás-os-Montes. Nove Passos. PDF link below:

https://9passos.cim-ttm.pt/wp-content/uploads/2021/07/220012_02_BROCHURA_GERAL_EN_2A.pdf

Corder, G. W., & Foreman, D. I. (2014). *Nonparametric statistics: A step-by-step approach*. John Wiley & Sons.

Cortés-Avizanda, A., Carrete, M., & Donázar, J. A. (2010). Managing supplementary feeding for avian scavengers: guidelines for optimal design using ecological criteria. *Biological conservation*, 143(7), 1707-1715. https://doi.org/10.1016/j.biocon.2010.04.016

Cortés-Avizanda, A., Colomer, M. A., Margalida, A., Ceballos, O., and Donázar, J. A. (2015). Modeling the consequences of the demise and potential recovery of a keystone-species: wild rabbits and avian scavengers in mediterranean landscapes. *Scientific Reports*, 5(1). https://doi.org/10.1038/srep17033

Cortés-Avizanda, A., Carrete, M., Serrano, D., & Donázar, J. A. (2016). Supplementary feeding and endangered avian scavengers: Benefits, caveats, and controversies. *Frontiers in Ecology and the Environment*, 14(4), 191-199. https://doi.org/10.1002/fee.1257

Díaz, G. I., Nahuelhual, L., Echeverría, C., & Marín, S. L. (2011). Drivers of land abandonment in southern Chile and implications for landscape planning. *Landscape and Urban Planning*, 99(3-4), 207-217. https://doi.org/10.1016/j.landurbplan.2010.11.005

Dias, A., Palma, L., Carvalho, F., Neto, D., Real, J., & Beja, P. (2017). The role of conservative versus innovative nesting behavior on the 25-year population expansion of an avian predator. *Ecology and Evolution*, 7(12), 4241-4253. https://doi.org/10.1002/ece3.3007

Dorber, M., Arvesen, A., Gernaat, D., & Verones, F. (2020). Controlling biodiversity impacts of future global hydropower reservoirs by strategic site selection. *Scientific Reports*, 10, 21777. https://doi.org/10.1038/s41598-020-78444-6

Duriez, O., Herman, S., & Sarrazin, F. (2012). Intra-specific competition in foraging Griffon Vultures Gyps fulvus: The influence of supplementary feeding management. *Bird Study*, 59(2), 193-206. https://doi.org/10.1080/00063657.2012.658640

EDP (2015). *Programa Integrado de Monitorização Ambiental* (PIMA). *REV.03*. Fases de Enchimento e de Exploração. Aproveitamento Hidroelétrico do Baixo Sabor. 126pp.

eLTER (2019). eLTER Site Catalogue. Eds.: Sier, A., Pugnetti, A. and Bergami, C. 189pp.

Elas, M., Rosendal, E., and Meissner, W. (2023). The effect of floods on nest survival probability of common sandpiper *Actitis hypoleucos* breeding in the riverbed of a large lowland European river. *Diversity*, 15(1), 90. https://doi.org/10.3390/d15010090

Elith J., Graham C.H., Anderson R.P., Ferrier M., Dudı´k S., Guisan A., Hijmans R.J., Huettmann F., Leathwick J.R., Lehmann A., Li J. (2006) Novel methods improve prediction of species' distributions from occurrence data. *Ecography* 29:129–151

Eriksson, O. (2014). Evolution of angiosperm seed disperser mutualisms: the timing of origins and their consequences for coevolutionary interactions between angiosperms and frugivores. *Biological Reviews*, 91(1), 168-186. https://doi.org/10.1111/brv.12164

Faust, L. J., Thompson, S. D., Earnhardt, J. M., Brown, E., Ryan, S., Sherman, M., & Yurenka, M. (2003). Using stage-based system dynamics modeling for demographic management of captive populations. *Zoo Biology: Published in affiliation with the American Zoo and Aquarium Association*, *22*(1), 45-64. https://doi.org/10.1002/zoo.10071

Fearnside, P. M. (2016). Environmental and social impacts of hydroelectric dams in Brazilian Amazonia: Implications for the aluminum industry. *World development*, *77*, 48-65. https://doi.org/10.1016/j.worlddev.2015.08.015

Fernández-Gil, A., Lamas, J. A., Ansola, L. M., Román, J., de Gabriel Hernando, M., & Revilla, E. (2023). Population dynamics of recovering apex predators: Golden eagles in a Mediterranean landscape. *Journal of Zoology*, 319(2), 99-111. https://doi.org/10.1111/jzo.13026

Ferreira, M., Filipe, A. F., Magalhães, M. F., Carona, S., & Beja, P. (2020). Spatial modelling of temporal dynamics in stream fish communities under anthropogenic change. *Diversity and Distributions*, 27(2), 313-326. https://doi.org/10.1111/ddi.13189

Fonseca, A. and Santos, J. (2021). The impact of a hydroelectric power plant on a regional climate in Portugal. *Atmosphere*, 12(11), 1400. https://doi.org/10.3390/atmos12111400

García-Heras, M. S., Cortés-Avizanda, A., & Donázar, J. A. (2013). Who are we feeding? Asymmetric individual use of surplus food resources in an insular population of the endangered Egyptian Vulture. *PLOS ONE*, 8(12), e80523. https://doi.org/10.1371/journal.pone.0080523

Gardner, T. A., Barlow, J., Chazdon, R., Ewers, R. M., Harvey, C. A., Peres, C. A., & Sodhi, N. S. (2016). Prospects for tropical forest biodiversity in a human-modified world. *Ecology Letters, 12*(6), 561–582. https://doi.org/10.1111/j.1461-0248.2009.01294.x

Gracey, E. O., & Verones, F. (2016). Impacts from hydropower production on biodiversity in an LCA framework—review and recommendations. *The International Journal of Life Cycle Assessment*, 21, 412–428. https://doi.org/10.1007/s11367-016-1039-3

Geist, J. (2021). Green or red: Challenges for fish and freshwater biodiversity conservation related to hydropower. *Aquatic Conservation*, 31(7), 1551-1558. https://doi.org/10.1002/aqc.3597

Geneletti, D. (2003). Biodiversity impact assessment of roads: an approach based on ecosystem rarity. *Environmental impact assessment review*, 23(3), 343-365. https://doi.org/10.1016/S0195-9255(02)00099-9

Gil-Tena, A. S. S. U., Brotons, L., & Saura, S. (2009). Mediterranean forest dynamics and forest bird distribution changes in the late 20th century. *Global Change Biology*, *15*(2), 474-485. http://dx.doi.org/10.1111/j.1365-2486.2008.01730.x

Guisan, A., & Zimmermann, N. E. (2000). Predictive habitat distribution models in ecology. *Ecological Modelling, 135*(2–3), 147–186. https://doi.org/10.1016/S0304-3800(00)00354-9

Gregory, R. D., Noble, D. G., & Custance, J. (2004). The state of play of farmland birds: population trends and conservation status of lowland farmland birds in the United Kingdom. *Ibis*, *146*, 1-13. https://doi.org/10.1111/j.1474-919X.2004.00358.x

Grimm, V., Berger, U., DeAngelis, D. L., Polhill, J. G., Giske, J., & Railsback, S. F. (2010). The ODD protocol: A review and first update. *Ecological Modelling, 221*(23), 2760–2768. https://doi.org/10.1016/j.ecolmodel.2010.08.019

Hanowski, J. M., & Niemi, G. J. (1995). Experimental design considerations for establishing an off-road, habitat specific bird monitoring program using point counts. *Monitoring bird populations by point counts*, 145-150

He, F., Zarfl, C., Tockner, K., Olden, J. D., Campos, Z., Muniz, F., Svenning, J-C., & Jähnig, S. C. (2024). Hydropower impacts on riverine biodiversity. *Nature Reviews Earth & Environment*, 5, 755-772. https://doi.org/10.1038/s43017-024-00596-0

Heikkinen, R. K., Luoto, M., Virkkala, R., & Rainio, K. (2004). Effects of habitat cover, landscape structure and spatial variables on the abundance of birds in an agricultural–forest mosaic. *Journal of Applied Ecology*, *41*(5), 824-835. https://doi.org/10.1111/j.0021-8901.2004.00938.x

Herrando, S., Brotons, L., & Llacuna, S. (2005). Post-fire dynamics in Mediterranean shrublands: are bird communities structured by arthropod availability? *Revista catalana d'ornitologia*, 17-28.

Herrando, S. et al., (2019). Contrasting impacts of precipitation on mediterranean birds and butterflies. *Scientific Reports*, 9(1). https://doi.org/10.1038/s41598-019-42171-4

Hesselbarth, M. H. K., Sciaini, M., With, K. A., Wiegand, K., & Nowosad, J. (2019). landscapemetrics: an open-source R tool to calculate landscape metrics. *Ecography*, 42(10), 1648–1657. https://doi.org/10.1111/ecog.04617

Hughes, S. J., Cabral, J. A., Bastos, R., Cortes, R., Vicente, J., Eitelberg, D., Yu, H., Honrado, J., & Santos, M. (2016). A stochastic dynamic model to assess land use change scenarios on the ecological status of fluvial water bodies under the Water Framework Directive. *Science of the Total Environment*, 565, 427–439. https://doi.org/10.1016/j.scitotenv.2016.04.153

Hunt, W. G., Wiens, J. D., Law, P. R., Fuller, M. R., Hunt, T. L., Driscoll, D., & Jackman, R. E. (2017). Quantifying the demographic cost of human-related mortality to a raptor population. *PLOS ONE*, 12, e0172232. https://doi.org/10.1371/journal.pone.0172232

Instituto da Conservação da Natureza e da Biodiversidade (ICN-B) (1999). Plano sectorial da Rede 2000, Zonas da Proteção Especial. File available in: https://www.icnf.pt/api/file/doc/3b441467eeea8f39 (consulted on 4 September 2024)

International Energy Agency, 2021. Hydropower Special Market Report, *IEA*, Paris https://www.iea.org/reports/hydropower-special-market-report, License: CC BY 4.0

Jackson, A. L. (2011). Renewable energy vs. biodiversity: policy conflicts and the future of nature conservation. *Global Environmental Change*, 21(4), 1195-1208. https://doi.org/10.1016/j.gloenvcha.2011.07.001

Jaeger, J.A., (2000). Landscape division, splitting index, and effective mesh size: new measures of landscape fragmentation. *Landscape Ecology,* 15, 115–130. https://doi.org/10.1023/A:1008129329289

Jenks, G. F. (1967). The Data Model Concept in Statistical Mapping. *International Yearbook of Cartography*, 7, 186-190.

Johnston, A. S., Sibly, R. M., & Thorbek, P. (2018). Forecasting tillage and soil warming effects on earthworm populations. *Journal of Applied Ecology*, *55*(3), 1498-1509. https://doi.org/10.1111/1365-2664.13096

Kajtoch, Ł. and Figarski, T. (2013). Short-term restoration of riverine bird assemblages after a severe flood. *Bird Study*, 60(3), 327-334. https://doi.org/10.1080/00063657.2013.798260

Katuwal, H. et al., (2016). Seasonal changes in bird species and feeding guilds along elevational gradients of the central Himalayas, Nepal. *Plos O*ne, 11(7), e0158362. https://doi.org/10.1371/journal.pone.0158362

Kingsford, R. T. (2000). Ecological impacts of dams, water diversions and river management on floodplain wetlands in Australia. *Austral Ecology, 25*(2), 109–127. https://doi.org/10.1046/j.1442-9993.2000.01036.x

Kochert, M. N., & Steenhof, K. (2012). Frequency of nest use by Golden Eagles in southwestern Idaho. *Journal of Raptor Research*, *46*(3), 239-247. https://doi.org/10.3356/JRR-12-00001.1

Lees, A. C., Peres, C. A., Fearnside, P. M., et al. (2016). Hydropower and the future of Amazonian biodiversity. *Biodiversity and Conservation*, 25, 451-466. https://doi.org/10.1007/s10531-016-1072-3

Lemieux, C. J., Groulx, M. W., Bocking, S., & Beechey, T. J. (2018). Evidence-based decision-making in Canada's protected areas organizations: Implications for management effectiveness. *Facets*, *3*(1), 392-414. https://doi.org/10.1139/facets-2017-0107

Linnaeus, C. (1758). Systema Naturae per Regna Tria Naturae, Secundum Classes, Ordines, Genera, Species, cum Characteribus, Differentiis, Synonymis, Locis (10th ed.). Laurentii Salvii.

Linnaeus, C. (1766). Systema naturae per regna tria naturae, secundum classes, ordinus, genera, species, cum characteribus, differentiis, synonymis, locis. Tomus I. Editio duodecima, reformata. Impensis Direct. Laurentii Salvii, *Holmiae*. 532 p.

López-López, P., García-Ripollés, C., & Verdejo, J. (2014). Food predictability determines space use of endangered vultures: Implications for management of supplementary feeding. *Ecological Applications*, 24(5), 938-949. https://doi.org/10.1890/13-2000.1

Margalida, A., and Colomer, M. A. (2012). Modelling the effects of sanitary policies on European vulture conservation. *Scientific Reports*, 2, 753. https://doi.org/10.1038/srep00753

Margalida, A., Campion, D., Donázar, J. (2014a). Vultures vs livestock: Conservation relationships in an emerging conflict between humans and wildlife. *Oryx*. 48. 172-176. DOI: 10.1017/S0030605312000889

Margalida, A., Colomer, M. À., & Oro, D. (2014b). Man-induced activities modify demographic parameters in a long-lived species: Effects of poisoning and health policies. *Ecological Applications*, 24(3), 436-444. https://doi.org/10.1890/13-0414.1

Mateo-Tomás, P., Olea, P. P., and Fombellida, I. (2010a). Status of the endangered Egyptian vulture (*Neophron percnopterus*) in the Cantabrian mountains, Spain, and assessment of threats. *Oryx*, 44(3), 434-440. https://doi.org/10.1017/s0030605310000505

Mateo-Tomás, P. and Olea, P. P. (2010b). Diagnosing the causes of territory abandonment by the endangered Egyptian vulture (*Neophron percnopterus*): the importance of traditional pastoralism and regional conservation. *Oryx*, 44(3), 424-433. https://doi.org/10.1017/s0030605310000189

McGarigal, K., S.A. Cushman, M.C. Neel, and E. Ene. 2002. FRAGSTATS: Spatial Pattern Analysis Program for Categorical Maps. Computer software program produced by the authors at the *University of Massachusetts*, Amherst, available at the following web site: https://www.fragstats.org.

Mor, J., Ruhí, A., Tornés, E., Valcárcel, H., Muñoz, I., and Sabater, S. (2018). Dam regulation and riverine food-web structure in a mediterranean river. *Science of the Total Environment*, 625, 301-310. https://doi.org/10.1016/j.scitotenv.2017.12.296

Monteiro-Henriques, T. (2010). Landscape and phytosociology of the Paiva river's hydrographical basin and contiguous basins of the Douro River's left margin, from the Paiva to the Tedo River. *Instituto Superior de Agronomia – University of Lisbon*

Morant, J., Zabala, J., Martínez, J. A., and Zuberogoitia, Í. (2018). Out of sight, out of mind? testing the effects of overwinter habitat alterations on breeding territories of a migratory endangered species. *Animal Conservation*, 21(6), 465-473. https://doi.org/10.1111/acv.12412

Moreira, F., Ferreira, P. G., Rego, F. C., & Bunting, S. (2001). Landscape changes and breeding bird assemblages in northwestern Portugal: the role of fire. *Landscape Ecology*, *16*, 175-187. https://doi.org/10.1023/A:1011169614489

Moreira, F., Beja, P., Morgado, R., Reino, L., Gordinho, L., Delgado, A., & Borralho, R. (2005). Effects of field management and landscape context on grassland wintering birds in Southern Portugal. *Agriculture, Ecosystems & Environment*, 109(1–2), 59–74. https://doi.org/10.1016/j.agee.2005.02.011

Moreira, *et al.*. (2012). Mosaic-level inference of the impact of land cover changes in agricultural landscapes on biodiversity: a case-study with a threatened grassland bird. *PLoS ONE*, 7(6), e38876. https://doi.org/10.1371/journal.pone.0038876

Moreno-Opo, R., Trujillano, A., Arredondo, Á., Guzmán, J. L., Higuero, R., & Margalida, A. (2015). Manipulating size, amount and appearance of food inputs to optimize supplementary feeding programs for European vultures. *Biological Conservation*, 181, 27-35. https://doi.org/10.1016/j.biocon.2014.10.022

Moreno-Opo, R., Trujillano, A., Margalida, A. (2020). Larger size and older age confer competitive advantage: dominance hierarchy within European vulture guild. *Scientific Reports*, 10, 2430. https://doi.org/10.1038/s41598-020-59387-4

Morgado, R., Santana, J., Porto, M., Sánchez-Oliver, J. S., Reino, L., Herrera, J. M., Rego, F., Beja, P., & Moreira, F. (2020). A Mediterranean silent spring? The effects of olive farming intensification on breeding bird communities. *Agriculture, Ecosystems & Environment*, 288, 106694. https://doi.org/10.1016/j.agee.2019.106694

Mota P., Vingada J. V., Ferreira J., Diogo H. M., Morgado R. G., Rodrigues P., Garrido N., Eira C. I., Pinto N., Marques C., Múrias T. (2020a). EDP Baixo Sabor: Construction and Reservoir Filling Phases - Iberian Wolf (Canis lupus) [Sign surveys] [2010-2014]. Version 1.2. *EDP*. Sampling event dataset https://doi.org/10.15468/zsqtsy accessed via GBIF.org on 2025-04-30

Mota P., Gomes C., Zina H. A., Araújo P. M., Oliveira C. A., Marques S. M., Mendes J. D., Múrias T., (2020b). EDP Baixo Sabor: Construction and Reservoir Filling Phases - Cliff-nesting species: Breeding sites [2010-2014]. *EDP*. Sampling event dataset https://doi.org/10.15468/4aqk8t accessed via GBIF.org on 2025-01-21.

Mota P., Gomes C., Zina H. A., Araújo P. M., Oliveira C. A., Marques S. M., Mendes J. D., Múrias T., (2020c). EDP Baixo Sabor: Construction and Reservoir Filling Phases – Cliff-nesting birds, prioritary conservation species: fixed observation points [2010-2014]. Version 1.1. *EDP*. Sampling event dataset https://doi.org/10.15468/zikgab accessed via GBIF.org on 2025-01-21.

Mota-Ferreira, M., Filipe, A. F., Filomena Magalhaes, M., Carona, S., & Beja, P. (2021). Spatial modelling of temporal dynamics in stream fish communities under anthropogenic change. *Diversity and Distributions*, 27(2), 313-326. https://doi.org/10.1111/ddi.13189

Mulatu, T., Bastos, R., Santos, M., Sousa, J. P., Silva, P. M. d., & Cabral, J. A. (2016). Do the passerine traits' dynamic patterns indicate the ecological status of agro-forestry ecosystems? a modelling approach for "montado" management assessments. *Global Ecology and Conservation*, 8, 154-169. https://doi.org/10.1016/j.gecco.2016.09.001

Nasruddin-Roshidi, A., Mansor, M., Ismail, N. A., Ngadi, E., Izzat-Husna, M., Husin, S., and Nor, S. M. (2021). Recovery of bird communities following the construction of a large-scale hydroelectric dam. *Ecological Processes*, 10(1). https://doi.org/10.1186/s13717-021-00298-1

Neter, J., Kutner, M., Nachtshei, C., Wasserma, W., 1996. Applied Linear Regression Models, third ed. McGraw-Hill, Boston.

Newbold, T., Hudson, L., Hill, S. *et al.,* (2015). Global effects of land use on local terrestrial biodiversity. *Nature,* 520, 45–50. https://doi.org/10.1038/nature14324

Nilsson, C., & Berggren, K. (2000). Alterations of riparian ecosystems caused by river regulation: Dam operations have caused global-scale ecological changes in riparian ecosystems. How to protect river environments and human needs of rivers remains one of the most important questions of our time. *BioScience*, *50*(9), 783-792.

https://doi.org/10.1641/0006-3568(2000)050[0783:AORECB]2.0.CO;2

O'Hara, R., & Kotze, J. (2010). Do not log-transform count data. *Nature Precedings*, 1-1. https://doi.org/10.1111/j.2041-210X.2010.00021.x

Olimpi, E. M., *et al.,* (2022). Semi-natural habitat surrounding farms promotes multifunctionality in avian ecosystem services. *Journal of Applied Ecology*, 59(4), 898-908. https://doi.org/10.1111/1365-2664.14124

Pearce-Higgins, J., Eglington, S., Martay, B., & Chamberlain, D. (2015). Drivers of climate change impacts on bird communities. *Journal of Animal Ecology*, 84(4), 943-954. https://doi.org/10.1111/1365-2656.12364

Pinheiro, J. C., and Bates, D. M. (2000). Mixed-Effects Models in S and S-PLUS. *Springer*. https://doi.org/10.1007/b98882

Poff, N. L., & Zimmerman, J. K. (2010). Ecological responses to altered flow regimes: a literature review to inform the science and management of environmental flows. *Freshwater biology*, *55*(1), 194-205. https://doi.org/10.1111/j.1365-2427.2009.02272.x

QGIS Development Team (2020). QGIS Geographic Information System. Open-Source Geospatial Foundation Project.

QGIS Development Team (2024) QGIS Geographic Information System. Open-Source Geospatial Foundation Project.

R Development Core Team (2020) R: A Language and Environment for Statistical Computing. R Foundation for Statistical Computing, Vienna, Austria. https://www.r-project.org/

R Core Team (2024) R: A Language and Environment for Statistical Computing. R Foundation for Statistical Computing.

Railsback, S. F. and Johnson, M. D. (2014). Effects of land use on bird populations and pest control services on coffee farms. Proceedings of the *National Academy of Sciences*, 111(16), 6109-6114. https://doi.org/10.1073/pnas.1320957111

Ralph, C. J., Sauer, J. R., & Droege, S. (1993). Monitoring bird populations by point counts. *USDA Forest Service General Technical Report PSW-GTR*-149. https://doi.org/10.2737/PSW-GTR-149

Regos, A., D'Amen, M., Herrando, S., Guisan, A., & Brotons, L. (2015). Fire management, climate change and their interacting effects on birds in complex Mediterranean landscapes: dynamic distribution modelling of an early-successional species—the near-threatened Dartford Warbler (Sylvia undata). *Journal of Ornithology*, *156*, 275-286. https://doi.org/10.1007/s10336-015-1174-9

Reino, L., Beja, P., Osborne, P., Morgado, R., Fabião, A., & Rotenberry, J. (2009). Distance to edges, edge contrast and landscape fragmentation: interactions affecting farmland birds around forest plantations. *Biological Conservation*, 142(4), 824-838. https://doi.org/10.1016/j.biocon.2008.12.011

Roscioni, F., Russo, D., Di Febbraro, M., Frate, L., Carranza, M. L., & Loy, A. (2013). Regional-scale modelling of the cumulative impact of wind farms on bats. *Biodiversity and Conservation*, *22*, 1821-1835. https://doi.org/10.1007/s10531-013-0515-3

Salaberría, C., Celis, P., López-Rull, I., & Gil, D. (2013). Effects of temperature and nest heat exposure on nestling growth, dehydration and survival in a mediterranean hole-nesting passerine. *Ibis*, 156(2), 265-275. https://doi.org/10.1111/ibi.12121

Sánchez-Zapata, J.A. et al. (2016). Effects of Renewable Energy Production and Infrastructure on Wildlife. In: Mateo, R., Arroyo, B., Garcia, J. (eds) Current Trends in Wildlife Research. Wildlife Research Monographs, vol 1. *Springer*, Cham. https://doi.org/10.1007/978-3-319-27912-1_5

Santos, M., & Cabral, J. A. (2004). Development of a stochastic dynamic model for ecological indicators' prediction in changed Mediterranean agroecosystems of north-eastern Portugal. *Ecological Indicators, 3*(4), 285–303. https://doi.org/10.1016/j.ecolind.2003.11.007

Santos, M., Bastos, R., & Cabral, J. A. (2013). Converting conventional ecological datasets in dynamic and dynamic spatially explicit simulations: current advances and future applications of the stochastic dynamic methodology (StDM). *Ecological Modelling*, 258, 91-100. https://doi.org/10.1016/j.ecolmodel.2013.02.028

Santos M., Ferreira D., Bastos R., Vicente J., Honrado J., Kueffer C., Kull C., Berger U. & Cabral J.A. (2016a). Linking landscape futures with biodiversity conservation strategies in northwest Iberia - a simulation study combining surrogates with a spatio-temporal modelling approach. *Ecological Informatics*, 33: 85-100. https://doi.org/10.1016/j.ecoinf.2016.04.008

Santos, M., Santos, R., Cabral, J., Pacheco, F., Leitão, D., Moreira, F., & Silva, J. (2016b). Impacts of land use and infrastructural changes on threatened little bustard *Tetrax tetrax* breeding populations: quantitative assessments using a recently developed spatially explicit dynamic modelling framework. *Bird Conservation International*, 26(4), 418-435. https://doi.org/10.1017/s0959270915000258

Santos, M., Silva, S., Bastos, R., Carvalho, D., & Cabral, J. A. (2018). How good are the ecological assumptions and predictions made in the past? insights from a dynamic modelling approach applied to changing landscapes. *Ecological Indicators*, 90, 226-230. https://doi.org/10.1016/j.ecolind.2018.03.023

Santos, M., Bastos, R., Vicente, J., Berger, U., & Cabral, J. A. (2022). Why do agroforestry systems enhance biodiversity? evidence from habitat amount hypothesis predictions. *Frontiers in Ecology and Evolution, 9*. https://doi.org/10.3389/fevo.2021.630151

Santos, R., Fernandes, L., Cortes, R., & Pacheco, F. (2019a). Development of a hydrologic and water allocation model to assess water availability in the Sabor river basin (Portugal). International Journal of Environmental Research and Public Health, 16(13), 2419. https://doi.org/10.3390/ijerph16132419

Santos, R., Fernandes, L., Cortes, R., & Pacheco, F. (2019b). Hydrologic impacts of land use changes in the Sabor river basin: a historical view and future perspectives. *Wate*r, 11(7), 1464. https://doi.org/10.3390/w11071464

Santos, R., Fernandes, L. F. S., Pacheco, F. A. L., Monteiro, S. M., & Jesus, J. (2021). River restoration for the replacement of lost spawning grounds due to dam construction. *WIT Transactions on Ecology and the Environment*. https://doi.org/10.2495/wrm210041

Sappington, J. M., Longshore, K. M., & Thompson, D. B. (2007). Quantifying landscape ruggedness for animal habitat analysis: A case study using bighorn sheep in the Mojave Desert. *Journal of Wildlife Management, 71*(5), 1419–1426. https://doi.org/10.2193/2005-723

Şekercioğlu, C. H., Daily, G. C., & Ehrlich, P. R. (2016). Ecosystem consequences of bird declines. Proceedings of the *National Academy of Sciences* (PNAS), 101(52), 18042–18047. https://doi.org/10.1073/pnas.0408049101

Shono, H., 2000. Efficiency of the finite correction of Akaike's information criteria. Fish. Sci. 66, 608–610.

Smith, E. P. (2006). BACI design. *Encyclopedia of Environmetrics*, 1, 141-148. https://doi.org/10.1002/9780470057339.vab001

Srinivasan, U., Elsen, P., & Wilcove, D. (2019). Annual temperature variation influences the vulnerability of montane bird communities to land-use change. *Ecography,* 42(12), 2084-2094. https://doi.org/10.1111/ecog.04611

Tack, J. D., Noon, B. R., Bowen, Z. H., & Fedy, B. C. (2019). Ecosystem processes, land cover, climate, and human settlement shape dynamic distributions for Golden Eagles across the Western US. *Animal Conservation*, 23(1), 72-82. https://doi.org/10.1111/acv.12511

Tirozzi, P., Massimino, D., & Bani, L. (2024). Avian responses to climate extremes: insights into abundance curves and species sensitivity using the UK breeding bird survey. *Oecologia*, 204(1), 241-255. https://doi.org/10.1007/s00442-023-05504-9

Topping C.J., Odderskær P., Kahlert J. (2013). Modelling skylarks (*Alauda arvensis*) to predict impacts of changes in land management and policy: development and testing of an Agent-Based Model. *PLOS ONE* 8(6): e65803. https://doi.org/10.1371/journal.pone.0065803

Vandewalle, M., de Bello, F., Berg, M. P., et al. (2010). Functional traits as indicators of biodiversity response to land use changes across ecosystems and organisms. *Biodiversity and Conservation, 19*, 2921–2947. https://doi.org/10.1007/s10531-010-9798-9

Velevski, M. et al. (2014). Population decline and range contraction of the Egyptian Vulture (*Neophron percnopterus*) in the Balkan Peninsula. *Bird Conservation International*, 25(4), 440-450. https://doi.org/10.1017/s0959270914000343

Watson, J. (2010). The Golden Eagle, Second Edition. *Bloomsbury Publishing*.

Watson, J. and Davies, R. (2015). Comparative diets of nesting golden eagles in the Columbia basin between 2007–2013 and the late 1970s. *Northwestern Naturalist*, 96(1), 81-86. https://doi.org/10.1898/nwn13-31.1

Wilensky, U. (1999). NetLogo (and NetLogo User Manual. Center for Connected Learning and Computer-Based Modeling, Northwestern University. https://ccl.northwestern.edu/netlogo/docs/

Wisz, M., Guisan, A., 2009. Do pseudo-absence selection strategies affect geographic predictions of species? A virtual species approach. *BMC Ecol*. 9, 8. https://doi.org/10.1186/1472-6785-9-8.

Zarfl, C., Lumsdon, A. E., Berlekamp, J., Tydecks, L., & Tockner, K. (2015). A global boom in hydropower dam construction. *Aquatic Sciences*, 77(1), 161-170. https://doi.org/10.1007/s00027-014-0377-0

Zarfl, C., Berlekamp, J., He, F., Jähnig, S. C., & Darwall, W. (2019). Future large hydropower dams impact global freshwater megafauna. *Scientific Reports*, 9, 18531. https://doi.org/10.1038/s41598-019-54980-8

Zuberogoitia, Í., Zabala, J., Martínez, J. A., Martínez, J. E., & Azkona, A. (2008). Effect of human activities on Egyptian Vulture breeding success. *Animal Conservation*, 11(4), 313-320. https://doi.org/10.1111/j.1469-1795.2008.00184.x

Zuberogoitia, Í., González-Oreja, J. A., Martínez, J. E., et al. (2013). Foraging movements of Eurasian Griffon Vultures (*Gyps fulvus*): implications for supplementary feeding management. *European Journal of Wildlife Research*, 59, 421–429. https://doi.org/10.1007/s10344-012-0687-2

Zuberogoitia, Í., Zabala, J., Martínez, J. A., González-Oreja, J. A., & López-López, P. (2014). Effective conservation measures to mitigate the impact of human disturbances on the endangered Egyptian Vulture. *Animal Conservation*, 17(5), 410-418. https://doi.org/10.1111/acv.12107

Zurell, D., *et al.,* (2015). Individual-based modelling of resource competition to predict density-dependent population dynamics: a case study with white storks. *Oikos*, *124*(3), 319-330. https://doi.org/10.1111/oik.01294

Supplementary information:

Appendix I - Classification and ecological relevance of LU/LC categories in the Baixo Sabor study area.

Aggregated Category	Component Land Uses	Ecological Function	Key Species Benefits
Traditional Agricultural Mosaics	Improved pastures, olive groves, cultural mosaics, semi-natural agriculture	Heterogeneous landscape providing diverse feeding and nesting opportunities	Passerines thrive in mixed agricultural systems
Coniferous Forest	Maritime pine forests, umbrella pine forests, other coniferous forests	Provides nesting sites and shelter	Forest bird species
Olive Groves and Orchards	Olive groves, fruit orchards	Semi-open canopy with spaced trees and open understory	Insectivorous and granivorous passerines
Deciduous Forest	Agroforestry systems, cork oak forests, chestnut forests, eucalyptus forests, holm oak forests, other deciduous forests	High biodiversity support, essential resources provision	Multiple passerine species
Pastures	Spontaneous and improved pastures	Critical seed resources for ground-foraging birds	Ground-foraging species
Urban Areas	Horizontal and discontinuous fabric, low-density fabric, road networks, construction areas, cultural facilities	Artificial nesting sites and food resources, habitat fragmentation	Urban-adapted species
Temporary Crops	Annual crops, rotational cultivation	Open habitats with low vegetation cover	Ground-nesting birds
Vineyards	Vineyard cultivation	Semi-open habitats with structured vegetation	Ground-nesting species
Shrublands	Natural and semi-natural shrub-dominated areas	Provision of dense cover for nesting and shelter in open landscapes	Shrubland-associated bird species
Natural Water Sources	Rivers, streams, natural ponds	Hydration and insect attraction	Multiple species
Reservoir	Dam-created water body	Modified aquatic habitat	Waterbirds and passerines

Appendix II - ODD Protocol for the Agent-Based Model

Overview

The purpose of this agent-based model (ABM) is to assess the ecological impacts of hydroelectric infrastructures on local avifauna, with a focus on passerine birds. The model simulates how changes in habitat structure, resource availability, and environmental conditions caused by hydroelectric projects influence the distribution, behaviour, and interactions of bird populations. The model aims to provide insights into the mechanisms driving biodiversity changes by integrating field data and ecological principles, and to inform conservation strategies for mitigating the impacts of hydroelectric infrastructures.

This approach is consistent with the methodologies described in Santos et al. (2020) and Santos et al. (2022), where agent-based models were used to explore ecological interactions and biodiversity patterns in complex landscapes. The model also follows the ODD protocol framework proposed by Grimm et al. (2010), ensuring transparency and reproducibility in its design and implementation.

The entities in the model include individual birds, which are characterized by species identity, habitat preferences, and resource use (e.g., insects, seeds, etc). The environment is represented as a spatially explicit landscape divided into habitat patches, each defined by vegetation type, resource availability, and proximity to hydroelectric infrastructures. The temporal scale of the model is designed to capture seasonal variations in bird activity, while the spatial scale reflects the study area impacted by hydroelectric projects.

The processes in the model are structured to simulate the interactions between birds and their environment, including habitat selection, resource use, and the effects of habitat fragmentation. These processes are informed by ecological data and field observations, ensuring that the model reflects the specific dynamics of passerine populations in the context of hydroelectric infrastructures.

Design Concepts

The model is grounded in the principles of landscape ecology and avian ecology, emphasizing the interactions between individual birds and their environment. Emergent properties, such as changes in species distribution and community composition, arise from the interactions between birds and habitat patches. The model assumes that birds adapt their habitat use based on resource availability and environmental conditions, but it does not explicitly include learning or predictive behaviours. Instead, birds respond to current conditions in their local environment, reflecting the ecological constraints observed in field studies.

The model incorporates stochasticity to account for variability in resource availability and environmental conditions, ensuring that the simulations capture the inherent uncertainty in ecological systems. Observations from the model include changes in species richness, abundance, and habitat use, which are analysed to evaluate the impacts of hydroelectric infrastructures on avian biodiversity.

Details

The model is initialized with a predefined number of bird agents distributed across the landscape based on habitat suitability. Habitat patches are characterized by their vegetation type, resource levels, and proximity to hydroelectric infrastructures. Input data for the model are derived from field studies and ecological surveys, ensuring that the simulations are grounded in empirical evidence.

The submodels in the ABM simulate key ecological processes, including habitat selection and resource use. These submodels are informed by the ecological characteristics of passerine birds and the specific impacts of hydroelectric infrastructures, as described in the literature. The outputs of the model are analysed to identify patterns and trends in avian biodiversity, providing insights into the mechanisms driving ecological changes in the study area.

The model interface: the world's view and commands associated with initial models settings:

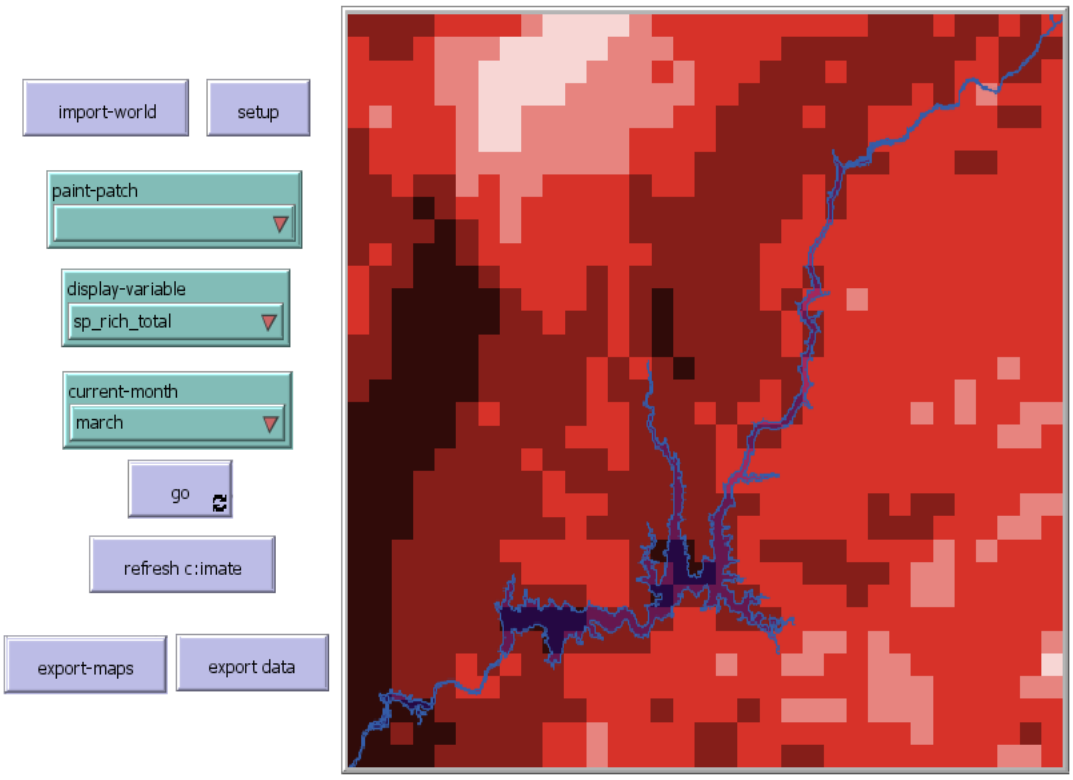

Commands	Type	Functions
Import-world	Button	To load environmental data (e.g., shapefiles) into NetLogo.
Setup	Button	To define the world's view and initializes model conditions, displaying environmental data dominance per pixel.
Paint-patch	Chooser	Pre-selected before running the 'Setup' button to display the dominant environmental variable per pixel.
Display-variable	Chooser	To display the selected response variable (e.g., total species richness).
Current-month	Chooser	To define the month for which data is displayed in the world.
Go	Button	To run the model, simulating species distribution across space and time.
Refresh climate	Button	To update climate variable data for the selected month.
Export-maps	Button	To export the generated maps for further visualization.
Export-data	Button	To export the data as a CSV file for metrics calculation in R.

Appendix III – Framework of the Netlogo code

a) Loading of environmental data in Netlogo

```
to setup_world
  clear-all

  ;  LULC importation
  set vin gis:load-dataset "C:/Users/tijse/Downloads/ETUDES/LEFT/M_shape_datas/NetLogo_World_Works/LULC_COS2015/bis/vinhas.shp"
  set cultemp gis:load-dataset "C:/Users/tijse/Downloads/ETUDES/LEFT/M_shape_datas/NetLogo_World_Works/LULC_COS2015/bis/cultemp2015.shp"
  set mat gis:load-dataset "C:/Users/tijse/Downloads/ETUDES/LEFT/M_shape_datas/NetLogo_World_Works/LULC_COS2015/bis/matos.shp"
  set olivpom gis:load-dataset "C:/Users/tijse/Downloads/ETUDES/LEFT/M_shape_datas/NetLogo_World_Works/LULC_COS2015/bis/olivpomare.shp"
  set conif gis:load-dataset "C:/Users/tijse/Downloads/ETUDES/LEFT/M_shape_datas/NetLogo_World_Works/LULC_COS2015/bis/coniferous2015.shp"
  set curso_agua gis:load-dataset "C:/Users/tijse/Downloads/ETUDES/LEFT/M_shape_datas/NetLogo_World_Works/LULC_COS2015/bis/watersource.shp"
  set decid gis:load-dataset "C:/Users/tijse/Downloads/ETUDES/LEFT/M_shape_datas/NetLogo_World_Works/LULC_COS2015/bis/deciduous2015.shp"
  set past gis:load-dataset "C:/Users/tijse/Downloads/ETUDES/LEFT/M_shape_datas/NetLogo_World_Works/LULC_COS2015/bis/pastagens2015.shp"
  set trad_agro gis:load-dataset "C:/Users/tijse/Downloads/ETUDES/LEFT/M_shape_datas/NetLogo_World_Works/LULC_COS2015/bis/tradi_agro_mos2015.shp"
  set dist gis:load-dataset "C:/Users/tijse/Downloads/ETUDES/LEFT/M_shape_datas/NetLogo_World_Works/COS2010/distance2015.shp"
  set urb gis:load-dataset "C:/Users/tijse/Downloads/ETUDES/LEFT/M_shape_datas/NetLogo_World_Works/LULC_COS2015/bis/urban_area2015.shp"
  set albuf gis:load-dataset "C:/Users/tijse/Downloads/ETUDES/LEFT/M_shape_datas/NetLogo_World_Works/albufeira/AHBS_Albufeira.shp"

  set rug gis:load-dataset "C:/Users/tijse/Downloads/ETUDES/LEFT/M_shape_datas/NetLogo_World_Works/RUGOSITY SLOPE/rugosity_shape.shp"
  set elev gis:load-dataset "C:/Users/tijse/Downloads/ETUDES/LEFT/M_shape_datas/NetLogo_World_Works/topography/elevation.shp"


 ; Load climate files dynamically based on selected month
  set temp gis:load-dataset get-temperature-file current-month
  set prec gis:load-dataset get-precipitation-file current-month
```

b) Displaying of the river/reservoir layer onto the world map:

```
to display-albufeira
  ; Set the color for the watersource shapefile with transparency
  gis:set-drawing-color (list 0 0 255 60)  ; RGB + alpha (0-255)

  ; Draw the filled polygon
  gis:fill albuf 1

  ; Set the color for the watersource shapefile
  gis:set-drawing-color blue

  ; Draw the shapefile on the world
  gis:draw albuf 1
end

to display-sabor
  ; Set the color for the watersource shapefile
  gis:set-drawing-color blue

  ; Draw the shapefile on the world
  gis:draw rio 1
end
```

c) Application of environmental data coverage to the patches

```
gis:set-world-envelope (gis:envelope-union-of (gis:envelope-of vin) (gis:envelope-of cultemp) (gis:envelope-of mat) (gis:envelope-of olivpom) (gis:envelope-of conif) (gis:envelope-of curso_agua)
  (gis:envelope-of decid) (gis:envelope-of past) (gis:envelope-of trad_agro) (gis:envelope-of dist) (gis:envelope-of urb) (gis:envelope-of albuf) (gis:envelope-of rio))

gis:set-world-envelope-ds gis:envelope-of rug
gis:set-world-envelope-ds gis:envelope-of elev
gis:set-world-envelope-ds gis:envelope-of temp
gis:set-world-envelope-ds gis:envelope-of prec
```

```
 ; Apply shapefile coverage to patches
 gis:apply-coverage vin "AREA_HA" vinhas
 gis:apply-coverage cultemp "AREA_HA" cultemporario
 gis:apply-coverage mat "AREA_HA" matos
 gis:apply-coverage olivpom "AREA_HA" olivepomare
 gis:apply-coverage conif "AREA_HA" coniferous
 gis:apply-coverage curso_agua "AREA_HA" watersource
 gis:apply-coverage decid "AREA_HA" deciduous
 gis:apply-coverage past "AREA_HA" pasture
 gis:apply-coverage trad_agro "AREA_HA" traditional_agro
 gis:apply-coverage dist "DISTBY" distancewater
 gis:apply-coverage urb "AREA_HA" urban_area
 gis:apply-coverage albuf "AREA_HA" albufeira
 gis:apply-coverage rug "DN" rugosity
 gis:apply-coverage elev "DN" elevation
 gis:apply-coverage prec "DN" precipitation
 gis:apply-coverage temp "DN" temperature
```

d) Specification of equations included in the model and calculation of the response variables

```
to calculate_sp_rich_total
 ask patches [

 ; Coefficients derived from Multiple Linear Regression analysis in R

 ; These coefficients represent the relationship between environmental variables

 ; and total species richness (response variable)

  let intercept 2.645651552972
  let coef_matos 0.000000002982
  let coef_olivepomare 0.000000261309
  let coef_elevation -0.000907683167
  let coef_rugosity -0.019450948057
  let coef_precipitattion -0.000231393422
  let coef_distancewater  0.000035247339
  let coef_pasture 0.000000244850
  let coef_coniferous -0.000000205709
  let coef_urban_area -0.000000202522
  let coef_cultemporario 0.000000039091
  let coef_temperature -0.010784576320
  let coef_albufeira -0.000000624773


; Calculate predicted species richness using the linear predictor

; Combines all environmental variables with their respective coefficients
     let log_prediction intercept +
     (coef_matos * matos) +
     (coef_olivepomare * olivepomare) +
     (coef_elevation * elevation) +
     (coef_rugosity * rugosity) +
     (coef_precipitation * precipitation) +
     (coef_distancewater * distancewater) +
     (coef_pasture * pasture) +
     (coef_coniferous * coniferous) +
     (coef_urban_area * urban_area) +
     (coef_cultemporario * cultemporario) +
     (coef_temperature * temperature) +
     (coef_albufeira * albufeira)


  ; Back-transform the prediction from log scale to original scale
  let raw_prediction exp(log_prediction)

  ; ; Assign the predicted value to sp_rich_total and round to nearest integer
  set sp_rich_total raw_prediction
  set sp_rich_total round sp_rich_total


  ; Constrain predictions to non-negative values
  if sp_rich_total < 0 [ set sp_rich_total 0 ]

 ]

end
```

e) Dominant variable parametrization from Netlogo

```
to dominant_variable
  ask patches [
    let max-value max (list vinhas cultemporario matos olivepomare coniferous watersource deciduous pasture traditional_agro distancewater urban_area rugosity elevation temperature precipitation )
    ifelse  vinhas = max-value [ set pcolor green + 21] [
      ifelse  cultemporario = max-value [ set pcolor 94 ] [
       ifelse  matos = max-value [ set pcolor yellow + 3] [
          ifelse  olivepomare = max-value [ set pcolor green + 19] [
          ifelse  coniferous = max-value [ set pcolor green ] [
              ifelse  watersource = max-value [ set pcolor 72] [
                ifelse  deciduous = max-value [ set pcolor green + 11 ] [
                ifelse  pasture = max-value [ set pcolor green ] [
                ifelse  traditional_agro = max-value [ set pcolor  gray] [
                ifelse  urban_area = max-value [ set pcolor violet ] [
                ifelse  albufeira = max-value [ set pcolor 73 ] [
                ifelse  distancewater = max-value [ set pcolor 86] [
                ifelse  rugosity = max-value [ set pcolor lime ] [
                ifelse  elevation = max-value [ set pcolor red + 1 ] [
                ifelse  temperature = max-value [ set pcolor 123  ] [
                ifelse  precipitation = max-value [ set pcolor 93 ] [
                                        set pcolor white
                                      ]
                                    ]
                                  ]
                                ]
                              ]
                            ]
                          ]
                        ]
                      ]
                    ]
                  ]
                ]
              ]
            ]
          ]
        ]
      ]
    ]
end


to paint-patches
  let var-name paint-patch
            ifelse paint-patch != "" [ ; check if a variable is selected
  ask patches [
    let value (runresult (word "[ " var-name " ] of self "))  ; dynamically execute the code to get the value of the variable
    let max-val max [runresult (word "[ " var-name " ]  of self")] of patches ; calculates the maximum value of this variable on all patches

      set pcolor scale-color blue value 0 max-val ] ;; applies the color in scale
  ] [
    dominant_variable ; execute this variable if no procedure is selected
  ]
end
```

f) Netlogo interface with the dominant variable represented on each patch

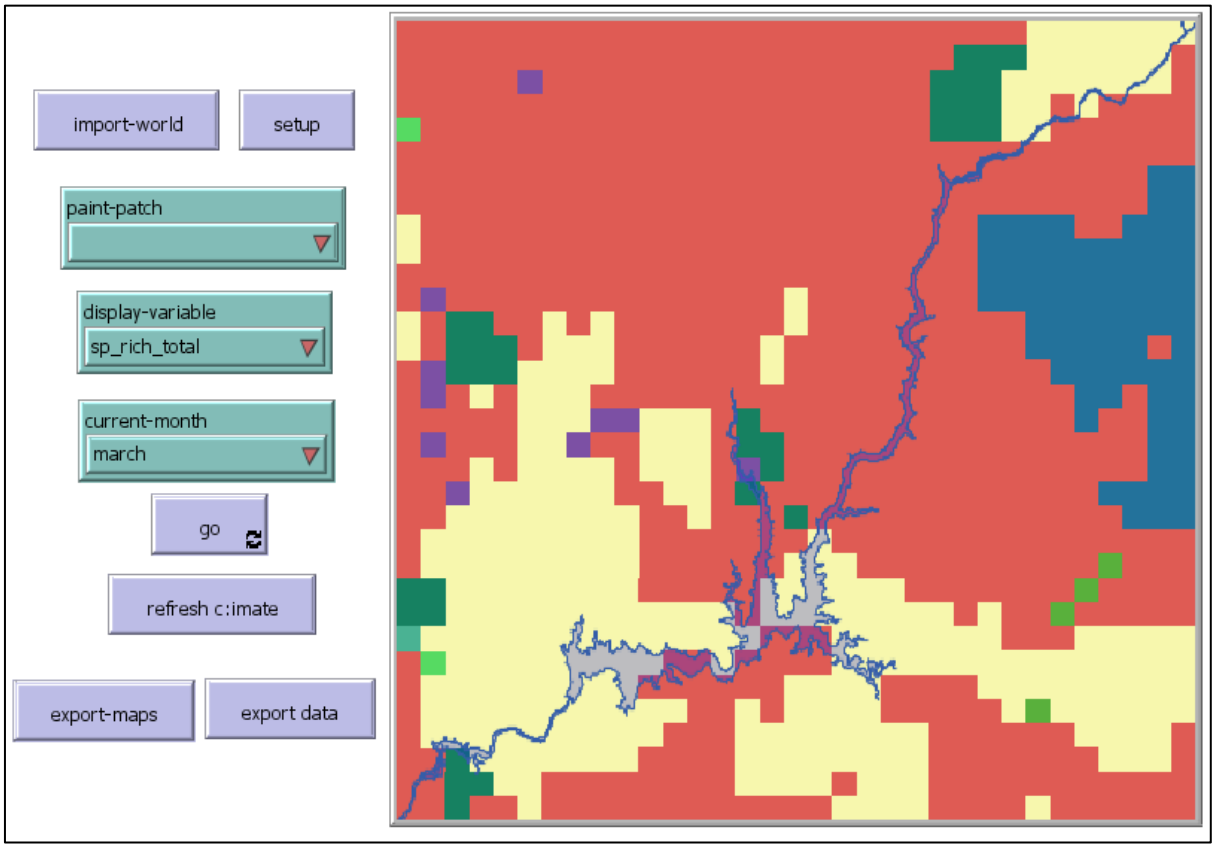

g) Parametrization of the visualization of the prediction maps:

```
to update-visuals
 ;; Clear the drawing layer before adding new elements
  clear-drawing


  ask patches [
    let val sp_rich_total
    ifelse val <= item 1 natural-breaks [
      set pcolor 19  ; lightest red
    ][
      ifelse val <= item 2 natural-breaks [
        set pcolor 17
      ][
        ifelse val <= item 3 natural-breaks [
          set pcolor 15
        ][
          ifelse val <= item 4 natural-breaks [
            set pcolor 13
          ][
            set pcolor 11  ; darkest red
          ]
        ]
      ]
    ]
  ]


    display-albufeira
    display-sabor


end
```

h) Export function of data and maps from Netlogo

```
to export-data-for-metrics-2015
  let filename (word "total_metrics_2015_" current-month ".csv")
  file-open filename
  file-print "x,y,sp_rich_total"
  ask patches [
    file-print (word pxcor "," pycor "," sp_rich_total)
  ]
  file-close
  print (word "Exported data for " current-month " 2015")
end

to export-maps
     let file-name (word "sp_rich_total_2015_" current-month ".png")
     export-view file-name
     show (word "World exported as image: " file-name)
end
```

Appendix IV – Statistical outputs (MMI) for passerine species richness and abundance, discriminated by functional group.

a) Grassland specie richness

Variables	Coefficient	Std. Error	Adjusted SE	z value	P-value
(Intercept)	2.092e+00	3.845e-01	3.852e-01	5.432	1.00e-07 ***
area_coniferous_forest	-1.175e-06	3.923e-07	3.931e-07	2.989	0.002798 **
area_temporary_crops	1.436e-06	8.990e-07	9.003e-07	1.595	0.110608
area_deciduous_forest	-1.529e-06	3.618e-07	3.626e-07	4.216	2.48e-05 ***
area_olives_orchards	-4.617e-07	3.768e-07	3.773e-07	1.224	0.221103
area_vineyards	-1.640e-06	1.450e-06	1.452e-06	1.129	0.258863
average_precip_buffer	4.346e-03	1.200e-03	1.202e-03	3.614	0.000301 ***
distance_water	-1.937e-05	2.544e-05	2.547e-05	0.761	0.446896
elevation_pc	-2.103e-03	4.621e-04	4.630e-04	4.543	5.50e-06 ***
rugosity_slope_buffer	-4.523e-02	1.503e-02	1.506e-02	3.003	0.002669 **
area_reservoir	-1.892e-07	4.237e-07	4.242e-07	0.446	0.655507
average_temperature_buffer	2.934e-03	7.539e-03	7.548e-03	0.389	0.697442
area_pasture	3.871e-07	1.179e-06	1.181e-06	0.328	0.743061
traditional_agricultural_mosaic	-1.464e-07	7.936e-07	7.949e-07	0.184	0.853903

b) Shrubland specie richness

Variables	Coefficient	Std. Error	Adjusted SE	z value	P-value
(Intercept)	1.020e+00	3.291e-01	3.299e-01	3.091	0.00199 **
area_reservoir	-1.102e-06	8.301e-07	8.315e-07	1.326	0.18497
area_shrubland	8.274e-07	3.181e-07	3.189e-07	2.595	0.00946 **
area_olives_orchards	9.854e-07	3.303e-07	3.311e-07	2.976	0.00292 **
distance_water	6.136e-05	2.324e-05	2.329e-05	2.634	0.00843 **
elevation_pc	-1.690e-03	3.705e-04	3.714e-04	4.552	5.3e-06 ***
rugosity_slope_buffer	-3.954e-02	1.207e-02	1.210e-02	3.268	0.00108 **
average_precip_buffer	-4.934e-04	1.029e-03	1.030e-03	0.479	0.63202
area_pasture	2.393e-07	9.578e-07	9.593e-07	0.249	0.80300
traditional_agricultural_mosaic	2.472e-07	1.015e-06	1.017e-06	0.243	0.80796
area_deciduous_forest	-2.199e-08	1.234e-07	1.236e-07	0.178	0.85879
average_temperature_buffer	4.024e-04	3.030e-03	3.036e-03	0.133	0.89454
area_temporary_crops	-2.979e-08	2.422e-07	2.427e-07	0.123	0.90230
urban_areas	6.166e-08	5.412e-07	5.423e-07	0.114	0.90947
area_watersource	-9.375e-08	8.718e-07	8.735e-07	0.107	0.91454

c) Woodland specie richness

Variables	Coefficient	Std. Error	Adjusted SE	z value	P-value
(Intercept)	2.105e+00	2.189e-01	2.193e-01	9.599	< 2e-16 ***
area_coniferous_forest	-5.261e-07	1.867e-07	1.871e-07	2.812	0.004929 **
area_temporary_crops	-7.337e-07	5.332e-07	5.339e-07	1.374	0.169390
area_shrubland	-7.619e-07	2.057e-07	2.062e-07	3.695	0.000220 ***
average_precip_buffer	-3.331e-03	8.854e-04	8.875e-04	3.753	0.000175 ***
average_temperature_buffer	-3.198e-02	7.372e-03	7.390e-03	4.328	1.51e-05 ***
distance_water	7.460e-05	1.273e-05	1.276e-05	5.848	< 2e-16 ***
urban_areas	-3.089e-06	1.278e-06	1.281e-06	2.412	0.015883 *

area_olives_orchards	1.398e-07	2.062e-07	2.065e-07	0.677	0.498408
area_vineyards	-7.604e-07	1.243e-06	1.245e-06	0.611	0.541302
elevation_pc	-9.067e-05	1.849e-04	1.851e-04	0.490	0.624181
area_watersource	2.358e-07	8.481e-07	8.494e-07	0.278	0.781323
rugosity_slope_buffer	9.886e-04	3.808e-03	3.813e-03	0.259	0.795400

d) Abundance of grassland species

Variables	Coefficient	Std. Error	Adjusted SE	z value	P-value
(Intercept)	2.021e+00	2.611e-01	2.616e-01	7.723	< 2e-16 ***
area_temporary_crops	2.197e-06	5.196e-07	5.209e-07	4.218	2.47e-05 ***
area_deciduous_forest	-7.159e-07	2.493e-07	2.499e-07	2.864	0.00418 **
area_shrubland	1.033e-06	2.364e-07	2.370e-07	4.359	1.31e-05 ***
area_olives_orchards	5.722e-07	2.352e-07	2.357e-07	2.428	0.01520 *
area_pasture	2.223e-06	1.721e-06	1.724e-06	1.290	0.19715
average_precip_buffer	4.922e-03	8.481e-04	8.501e-04	5.790	< 2e-16 ***
distance_water	-5.131e-05	1.698e-05	1.702e-05	3.014	0.00257 **
elevation_pc	-2.103e-03	2.542e-04	2.548e-04	8.252	< 2e-16 ***
rugosity_slope_buffer	-4.416e-02	1.026e-02	1.028e-02	4.294	1.75e-05 ***
urban_areas	3.419e-06	1.291e-06	1.294e-06	2.642	0.00823 **
average_temperature_buffer	1.587e-03	4.852e-03	4.859e-03	0.327	0.74394
area_watersource	-2.270e-07	9.699e-07	9.716e-07	0.234	0.81526
area_vineyards	-4.788e-08	3.627e-07	3.634e-07	0.132	0.89519

e) Abundance of shrubland species

Variables	Coefficient	Std. Error	Adjusted SE	z value	P-value
(Intercept)	2.373e+00	3.462e-01	3.469e-01	6.840	< 2e-16 ***
area_reservoir	-1.933e-06	6.482e-07	6.497e-07	2.975	0.002930 **
area_deciduous_forest	-8.773e-07	2.994e-07	3.000e-07	2.925	0.003448 **
area_shrubland	2.433e-07	3.219e-07	3.222e-07	0.755	0.450232

area_olives_orchards	3.489e-07	3.406e-07	3.409e-07	1.023	0.306092
area_vineyards	-4.681e-06	1.656e-06	1.659e-06	2.820	0.004795 **
average_precip_buffer	-1.209e-03	1.233e-03	1.235e-03	0.979	0.327430
distance_water	6.816e-05	1.941e-05	1.946e-05	3.503	0.000459 ***
elevation_pc	-2.314e-03	3.550e-04	3.558e-04	6.503	< 2e-16 ***
rugosity_slope_buffer	-5.770e-02	1.219e-02	1.222e-02	4.721	2.3e-06 ***
urban_areas	1.456e-06	1.712e-06	1.713e-06	0.850	0.395355
area_temporary_crops	-1.183e-07	3.967e-07	3.973e-07	0.298	0.765963
average_temperature_buffer	-1.464e-04	2.185e-03	2.190e-03	0.067	0.946697

f) Abundance of woodland species

Variables	Coefficient	Std. Error	Adjusted SE	z value	P-value
(Intercept)	2.414e+00	2.182e-01	2.187e-01	11.037	< 2e-16 ***
area_reservoir	-9.279e-07	4.297e-07	4.308e-07	2.154	0.031236 *
area_deciduous_forest	4.657e-07	1.677e-07	1.681e-07	2.771	0.005592 **
area_shrubland	-5.212e-07	2.112e-07	2.118e-07	2.461	0.013839 *
area_olives_orchards	7.877e-07	1.918e-07	1.923e-07	4.096	4.20e-05 ***
area_vineyards	-1.908e-06	1.326e-06	1.328e-06	1.436	0.150907
average_precip_buffer	-3.026e-03	8.301e-04	8.321e-04	3.637	0.000276 ***
average_temperature_buffer	-3.042e-02	6.989e-03	7.006e-03	4.343	1.41e-05 ***
distance_water	7.041e-05	1.271e-05	1.274e-05	5.527	< 2e-16 ***
elevation_pc	-4.978e-04	2.037e-04	2.041e-04	2.439	0.014742 *
urban_areas	-2.811e-06	1.176e-06	1.179e-06	2.384	0.017137 *
traditional_agricultural_mosaic	2.557e-07	7.263e-07	7.271e-07	0.352	0.725103
area_watersource	-1.311e-07	6.671e-07	6.683e-07	0.196	0.844518
rugosity_slope_buffer	-5.659e-04	2.941e-03	2.946e-03	0.192	0.847704
area_temporary_crops	2.196e-08	1.532e-07	1.535e-07	0.143	0.886250
area_pasture	5.168e-08	3.745e-07	3.753e-07	0.138	0.890482

Appendix V – Elevation range within the study area (ABM layout), showing topographic variation from 117m (very low, dark areas) to 1120m (very high, light areas) above sea level, with the reservoir extent highlighted in blue

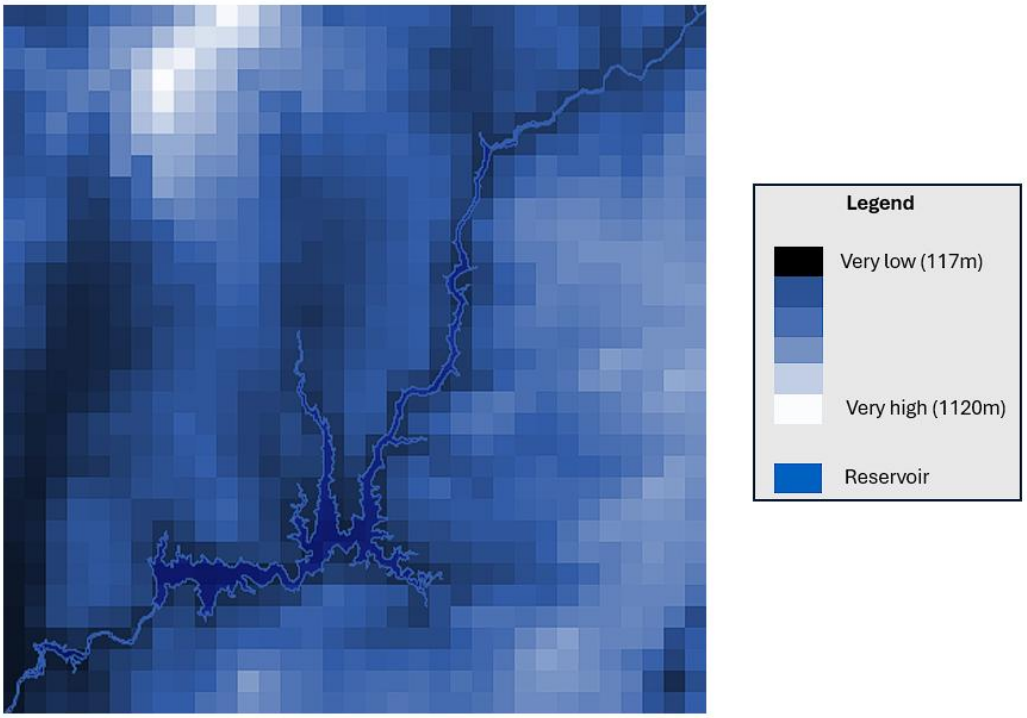

Appendix VI – Monthly microclimatic variation maps of the Baixo Sabor region from March to July across four consecutive years (2013-2016) (ABM layout) showing: (a) Temperature distribution patterns with darker shades representing lower temperatures and lighter shades indicating higher temperatures; (b) Precipitation distribution patterns with darker shades representing lower precipitation levels and lighter shades indicating higher precipitation levels. Both maps include the Sabor River (blue line) and reservoir area (light blue) overlaid for geographic reference.

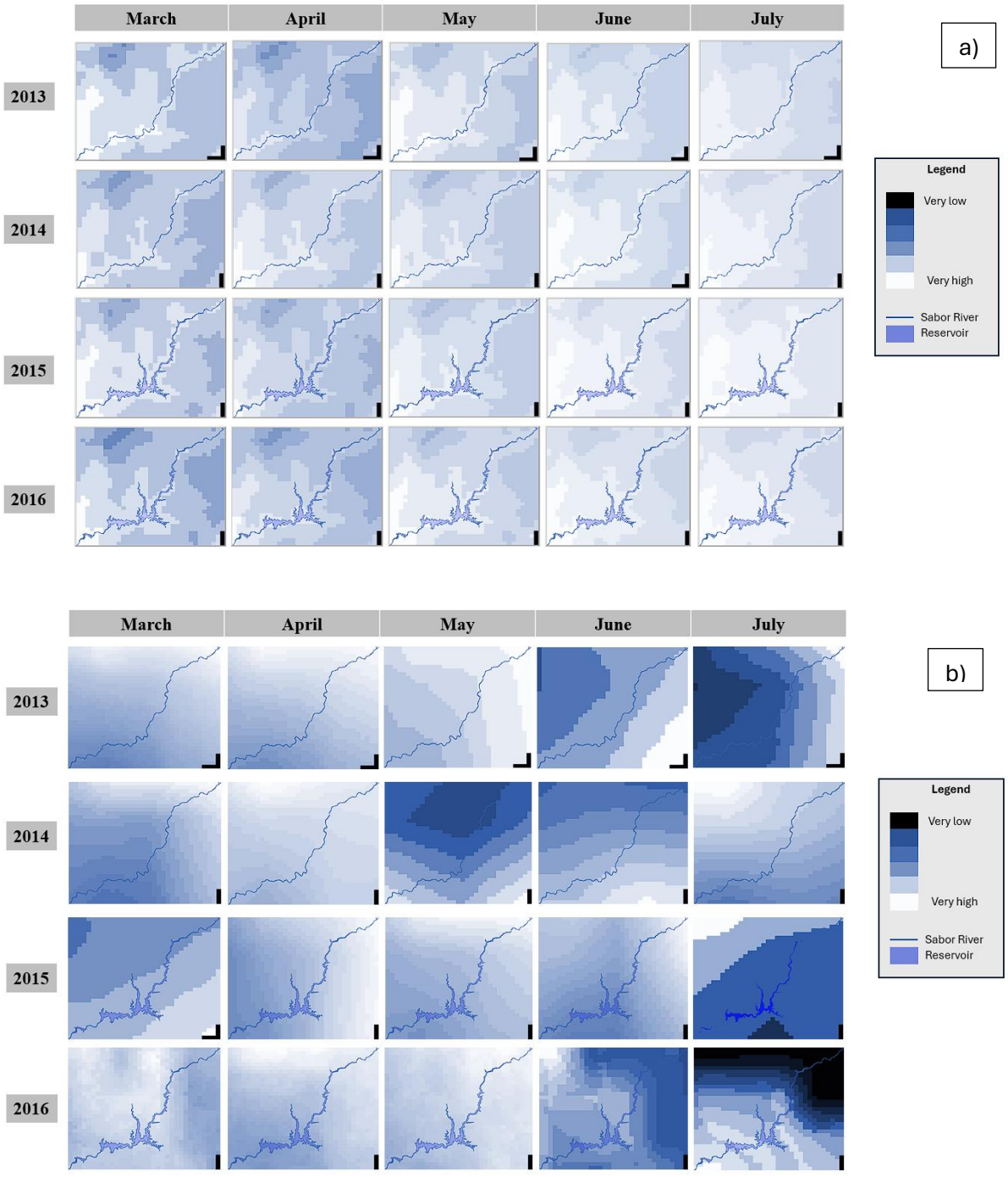

Appendix VII – Monthly spatial distribution maps of passerine species richness by functional group in the study area from March to July across four consecutive years (2013-2016): (a) Grassland species richness, with color intensity indicating number of species; (b) Shrubland-associated bird species richness, with color intensity indicating number of species; (c) Woodland-associated bird species richness, with color intensity indicating number of species. All maps include the Sabor River (blue line) and reservoir area (light blue) for geographic reference.

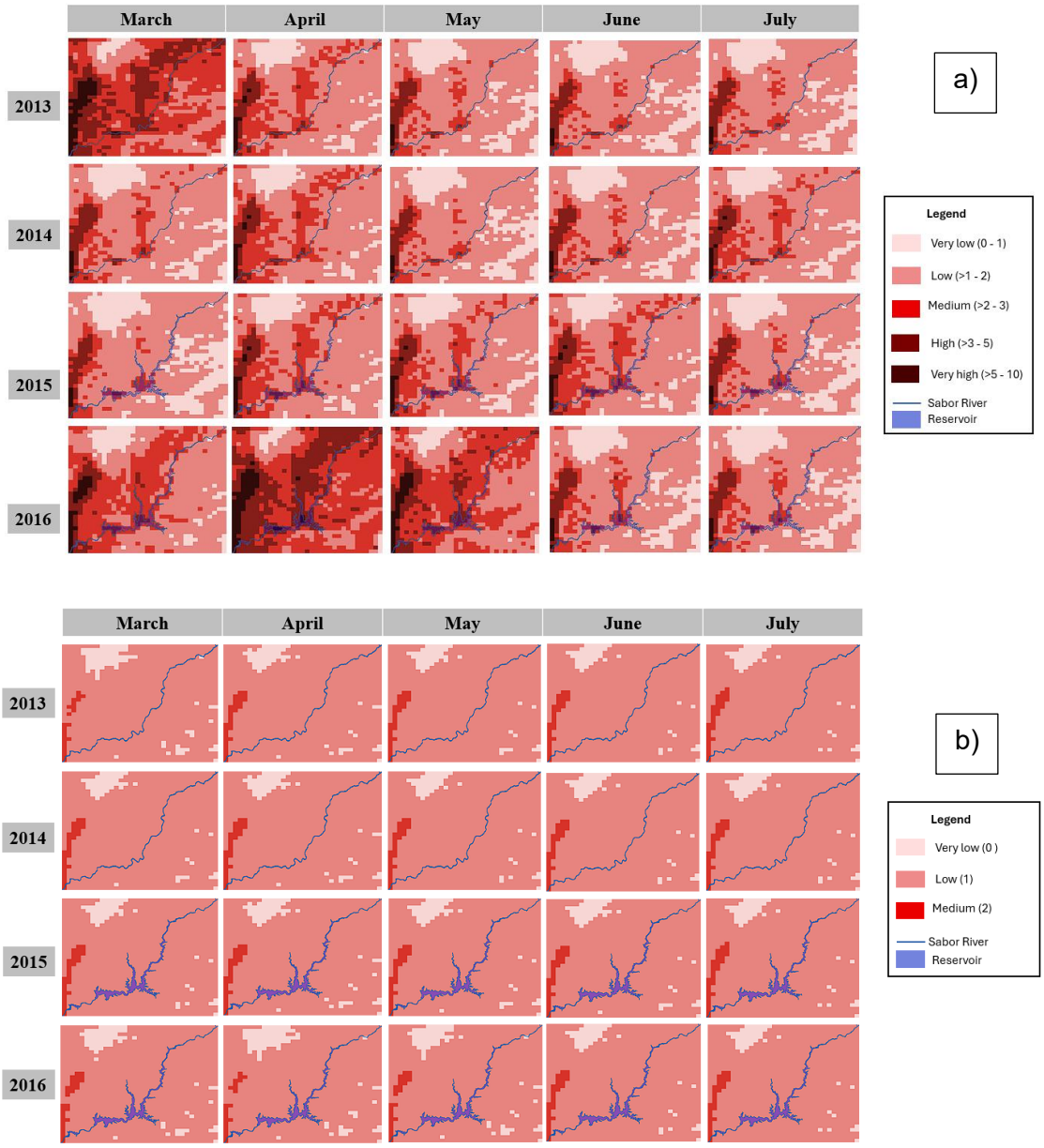

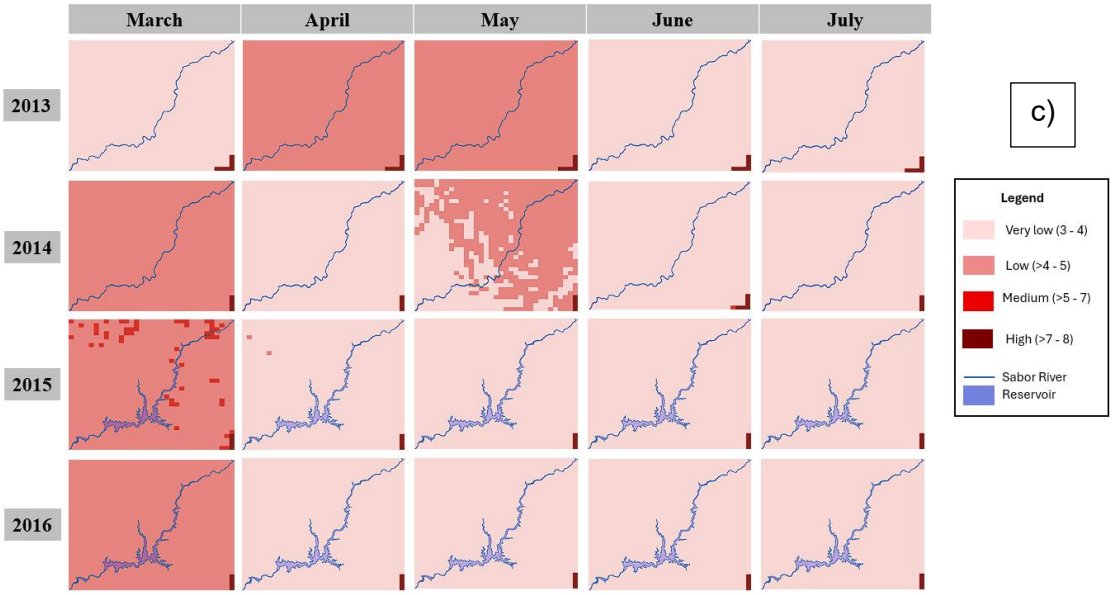
March
April
May
June
July
2013
2014
2015
2016
c)
Legend
Very low (3 - 4)
Low (>4 - 5)
Medium (>5 - 7)
High (>7 - 8)
Sabor River
Reservoir

Appendix VIII – Monthly spatial distribution maps of abundance of passerine birds discrimated by functional group in the study area from March to July across four consecutive years (2013-2016): (a) Abundance of grassland species, with color intensity indicating number of species; (b) Abudance of Shrubland species, with color intensity indicating number of species; (c) Abundance of woodland species, with color intensity indicating number of species. All maps include the Sabor River (blue line) and reservoir area (light blue) for geographic reference.

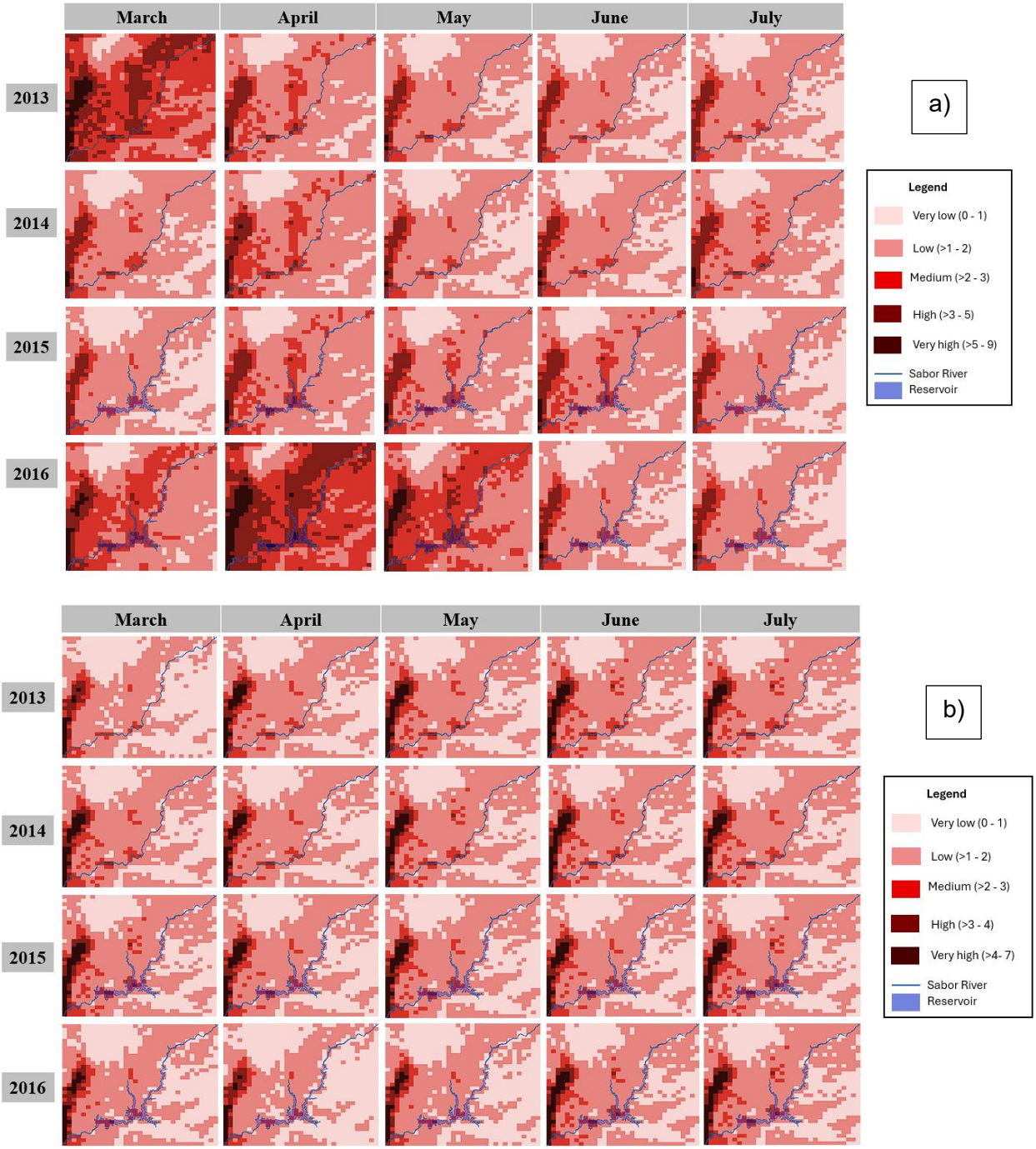

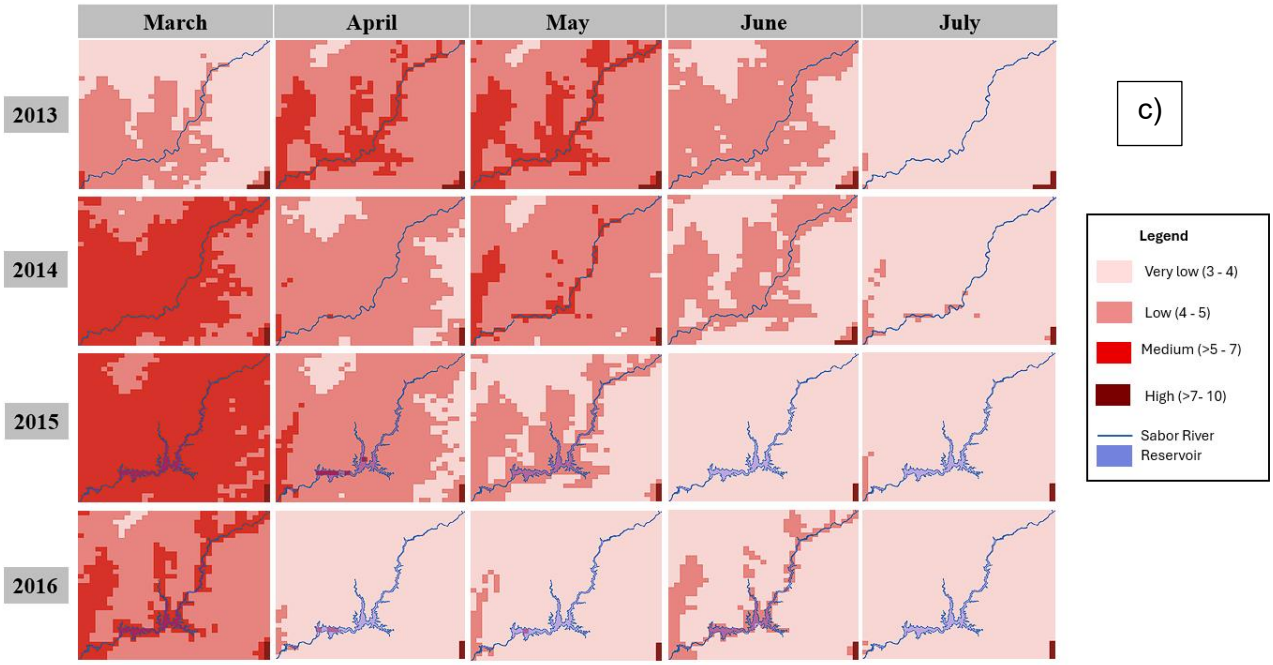
March
April
May
June
July
2013
2014
2015
2016
c)
Legend
Very low (3 - 4)
Low (4 - 5)
Medium (>5 - 7)
High (>7- 10)
Sabor River
Reservoir

Appendix IX - Statistical outputs (Kruskal-Wallis test and Dunn's test) for inter-annual variation of passerine species richness, discriminated by landscape metrics (SHDY, CI, DI).

1.1. SHDI

```
Summary Statistics:

   Min. 1st Qu.  Median    Mean 3rd Qu.    Max.

  1.159   1.167   1.215   1.201   1.226   1.233

Detailed Summary by Year:

     Year     Mean         SD   Median      Min      Max

2013 2013 1.208492 0.02890031 1.225988 1.168317 1.232624

2014 2014 1.201528 0.02732786 1.213261 1.163167 1.228423

2015 2015 1.195057 0.03183919 1.202045 1.159441 1.226563

2016 2016 1.197673 0.03264920 1.215801 1.160755 1.227400

Kruskal-Wallis Test:

    Kruskal-Wallis rank sum test

data:  value by year

Kruskal-Wallis chi-squared = 1.7086, df = 3, p-value = 0.635
```

1.2. CI

```
Summary Statistics:

   Min. 1st Qu.  Median    Mean 3rd Qu.    Max.

  94.42   94.66   94.91   95.06   95.50   95.93

Detailed Summary by Year:

     Year     Mean        SD   Median      Min      Max

2013 2013 94.91064 0.5745060 94.65539 94.41900 95.87824

2014 2014 95.14528 0.5236218 95.07761 94.58373 95.77748

2015 2015 94.98828 0.4855404 94.88693 94.61420 95.82494

2016 2016 95.20855 0.5406657 95.28823 94.65461 95.92818
```

```
Kruskal-Wallis Test:

    Kruskal-Wallis rank sum test

data:  value by year

Kruskal-Wallis chi-squared = 1.3314, df = 3, p-value = 0.7217
```

1.3. DI

```
Summary Statistics:

   Min. 1st Qu.  Median    Mean 3rd Qu.    Max.

 0.6736  0.6926  0.7358  0.7316  0.7583  0.7905

Detailed Summary by Year:

     Year      Mean         SD    Median       Min       Max

2013 2013 0.7478667 0.04006522 0.7544634 0.6931440 0.7904692

2014 2014 0.7201491 0.04338745 0.7347134 0.6735710 0.7765273

2015 2015 0.7384731 0.03117263 0.7412248 0.6911034 0.7756436

2016 2016 0.7197437 0.04130241 0.7204696 0.6779372 0.7699467

Kruskal-Wallis Test:

    Kruskal-Wallis rank sum test

data:  value by year

Kruskal-Wallis chi-squared = 2.6343, df = 3, p-value = 0.4515
```

Appendix X - Statistical outputs (Kruskal-Wallis test and Dunn's test) for inter-annual variation of passerine abundance, discriminated by landscape metrics (SHDY, CI, DI).

1.1. SHDI

```
Summary Statistics:

   Min. 1st Qu.  Median    Mean 3rd Qu.    Max.

  1.008   1.054   1.154   1.123   1.183   1.208

Detailed Summary by Year:

     Year     Mean         SD   Median      Min      Max

2013 2013 1.134575 0.08390472 1.182018 1.007665 1.207765

2014 2014 1.127457 0.06691342 1.147377 1.036563 1.198670

2015 2015 1.106151 0.08023505 1.110726 1.014504 1.189155

2016 2016 1.123755 0.08000916 1.160530 1.019073 1.204796

Kruskal-Wallis Test:

    Kruskal-Wallis rank sum test

data:  value by year

Kruskal-Wallis chi-squared = 0.56571, df = 3, p-value = 0.9042
```

1.2. CI

```
Summary Statistics:

   Min. 1st Qu.  Median    Mean 3rd Qu.    Max.

  94.54   94.79   95.30   95.29   95.85   96.19

Detailed Summary by Year:

     Year     Mean        SD   Median      Min      Max

2013 2013 95.19039 0.5018488 95.22147 94.56399 95.89434

2014 2014 95.44773 0.6066776 95.66530 94.72390 96.01117

2015 2015 95.40355 0.6591634 95.48802 94.54372 96.19051

2016 2016 95.12077 0.5661212 94.81533 94.66499 95.94980
```

```
Kruskal-Wallis Test:

    Kruskal-Wallis rank sum test

data:  value by year

Kruskal-Wallis chi-squared = 1.6057, df = 3, p-value = 0.6581
```

1.3. DI

```
Summary Statistics:

   Min. 1st Qu.  Median    Mean 3rd Qu.    Max.

 0.6038  0.6276  0.7121  0.6975  0.7532  0.7673

Detailed Summary by Year:

     Year      Mean         SD    Median       Min       Max

2013 2013 0.7102773 0.06443969 0.7406126 0.6115163 0.7672805

2014 2014 0.6813982 0.07505330 0.6814838 0.6038497 0.7622042

2015 2015 0.6884678 0.07084453 0.6835177 0.6065531 0.7672771

2016 2016 0.7097673 0.06642790 0.7473179 0.6071855 0.7600692

Kruskal-Wallis Test:

    Kruskal-Wallis rank sum test

data:  value by year

Kruskal-Wallis chi-squared = 0.61143, df = 3, p-value = 0.8938
```

Appendix XI - Statistical outputs (Kruskal-Wallis Test and Dunn's test) for seasonal variation of passerine species richness, discriminated by landscape metrics (SHDY, CI, DI).

1.1. SHDI

```
Summary Statistics:

   Min. 1st Qu.  Median    Mean 3rd Qu.    Max.

  1.159   1.167   1.215   1.201   1.226   1.233

Detailed Summary by Month (Years as replicates):

  month  Mean      SD Median   Min   Max     N

1 march  1.23 0.00269   1.23  1.23  1.23     4

2 april  1.22 0.00684   1.22  1.21  1.23     4

3 may    1.22 0.0104    1.22  1.20  1.23     4

4 june   1.17 0.0147    1.17  1.16  1.19     4

5 july   1.16 0.00237   1.16  1.16  1.17     4

Kruskal-Wallis Test for Seasonal Differences:

       Kruskal-Wallis rank sum test

data:  value by month

Kruskal-Wallis chi-squared = 15.871, df = 4, p-value = 0.003197
```

Dunn's Test Results (Monthly Comparisons):

```
      Comparison          Z     P.unadj      P.adj

1   april - july  2.0916501 0.036469830 0.36469830

2   april - june  2.0916501 0.036469830 0.36469830

3    july - june  0.0000000 1.000000000 1.00000000

4  april - march -1.1354672 0.256179626 1.00000000

5   july - march -3.2271172 0.001250442 0.01250442

6   june - march -3.2271172 0.001250442 0.01250442

7    april - may  0.2390457 0.811070129 1.00000000

8     july - may -1.8526043 0.063939089 0.63939089

9     june - may -1.8526043 0.063939089 0.63939089

10   march - may  1.3745129 0.169282508 1.00000000
```

1.2. CI

```
Summary Statistics:
   Min. 1st Qu.  Median    Mean 3rd Qu.    Max.
  94.42   94.66   94.91   95.06   95.50   95.93
Detailed Summary by Month (Years as replicates):
  month  Mean     SD Median   Min   Max     N
1 march  94.6 0.0479   94.6  94.6  94.7     4
2 april  95.4 0.656    95.6  94.4  95.8     4
3 may    95.6 0.462    95.7  94.9  95.9     4
4 june   95.0 0.242    94.9  94.7  95.3     4
5 july   94.8 0.209    94.7  94.6  95.1     4
Kruskal-Wallis Test for Seasonal Differences:
    Kruskal-Wallis rank sum test
data:  value by month
Kruskal-Wallis chi-squared = 9.7429, df = 4, p-value = 0.04499
```

Dunn's Test Results (Monthly Comparisons):

```
       Comparison          Z    P.unadj     P.adj
1   april - july  1.3147515 0.18859344 1.0000000
2   april - june  0.3585686 0.71991785 1.0000000
3    july - june -0.9561829 0.33897984 1.0000000
4  april - march  1.9123658 0.05582929 0.5582929
5   july - march  0.5976143 0.55009732 1.0000000
6   june - march  1.5537972 0.12023280 1.0000000
7    april - may -0.8964215 0.37002771 1.0000000
8     july - may -2.2111729 0.02702386 0.2702386
9     june - may -1.2549900 0.20948238 1.0000000
10   march - may -2.8087872 0.00497285 0.0497285
```

1.3. DI

```
Summary Statistics:
   Min. 1st Qu.  Median    Mean 3rd Qu.    Max.
 0.6736  0.6926  0.7358  0.7316  0.7583  0.7905
Detailed Summary by Month (Years as replicates):
  month  Mean      SD Median   Min   Max     N
1 march 0.775 0.00367  0.776 0.770 0.778     4
2 april 0.709 0.0550   0.685 0.674 0.790     4
3 may   0.695 0.0251   0.686 0.678 0.732     4
4 june  0.730 0.00985  0.729 0.720 0.741     4
5 july  0.749 0.00803  0.752 0.737 0.754     4
Kruskal-Wallis Test for Seasonal Differences:
    Kruskal-Wallis rank sum test
data:  value by month
Kruskal-Wallis chi-squared = 11.129, df = 4, p-value = 0.02516
```

Dunn's Test Results (Monthly Comparisons):

```
      Comparison          Z     P.unadj      P.adj
1   april - july -1.3745129 0.169282508 1.00000000
2   april - june -0.4183300 0.675705849 1.00000000
3    july - june  0.9561829 0.338979844 1.00000000
4  april - march -2.3904572 0.016827409 0.16827409
5   july - march -1.0159443 0.309655903 1.00000000
6   june - march -1.9721272 0.048595087 0.48595087
7    april - may  0.5976143 0.550097317 1.00000000
8     july - may  1.9721272 0.048595087 0.48595087
9     june - may  1.0159443 0.309655903 1.00000000
10   march - may  2.9880715 0.002807438 0.02807438
```

Appendix XII - Statistical outputs (Kruskal-Wallis Test and Dunn's test) for seasonal variation of passerine abundance, discriminated by landscape metrics (SHDY, CI, DI).

1.1. SHDI

```
Summary Statistics:

   Min. 1st Qu.  Median    Mean 3rd Qu.    Max.

  1.008   1.054   1.154   1.123   1.183   1.208

Detailed Summary by Month (Years as replicates):

  month  Mean      SD Median   Min   Max     N

1 march  1.20 0.00822   1.20  1.19  1.21     4

2 april  1.18 0.00535   1.18  1.17  1.18     4

3 may    1.15 0.0299    1.15  1.11  1.18     4

4 june   1.07 0.0244    1.07  1.04  1.09     4

5 july   1.02 0.0123    1.02  1.01  1.04     4

Kruskal-Wallis Test for Seasonal Differences:

    Kruskal-Wallis rank sum test

data:  value by month

Kruskal-Wallis chi-squared = 17.514, df = 4, p-value = 0.001535

Dunn's Test Results (Monthly Comparisons):

      Comparison          Z     P.unadj      P.adj

1   april - july  2.6295029 0.008550979 0.08550979

2   april - june  1.7928429 0.072998045 0.72998045

3    july - june -0.8366600 0.402783694 1.00000000

4  april - march -1.1354672 0.256179626 1.00000000

5   july - march -3.7649701 0.000166569 0.00166569

6   june - march -2.9283101 0.003408100 0.03408100

7    april - may  0.5976143 0.550097317 1.00000000

8     july - may -2.0318886 0.042164931 0.42164931

9     june - may -1.1952286 0.231997724 1.00000000

10   march - may  1.7330815 0.083081187 0.83081187
```

1.2. CI

```
Summary Statistics:
   Min. 1st Qu.  Median    Mean 3rd Qu.    Max.
  94.54   94.79   95.30   95.29   95.85   96.19
Detailed Summary by Month (Years as replicates):
  month  Mean    SD Median   Min   Max     N
1 march  95.0 0.178   94.9  94.8  95.2     4
2 april  94.7 0.145   94.7  94.5  94.9     4
3 may    95.3 0.742   95.2  94.6  96.0     4
4 june   96.0 0.129   96.0  95.9  96.2     4
5 july   95.5 0.122   95.5  95.4  95.7     4
Kruskal-Wallis Test for Seasonal Differences:
    Kruskal-Wallis rank sum test
data:  value by month
Kruskal-Wallis chi-squared = 11.829, df = 4, p-value = 0.01867
Dunn's Test Results (Monthly Comparisons):
      Comparison          Z     P.unadj      P.adj
1   april - july -1.9123658 0.055829295 0.55829295
2   april - june -3.2271172 0.001250442 0.01250442
3    july - june -1.3147515 0.188593442 1.00000000
4  april - march -0.8366600 0.402783694 1.00000000
5   july - march  1.0757057 0.282058876 1.00000000
6   june - march  2.3904572 0.016827409 0.16827409
7    april - may -1.1952286 0.231997724 1.00000000
8     july - may  0.7171372 0.473289465 1.00000000
9     june - may  2.0318886 0.042164931 0.42164931
10   march - may -0.3585686 0.719917853 1.00000000
```

1.3. DI

```
=== Seasonal Pattern Analysis for division ===

Summary Statistics:

   Min. 1st Qu.  Median    Mean 3rd Qu.    Max.

 0.6038  0.6276  0.7121  0.6975  0.7532  0.7673

Detailed Summary by Month (Years as replicates):

  month  Mean      SD Median   Min   Max     N

1 march 0.748 0.00505  0.749 0.741 0.752     4

2 april 0.760 0.00661  0.759 0.752 0.767     4

3 may   0.710 0.0647   0.721 0.633 0.767     4

4 june  0.607 0.00318  0.607 0.604 0.612     4

5 july  0.663 0.0357   0.679 0.609 0.684     4

Kruskal-Wallis Test for Seasonal Differences:

    Kruskal-Wallis rank sum test

data:  value by month

Kruskal-Wallis chi-squared = 14.071, df = 4, p-value = 0.007071
```

Dunn's Test Results (Monthly Comparisons):

```
       Comparison          Z      P.unadj       P.adj

1   april - july  2.3306958 0.0197694064 0.197694064

2   april - june  3.4064015 0.0006582529 0.006582529

3    july - june  1.0757057 0.2820588758 1.000000000

4  april - march  1.0757057 0.2820588758 1.000000000

5   july - march -1.2549900 0.2094823757 1.000000000

6   june - march -2.3306958 0.0197694064 0.197694064

7    april - may  0.9561829 0.3389798440 1.000000000

8     july - may -1.3745129 0.1692825080 1.000000000

9     june - may -2.4502186 0.0142769490 0.142769490

10   march - may -0.1195229 0.9048611295 1.000000000
```

Appendix XIII - Number of sampling days included in cliff-nesting birds surveys, discriminated by year.

year	Nr. of sampling days
2010	27
2011	46
2012	42
2013	53
2014	25
2015	25
2016	42
2017	37
2018	34
2019	31
2020	10
2021	31
2022	27

Appendix XIV - Location of breeding territories/colonies of Golden eagles, Egyptian vultures and Griffon vultures in the study area.